Journal of the National Academy of Forensic Engineers®

http://www.nafe.org

ISSN: 2379-3252

Vol. 35 No. 2 December 2018

National Academy of Forensic Engineers®

Journal Staff

Technical Review Process

The Technical Review Committee Chair chooses the reviewers for each Journal manuscript from amongst the members and affiliates of the NAFE according to their competence and the subject of the paper, and then arbitrates (as necessary) during the review process. External reviewers may also be utilized when necessary. This confidential process concludes with the acceptance of the finished paper for publication or its rejection/withdrawal. The name(s) of authors are included with their published works. However, unpublished drafts together with the names and comments of reviewers are entirely confidential during the review process and are excised upon publication of the finished paper.

National Academy of Forensic Engineers®

Board of Directors

President
Martin Gordon, P.E.
Senior Member

President-Elect
John Certuse, P.E.
Fellow

Senior Vice President
James Petersen, P.E.
Fellow

Vice President
Liberty Janson, P.E.
Senior Member

Treasurer
Jerry S. Ogden, Ph.D., P.E.
Fellow

Secretary
Paul Swanson, P.E.
Senior Member

Past Presidents
Michael D. Leshner, P.E.
Fellow

John P. Leffler, P.E.
Senior Member

Jeffrey D. Armstrong, P.E.
Fellow

Directors at Large
Samuel G. Sudler, P.E.
Senior Member

Richard A. Rice, P.E.
Fellow

Executive Director
Arthur E. Schwartz, Esq.

Executive Director Emeritus
Marvin M. Specter, P.E., L.S.
Life Member

Submitting Proposed Papers to NAFE for Consideration

A concise abstract of approximately 100 words shall be sent to the Journal Editor for initial consideration. Upon approval of the abstract, authors will be scheduled to present their work at one of the semi-yearly NAFE Technical Conferences. A 90% complete draft copy of the manuscript shall be submitted to the Journal Editor for review and approval no later than 30 days before the conference.

For details about requirements for manuscripts, visit:
https://www.nafe.org/assets/Journal/JournalContents.pdf

For details on the NAFE Journal peer review process, visit:
https://nafe.memberclicks.net/assets/Journal/NAFEPeerReviewProcess030719.pdf

For the NAFE Bylaws content "Responsibilities of, Obligations of and Guidelines for Authors, the Journal Editor, Technical Review Committee Chair, and Technical Reviewers," visit:
https://www.nafe.org/assets/docs/journalguidelines.pdf

Copies of the Journal

The Journal of the National Academy of Forensic Engineers® contains papers that have been accepted by NAFE. In most cases, papers have been presented at NAFE seminars. Members and Affiliates receive a PDF download of the Journal as part of their annual dues. All Journal papers may be individually downloaded from the NAFE website at www.nafe.org. There is no charge to NAFE Members & Affiliates. A limited supply of Volume 33 and earlier hardcopy Journals (black & white) are available. The costs are as follows: $15.00 for NAFE Members and Affiliates; $30.00 for members of the NSPE not included in NAFE membership; $45.00 for all others. Requests should be sent to Arthur Schwartz, Executive Director, NAFE, 1420 King St., Alexandria, VA 22314-2794.

Comments by Readers

Comments by readers are invited, and, if deemed appropriate, will be published. Send to: Arthur Schwartz, Esq., Executive Director, 1420 King St., Alexandria, VA 22314-2794. Comments can also be sent via email to journal@nafe.org.

Material published in this Journal, including all interpretations and conclusions contained in papers, articles, and presentations, are those of the specific author or authors and do not necessarily represent the view of the National Academy of Forensic Engineers® (NAFE) or its members.

Table of Contents

‡ Paper presented at the NAFE seminar held 1/14/17 in Phoenix.

* Paper presented at the NAFE seminar held 7/22/17 in Atlanta.

Forensic Engineering Application of the Matchmoving Process

By Richard M. Ziernicki, PhD, PE (NAFE 308F), Angelos G. Leiloglou (NAFE 956C), Taylor Spiegelberg, and Kurt Twigg

Abstract

This paper presents a methodology that uses the photogrammetric process of matchmoving for analyzing objects (vehicles, pedestrians, etc.) visible in video captured by moving cameras. Matchmoving is an established scientific process that is used to calibrate a virtual camera to "match" the movement and optic properties of the real-world camera that captured the video. High-definition 3D laser scanning technology makes it possible to accurately perform the matchmoving process and evaluate the results. Once a virtual camera is accurately calibrated, moving objects visible in the video can be tracked or matched to determine their position, orientation, path, speed, and acceleration. Specific applications of the matchmoving methodology are presented and discussed in this paper and include analysis performed on video footage from a metro bus onboard camera, police officer body-worn camera footage, and race track video footage captured by a drone. In all cases, the matchmoving process yielded highly accurate camera calibrations and allowed forensic investigators to accurately determine and evaluate the dynamics of moving objects depicted in the video.

Keywords

Matchmoving, photogrammetry, on-board video, photo-match, high-definition scanning, body-worn cameras, police cruiser cameras, drone video footage, accident reconstruction, lens distortion correction, SynthEyes, PFTrack, Boujou, forensic engineering

Introduction

Matchmoving (also referred to as "camera tracking") is a technique based upon photogrammetry, which is the science of attaining measurements from photographs or images. Accordingly, matchmoving is simply the application of photogrammetry to a sequence of individual images (i.e., video frames).

The purpose or goal of matchmoving is to take 2D information from an image sequence and solve for or "calibrate" a 3D virtual camera, which "matches" the movement and optic properties of the real-world camera that captured a given video. When done correctly, this technique allows computer-generated, 3D virtual objects to be accurately composited into the video footage with correct position, scale, and orientation.

With advancements in matchmoving software programs, high-definition laser scanning (also known as LIDAR - Light Detection and Ranging), and other related technologies, the matchmoving technique can be an effective tool for forensic engineering investigations and accident reconstruction to accurately determine and analyze the orientation, translation, velocity, and acceleration of vehicles, pedestrians, or other objects depicted in video footage.

Background

Photogrammetry (the basis of the matchmoving technique) is rooted in the principles of perspective and projective geometry, which were developed centuries ago by artists and mathematicians to transform 3D (or Euclidian) space into 2D (or projective) space (**Figure 1**). Matchmoving uses reverse projection to transform the 2D image back into 3D space by analyzing the change of perspective (parallax shift) in a sequence of images.

Before dedicated software programs for matchmoving existed, manual hand-tracking methods were used. In hand-tracking, the user makes an approximation as to the camera's position in each frame of the image sequence and then attempts to refine its position over many iterations

Richard M. Ziernicki, PhD, PE, 7185 S. Tucson Way, Centennial, CO 80112, 303-925-1900, rziernicki@knottlab.com

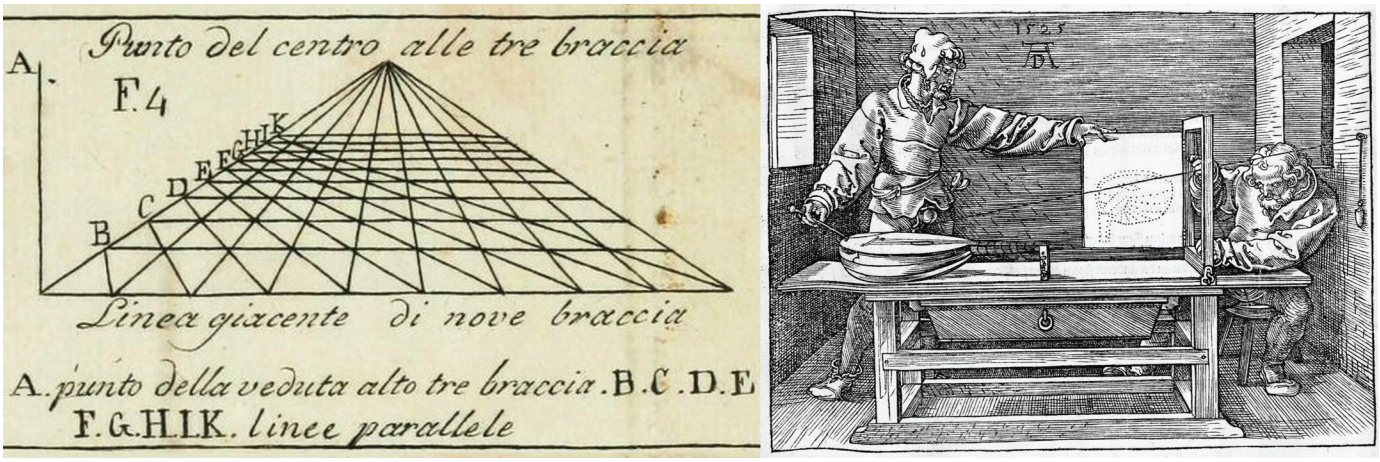

Figure 1
Left: Visual pyramid by Leon Battista Alberti, in "De Pictura," 1448;
Right: One of Albrecht Durer's perspective machines, "Underweysung der Messung," 1525.

until something close to a match is achieved. Hand-tracking methods would be very difficult, if not impossible, to implement in the matchmoving process to achieve an appropriate level of accuracy for forensic engineering. Now, with advanced matchmoving software programs and the accessibility of LIDAR, even videos with complex camera movements can be analyzed with great precision to accurately determine and evaluate the kinematics of moving objects depicted in the video.

Lens Distortion Correction

Before the matchmoving process can be performed, a major factor that must be addressed is lens distortion, which is attributed to the imperfections due to the physical characteristics of the components that make up the camera lens. The apparent effect causes the image or video to be distorted so that straight lines appear curved or bowed out toward the edges of the image. When the edges tend to bend inward, it is referred to as barrel distortion; when the edges flare outward, it is called pincushion distortion (**Figure 2**).

The amount of lens distortion can vary, but because the virtual cameras in 3D animation programs do not exhibit lens distortion, it must be corrected for accurate matchmoving and photogrammetry to be performed. Although most matchmoving programs are able to solve for and correct lens distortion, it is best to first correct the lens distortion ("undistort") the video footage using a camera calibration process.

Matchmoving software can calculate the type and amount of lens distortion in a video by using a calibration pattern or grid (**Figure 3**). A calibration grid is typically a grid of lines, points, or checkerboards. This grid can be recorded by either the same camera that shot the original video or an identical exemplar camera using the same settings that were used when the original footage was shot.

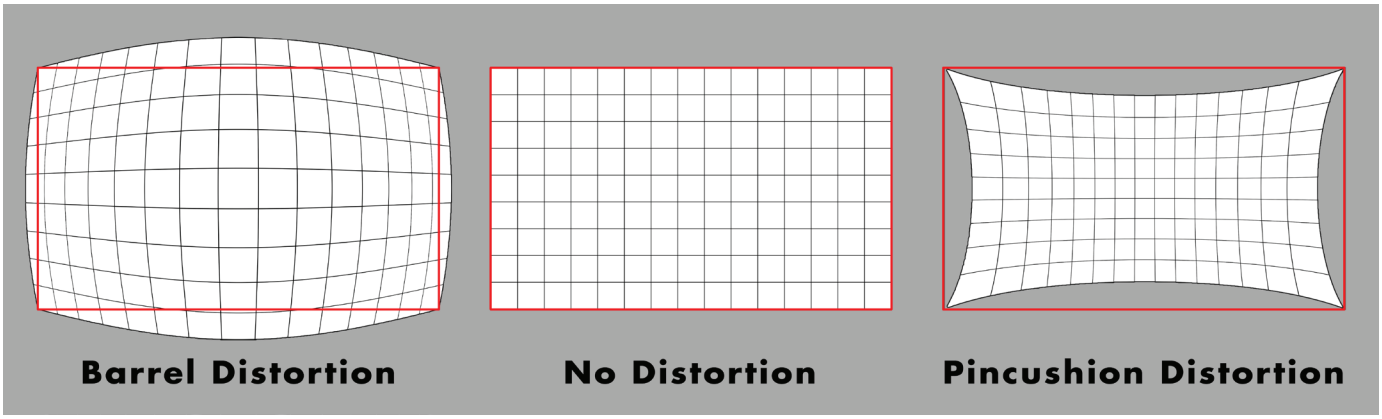

Figure 2
The two most common types of lens distortion are barrel distortion and pincushion distortion.

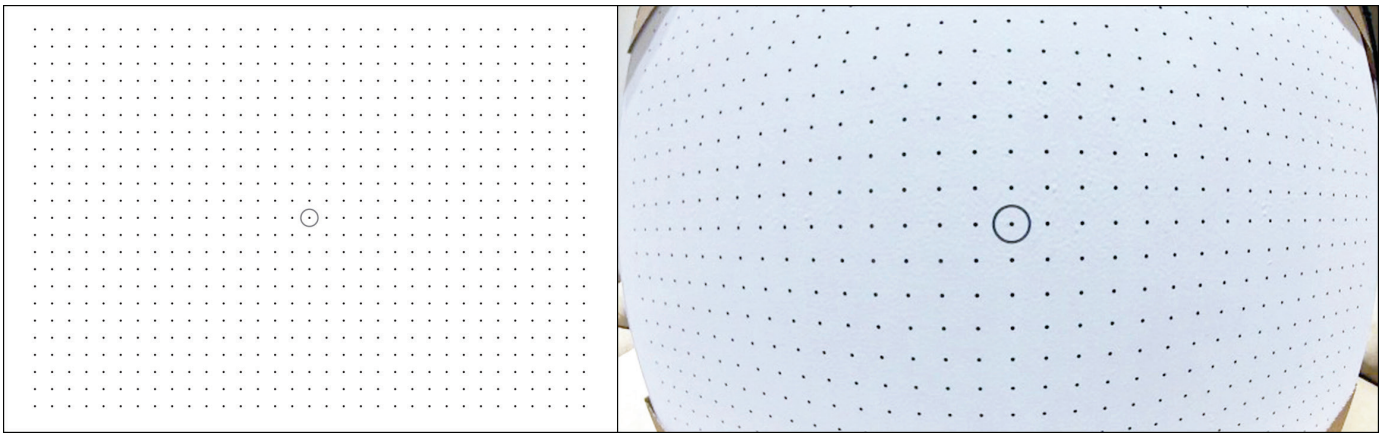

Figure 3
Left: Example of typical calibration grid used to determine the amount of lens distortion produced by a camera lens; Right: Calibration grid capture using wide-angle lens with barrel lens distortion.

If the subject camera or an exemplar camera are not available, there are other methods or algorithms that can be used to calculate the lens distortion.

Once the matchmoving software successfully calculates the lens distortion, it then applies the correct type and amount of "warping" to "undistort" or correct the footage so that there is no longer any lens distortion (i.e., straight line in the scene appears straight in the video footage), as shown in **Figure 4**.

Matchmoving Process

Matchmoving software programs analyze 2D information (x, y) and convert it into 3D information (x, y, z) about the camera and scene. There are many matchmoving software programs available today, such as SynthEyes, PFTrack, and Boujou. While these programs can vary in some areas and features, they all generally follow the same matchmoving procedure, which can be broken down into two basic steps: 2D tracking and 3D calibration.

2D Tracking

The first step in the matchmoving process is identifying 2D points (commonly referred to as "features") in the video frames or image sequence and then tracking them throughout the image sequence using 2D trackers. Features are specific points in an image that can be easily identified (i.e., corners of objects or high-contrast spots) and represent real-world 3D objects in the scene that are static. For most matchmoving software to solve for a calibration, a minimum number of 2D features must be tracked in each frame of the image sequence. There are generally two basic methods of 2D tracking: automatic tracking and manual ("supervised") tracking. Matchmoving projects will typically require a combination of these methods.

Automatic Tracking

Most matchmoving programs now have the capability to do automatic 2D tracking, which means the software searches for and tracks features with minimal user intervention.

Figure 4
Left: Original dash camera video footage with significant barrel distortion; Right: Same frame after being corrected for lens distortion.

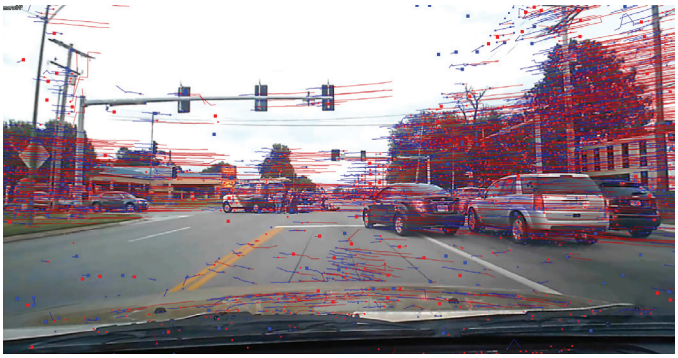

Figure 5
Blips and potential 2D tracks produced by automatic tracking method of dash camera video.

In automatic tracking, the software goes through the image sequence and identifies unique features in each individual frame and marks them as potential 2D tracking features (often referred to as blips). Then the software program tries to match or join these blips together into tracks that span several sequential frames (**Figure 5**). Finally, the software analyzes the 2D tracks to determine which tracks are valid and potentially useful for 3D calibration and eliminates those that are not.

Supervised Tracking

Supervised tracking is a "manual" method used to perform 2D tracking, only in the sense that it is the user who decides what feature he wants to track, instead of leaving it up to the software to find features to track automatically. In this method, the software uses its searching or tracking algorithms to automatically search for and track the features defined by the user, while the user "supervises" the tracking, intervening if or when the software loses track of the feature.

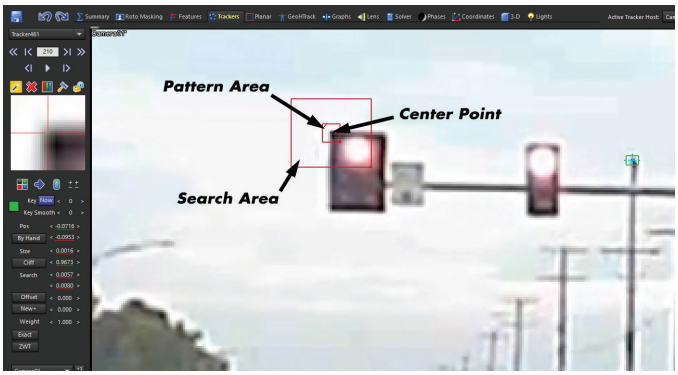

Figure 6
Using supervised tracking, the user places a tracker by defining the center point of the feature to be tracked (in this case, the upper left corner of the traffic signal), the pattern to search for, and the area in which to search for that pattern in subsequent frames.

Figure 7
2D tracks produced by manual (or "supervised") tracking. The blue/red sweeping lines represent the 2D paths of the tracked features.

To initiate the supervised tracking process, the user places a 2D tracker on a feature in a frame, defining the feature's center point. The user then defines the pattern area and search area to inform the software what pattern to search for and what part of the image it should search to find that pattern in subsequent frame (**Figure 6**).

If the software finds a similar pattern in that frame, it will automatically move the tracker's center point to match the center point of the pattern; and then the software will move on to the next frame and repeat the search process, and so on, resulting in a 2D path of that tracke feature (**Figure 7**).

If the software cannot find a similar pattern within the search area, the tracker will "slip" off-track. When this occurs, the user can go back to the frame where the tracker had slipped and "help" the software by moving the tracker to the proper position (and setting a keyframe). The user then tells the software to resume the tracking process as before.

Constrained Points

Once the 2D tracking step has been completed, the software technically has enough information to attempt to solve for or calibrate a virtual camera that matches the real-world camera that recorded the video. However, to increase the likelihood of an accurate calibration, most matchmoving software programs allow for the use of constraints — ways of forcing the software to calibrate a solution based on known 3D information. One very powerful type of constraint is using LIDAR data, which a user can use to force individual tracks to be solved to fit their corresponding real-world xyz coordinates (**Figure 8**).

Using this type of constraint assures the user that the calibration (if successful) will be accurate and in line with

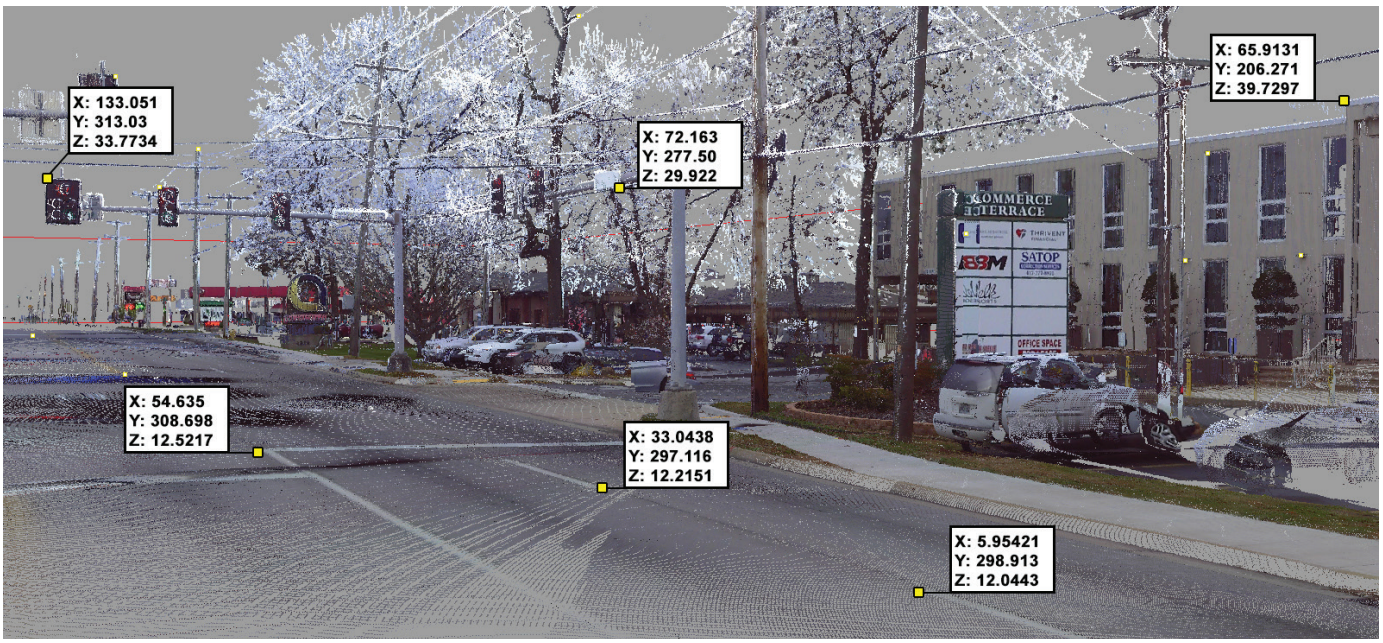

Figure 8

Sample of the 3D (XYZ) coordinates data (from accident scene point cloud) used to constrain the corresponding 2D trackers.

the real-world scene as defined by the point cloud captured by the high-definition 3D laser scanning. The accuracy of the calibration can also be assessed by comparing the difference between the constrained points' positions versus the solved 3D position. The smaller the difference, the greater the accuracy of the calibration (**Figure 9)**.

3D Calibration

The second and final step in the matchmoving process (after 2D tracking) is 3D calibration. The goal of 3D calibration is to determine the exact camera movement and optic properties (e.g., field of view [FOV], focal length, lens distortion, optical center, etc.) of the real-world camera that was used to record the video of the scene, and then to reproduce a 3D virtual camera that "matches" it.

To calibrate a virtual camera, the software analyzes the 2D tracking information from the first step (2D tracking) of the matchmoving process and uses triangulation between corresponding points/features in multiple frames of the image sequence (video) to solve for the virtual camera position. In addition to generating a virtual camera, which matches the real-world camera, the calibration process also generates virtual 3D markers that represent the 3D locations of the features that were tracked in the 2D tracking step.

Evaluating Error in 3D Calibration

When a matchmoving process is complete and solved correctly, the 3D virtual camera should accurately match the real-world camera. The simplest way to evaluate how

Axes	Tracker	Locked To	Distance	Solved Position (x y z)			Error (ft)
XYZ	#298	x=133.051 y=313.03 z=33.7734		133.051	313.030	33.773	0.000
XYZ	#299	x=55.4804 y=338.583 z=32.7554		55.480	338.583	32.756	0.001
XYZ	#300	x=55.065 y=316.18 z=33.3131		55.065	316.180	33.313	0.000
XYZ	#301	x=367.287 y=256.397 z=61.4309		367.287	256.397	61.431	0.000
XYZ	#302	x=201.716 y=362.838 z=33.4569		201.716	362.838	33.457	0.000
XYZ	#303	x=144.756 y=384.769 z=50.4419		144.756	384.769	50.442	0.000
XYZ	#304	x=51.3948 y=261.215 z=25.7705		51.395	261.215	25.771	0.000
XYZ	#305	x=64.553 y=388.033 z=27.8675		64.553	388.033	27.867	0.000
XYZ	#306	x=62.5352 y=275.258 z=53.8683		62.535	275.258	53.868	0.000
XYZ	#309	x=43.5314 y=205.455 z=37.896		43.531	205.455	37.896	0.000
XYZ	#310	x=44.6667 y=197.61 z=31.6698		44.667	197.610	31.670	0.000

Figure 9

Error (far right column) of the constrained point position versus the solved or calibrated 3D positions.

accurately a calibrated virtual camera matches the real-world camera is to look through the virtual camera and evaluate the alignment between the 2D tracked features with the 3D (calibrated) markers or features (**Figure 10**). In a good calibration, the 3D markers should be aligned with the feature they represent in the image. Most matchmoving software programs conveniently feature the ability to visually evaluate the error of each 3D marker's position versus the 2D tracker position in each frame of the video.

The difference between the alignment of the solved 3D marker and the 2D track is typically referred to as the "solution's error." Error values are usually expressed in pixels, which correlate to a unit of measure relative to the resolution of the video and the scale of the scene.

Once the 3D calibration step is done, the matchmoving process is complete. The virtual camera is then exported from the matchmoving software program and imported into a virtual scene within a 3D animation software program. Since the virtual camera was calibrated using constrained points from the LIDAR point cloud data, the virtual camera is accurately positioned, scaled, and oriented relative to the point cloud within the virtual scene.

In the case of body-worn cameras or cameras attached to vehicles (i.e., police cruiser camera, bus, etc.), the virtual camera's movement directly correlates to the movement of the pedestrian wearing the camera or the vehicle the camera is attached to. Therefore, the path, speed, and acceleration of the pedestrian wearing the camera or the vehicle that the camera is in can be attained from the virtual camera itself.

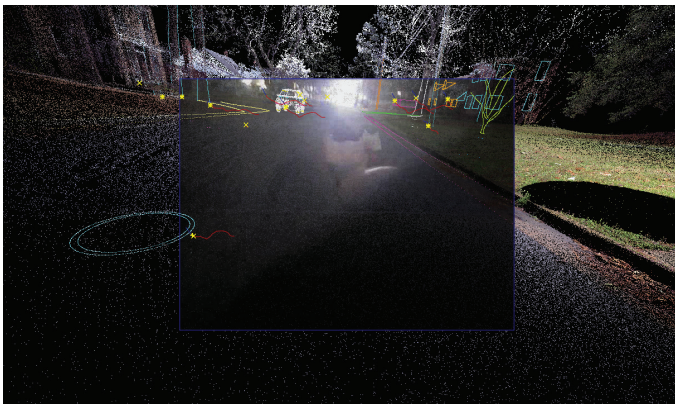

Figure 10
View through virtual camera within virtual scene with view from real-world camera (video frame) composited together to analyze the accuracy of the calibration process.

Object Tracking/Matching

The motion of vehicles, pedestrians, or other objects depicted in the video can also be determined by using a process called object tracking or object matching.

The process of object matching involves viewing the video footage through the virtual camera in the virtual scene, and manually positioning a surrogate virtual model, which has the same size and geometry as the real-world object in the video, so that it matches the object's position relative to the point cloud as depicted in each frame of the video (**Figure 11**).

Determining and Analyzing Object Dynamics

Once an object has been tracked/matched, the 3D translation (x,y,z) and orientation (roll, pitch, yaw) data of that object, for each frame, is exported from the 3D animation program and imported into an Excel spreadsheet where the object's motion data (i.e., speed, acceleration, heading angle, etc.) is calculated and graphed. The object's motion data is then evaluated to confirm that its motion is in line with the laws of physics.

Case Studies

Pedestrian vs. Bus

This case involved a female pedestrian crossing in the crosswalk with a walk signal when she was struck by a right-turning bus that failed to yield the right-of-way. The bus impact with the pedestrian can be seen in one of the four on-board video cameras (**Figure 12**). The authors were able to attain the path, speed, and acceleration of the bus using the matchmoving technique to match the on-board dash camera of the bus to the 3D point cloud of the environment (**Figure 13**). The placement of the on-board dash camera within the 3D point cloud of the bus was then aligned with the matchmoved camera to move

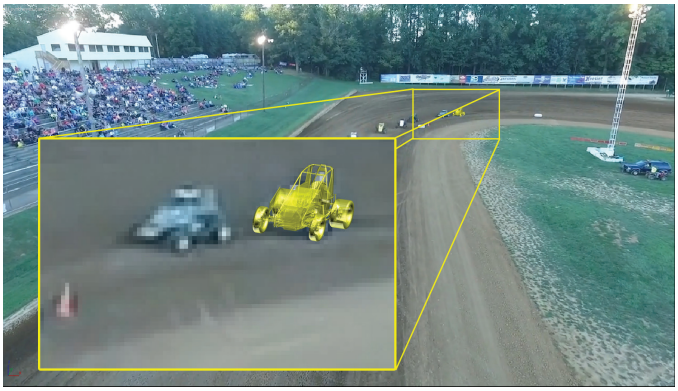

Figure 11
Virtual model of sprint car used to match the position of drifting sprint car depicted in video.

Figure 12
View of the bus's four on-board video cameras at the time of impact with the pedestrian.
Top left: Dash Cam; Top right: Step Cam — showing the impact with the pedestrian (circled in red).

a point cloud model of the bus along the appropriate motion path.

The analysis revealed that the maximum speed of the bus during the turn was 7.3 miles per hour, and the bus was traveling 6.5 miles per hour at the point of impact with the pedestrian. The relevant standard operating procedures of this commercial bus requires drivers to travel 3 to 5 miles per hour during a turn.

Further, the interior "step" camera footage was camera matched to the bus 3D point cloud that showed the passenger door of the bus (**Figure 14)**. Using contrast and color correction filters within Adobe After Effects, it was possible to view the pedestrian and other features through the bus door in the interior camera footage.

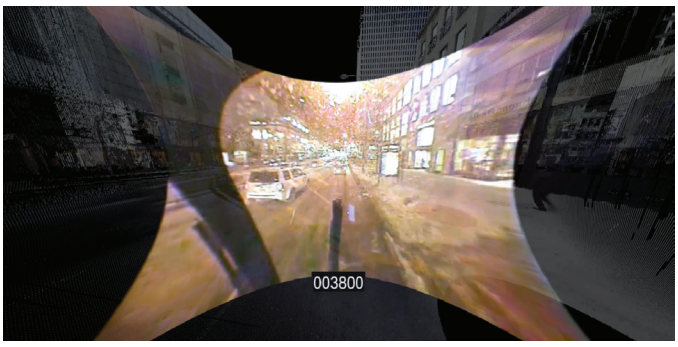

Figure 13
View through matchmoved virtual camera of the bus dash camera video footage, with point cloud in the virtual scene.

With this virtual interior "step" camera matched to the bus point cloud — and the bus point cloud parented to the virtual dash camera — it was possible to determine information regarding the motion of the pedestrian in the same 3D space, relative to the bus motion and 3D environment point cloud, as follows:

- The pedestrian, was visible to the bus driver for 6-plus seconds, but the bus had a dirty window and door. The driver failed to recognize the moving pedestrian. According to standard operating procedures, drivers are not allowed to operate a bus with dirty windows/mirrors.

- There were two signs present at the intersection: "turning vehicles YIELD to pedestrians." The bus driver failed to yield to the pedestrian.

The utilization of matchmoving revealed that the bus driver's failure to follow the standard operating procedures and posted signs at the intersection was the probable cause of the incident. Had the bus driver complied with the standard operating procedures by traveling within the designated turn speed, keeping windows/mirrors clean, and keeping proper lookout, it was opined that

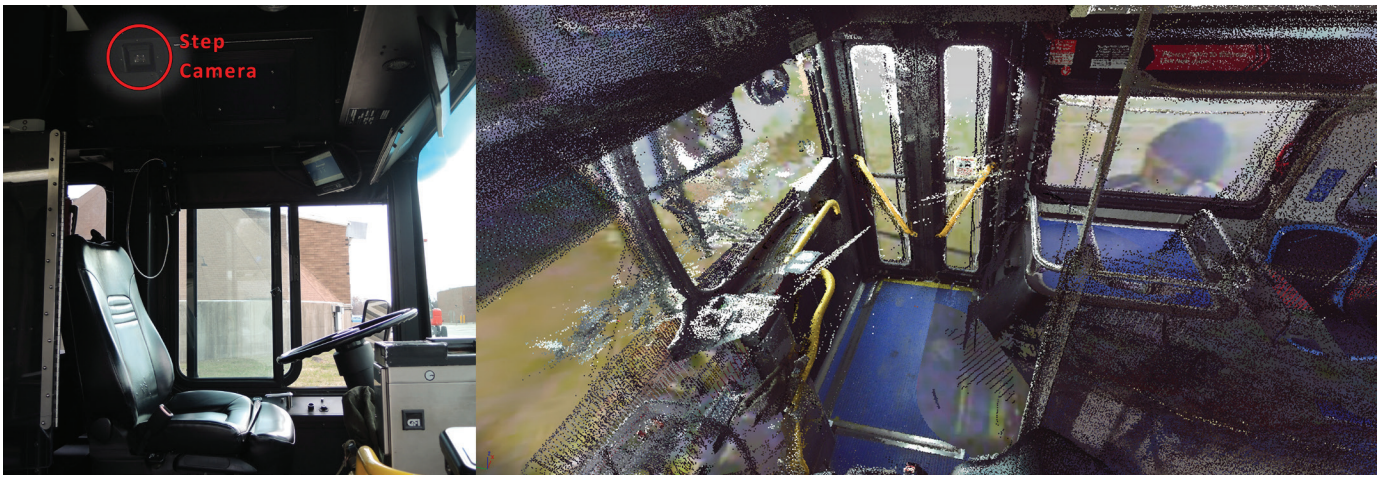

Figure 14

Left: Photograph showing location of step camera; Right: View through virtual camera match with point cloud of bus in virtual scene.

the bus driver would have been able to have ample time to observe and avoid hitting the pedestrian.

Police Officer Body-Worn Camera

This was an officer-involved shooting (OIS) case that resulted in the fatality of a 28-year-old male. The moments leading up to the shooting (and the shooting itself) were captured by the officer's body-worn camera. At the time of the shooting, the victim was sitting on the ground with his back to the officer.

By matchmoving the officer's body-worn camera and matching the pedestrian in the video, the authors were able to determine the movement of the officer (**Figure 15)** and the victim. From the analysis, the authors determined that the officer was approximately 23 feet away from the victim when he fatally shot the victim in the back and killed him (**Figure 16)**.

Sprint Car Race

In this case, aerial video footage captured by a drone during a sprint car race was used to verify whether a

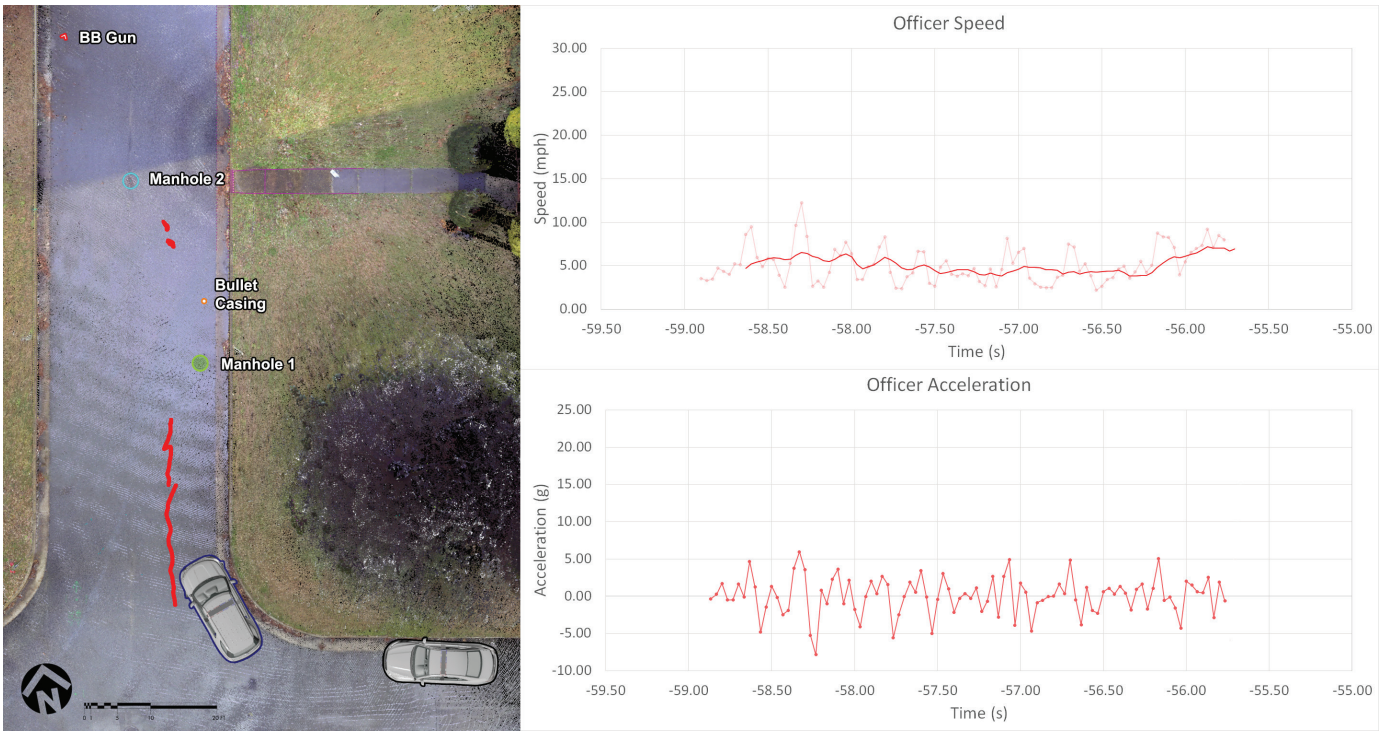

Figure 15

The path, speed, and acceleration of a calibrated virtual camera that directly correlates to the motion of the officer wearing a body camera.

sprint car could, in fact, drift at relatively low speeds. Aerial Imagery and LIDAR data attained from the United States Geological Survey (USGS) were used to accurately matchmove the video footage (**Figure 17**). Using object

Figure 16

Left: View through the virtual matchmoved camera with zoomed out to show shooting scene point cloud; Right: Top view of shooting scene point cloud depicting the location of the officer and the distance between him and the victim. * The names used are fictional.

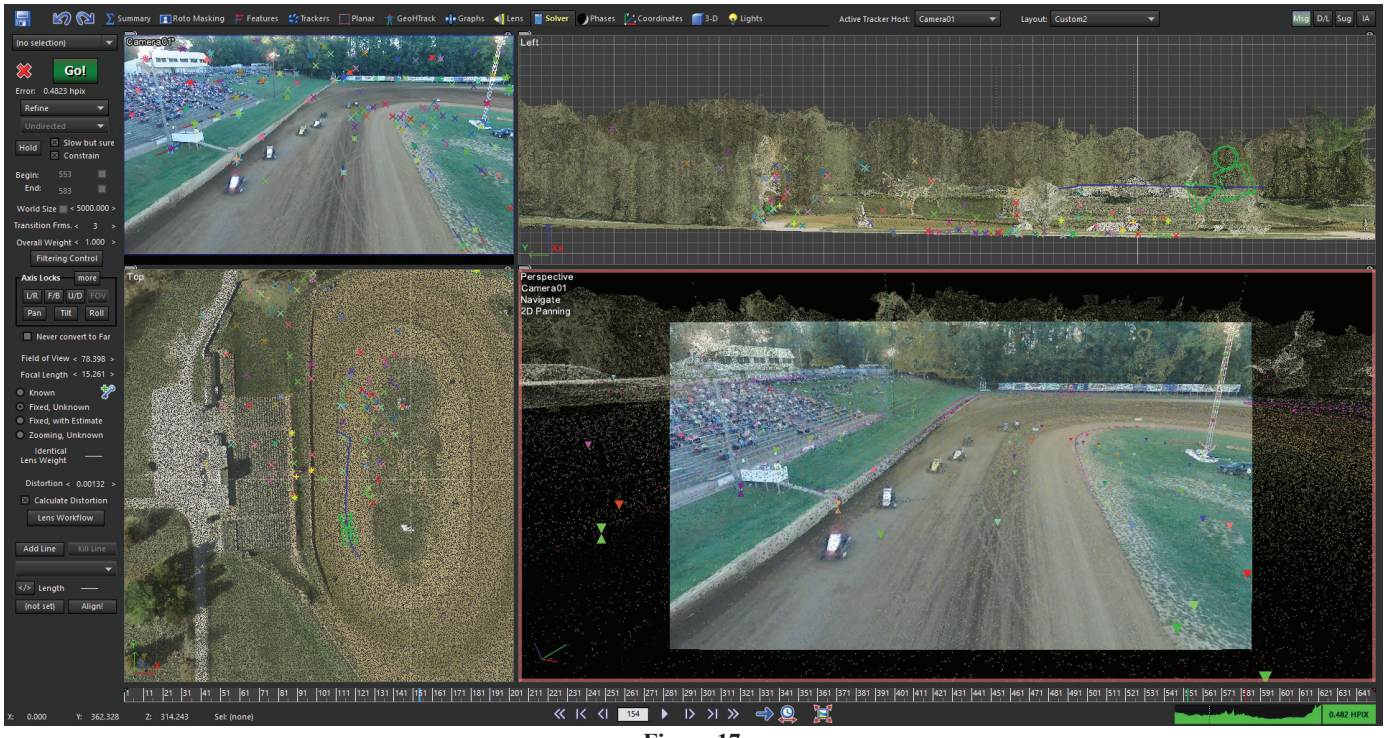

Figure 17

USGS LIDAR data used as constraint to accurately matchmove aerial video from a drone during sprint car race.

matching, the authors were able to match an exemplar sprint car model to one of the sprint cars depicted in the video (**Figure 18**). The position and rotational data of the sprint car was analyzed, and showed that the sprint car was drifting at speeds below 50 miles per hour.

Conclusion

The matchmoving process is based on the science of photogrammetry, which provides a solid foundation for forensic engineering investigations. The use of laser scanning technology (accurate to within a few millimeters) assures the accuracy and validity of the matchmoving process and the resulting analysis.

It is important to recognize that the matchmoving process must be done correctly to yield accurate results. The simplest way to verify whether this was done is to look through the virtual camera and evaluate the alignment between the 2D tracked features with the 3D (calibrated) markers. In a good calibration, the 3D markers should be aligned with the feature they represent in the image. In addition to visual verification, most matchmoving software programs conveniently feature the ability to evaluate the mathematical error of each 3D marker's position versus its corresponding 2D tracker position in each frame of the video.

With advancements in matchmoving software programs, high-definition laser scanning, and other related technologies, the matchmoving technique can be effective in forensic engineering investigations and accident reconstruction to accurately analyze video to determine the orientation, translation, velocity, and acceleration of vehicles, pedestrians, or other objects depicted in video footage.

Bibliography

1. Breen K, Anderson C. The Application of Photogrammetry to Accident Reconstruction. SAE Technical Paper 861422. Warrendale, PA: Society of Automotive Engineers; 1986.

2. Callahan M, LeBlanc B, Vreeland R, Bretting G. Close-Range Photogrammetry with Laser Scan Point Clouds. SAE Technical Paper 2012-01-0607. Warrendale, PA: Society of Automotive Engineers; 2012.

3. Coleman C, Tandy D, Colborn J, Ault N. Applying Camera Matching Methods to Laser Scanned

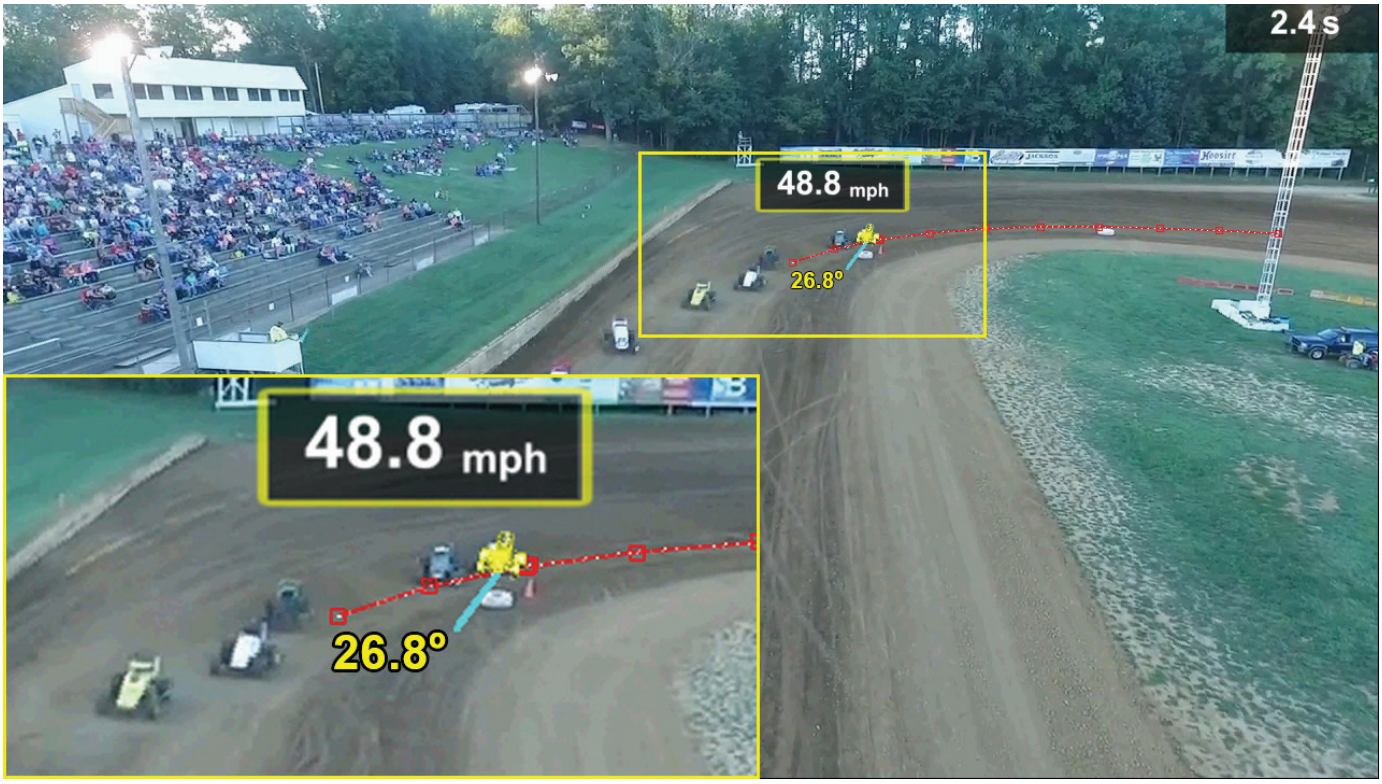

Figure 18
3D virtual model of sprint car matched to sprint car depicted in the video.

Three Dimensional Scene Data with Comparisons to Other Methods. SAE Technical Paper 2015-01-1416. Warrendale, PA: Society of Automotive Engineers; 2015.

4. Fenton S, Kerr R. Accident Scene Diagramming Using New Photogrammetric Technique. SAE Technical Paper 970944. Warrendale, PA: Society of Automotive Engineers; 1997.

5. Fenton S, Neale W, Rose N, Hughes W. Determining Crash Data Using Camera Matching Photogrammetric Technique. SAE Technical Paper 2001-01-3313. Warrendale, PA: Society of Automotive Engineers; 2001.

6. Dobbert, T. Matchmoving- The Invisible Art of Camera Tracking. 2nd Edition. Indianapolis, Indiana: John Wiley & Sons, Inc.; 2012..

7. Neale W, Fenton S, McFadden S, Rose N. A Video Tracking Photogrammetry Technique to Survey Roadways for Accident Reconstruction. SAE Technical Paper 2004-01-1221. Warrendale, PA: Society of Automotive Engineers; 2004.

8. Ziernicki R, Danaher D. Forensic Engineering Use of Computer Animations and Graphics. Journal of the National Academy of Forensic Engineers. 2006;23(2):1-9.

9. Ziernicki R, Danaher D, Ball J. Forensic Engineering Evaluation of Physical Evidence in Accident Reconstruction. Journal of the National Academy of Forensic Engineers. 2007;24(2):1-10.

10. Ziernicki R, Leiloglou A. Advanced Technologies Utilized in the Reconstruction of an Officer-Involved Shooting Incident. Journal of the National Academy of Forensic Engineers. 2017;34(2):1-12.

11. Ziernicki R, Pierce W, Leiloglou A. Forensic Engineering Usage of Surveillance Video in Accident Reconstruction. Journal of the National Academy of Forensic Engineers. 2014;31(2):9-19.

12. Ssontech.com. (2019). SynthEyes - Andersson Technologies LLC. [online] Available at: https://www.ssontech.com/ [Accessed 29 Apr. 2019].

13. The Pixel Farm Ltd. (2019). PFTrack - The Pixel Farm Ltd.. [online] Available at: https://www.thepixelfarm.co.uk/pftrack/ [Accessed 29 Apr. 2019].

14. VICON. (2019). Boujou Matchmoving Software by Vicon. [online] Available at: https://www.vicon.com/products/software/boujou [Accessed 29 Apr. 2019].

15. Adobe.com. (2019). Adobe After Effects Visual effects and motion graphics software. [online] Available at: https://www.adobe.com/products/aftereffects.html [Accessed 29 Apr. 2019].

Forensic Engineering Investigation of a Fatal Farm Tractor Incident

By Daniel P. Couture, PEng (NAFE 951M)

Abstract

A farm owner was found unresponsive with crushing head injuries on his property in rural Ontario. His small farm tractor was found 60 meters away down a small incline with the engine running and transmission in neutral. The owner's son alleged that when the parking brake was engaged (with the engine running and transmission in neutral), this tractor's parking brake would "pop out," allowing the tractor to move. Field tests were conducted on the tractor to attempt to duplicate the scenario and to determine if the alleged sequence of events was plausible. Components of the parking brake and one exemplar were assessed with specialized metrology to determine whether they were within the manufacturing specifications on the blueprint. A 3-D CAD model of fit was created, and several variances were identified between the parts and the factory drawing. The results of the analysis concurred with the scenario that these variances led to the disengagement of the parking brake and operator fatality.

Keywords

Tractor, parking brake, disengagement, 3-D modeling, laser scan, forensic engineering

Background

In 2016, there were 43 farm-related deaths in Canada, according to statistics from the Canadian Agricultural Safety Association (CASA), including 11 in Ontario, which is home to the largest farming population in Canada. Some recent facts are shown in **Figure 1**. There were 19 on-farm deaths in Ontario in 2013, while Saskatchewan was second with eight. These facts set the context for the incident described in this paper.

It was reported that the 83-year-old victim (referred to as "Mr. W" for the purpose of this paper) was found lying on the ground by the shed on the farm in the rural Ontario township where he lived. He died at the scene from his injuries, and there were no witnesses to the accident.

The Ontario Provincial Police conducted a homicide investigation into the sudden death of Mr. W, and foul play was ruled out. The autopsy revealed that the victim had fatal crushing injuries to the head, leading investigators to presume he had been run over by the tractor, which was found with its engine idling and transmission in neutral some distance away from the shed against a fence post at the bottom of a small hill, as shown in **Figures 2** through **4**. Mr. W had significant farm operator experience. It was believed by his son, "Mr. AW," that his father had been operating the tractor to pull a riding lawn mower out from within the shed. Mr. AW suspected involvement of the parking brake, which had unexpectedly "popped out" when AW had operated this tractor.

The author's original scope of involvement was to inspect the tractor's parking brake mechanism and provide

Farm Injury/Fatality Statistics in Canada	
+ Agriculture ranks as Canada's third most hazardous industry	
+ In terms of absolute numbers of fatalities, there is no more dangerous occupation	
+ 1769 agricultural fatalities in Canada from 1990-2005: 2 per week	
+ Agricultural machines were involved in 70.9% of fatalities	
+ 91.6% of those fatally injured from this work were male	
+ For children under 14, the following were the most predominant causes of farm-related fatalities:	
Machine runovers	41.9%
Drownings	15.2%
Machine rollovers	11.1%
Animal-related	6.5%
Crushed under an object	5.1%

Figure 1
Recent Canadian agricultural injury and fatality details.

Daniel P. Couture, 352 Consumers Road, Toronto, ON M2J 1P8, daniel.couture@arconforensics.com

Figure 2
View downhill from shed at farm site.

a report on its condition. As the investigation progressed, the forensic engineering firm was subsequently engaged to quantify the differences between the blueprint design of the parking brake mechanism, an unused exemplar of the parts purchased from stock, and the actual involved components from the tractor. The objective was to gain insight into the circumstances of the fatality and possibly determine the root cause(s).

Investigation

The fact-gathering and analysis portions of the investigation were executed in three distinct phases over a period of four years.

First Phase: Elements and Observations

The original fact-finding phase of the investigation incorporated the following elements:

- During attendance at the incident site in December 2006, the tractor and parking brake mechanism were inspected and documented;
- Mr. AW was briefly interviewed about the circumstances of the incident; and
- The neighbor's ("Mr. R") farm was visited to inspect the parking brake mechanism of an identical model tractor owned by Mr. R.

The small tractor, which had a 55-hp engine and a bale spear attachment accessory, had been purchased new by Mr. W in the fall of 2004 from the local brand distributor. At the time of the incident, it reportedly had about 63 hours on the operation clock. When inspected in December 2006, the clock read 132.6 hours. This would be characterized as occasional use of about one hour per week.

The Parking Brake Mechanism

The tractor braking system comprised independent mechanical wet disc brakes for the right and left traveling brakes. Separate pedals were provided for the right (outboard side) and left (inboard side). Depressing the pedals and pulling the parking brake lever locks the traveling brakes, and results in the same state as that obtained when the brake pedals are pressed. The inboard and outboard pedals can be split, but only the inboard pedal is required to be depressed to engage the parking brake, as shown in **Figure 5**.

The brake was engaged by depressing the pedal with the right foot and simultaneously pulling up and back on a hand lever at approximately even elevation with the right knee of a sitting operator. The hand lever was solidly fixed to a flat chisel-like bar such that, as the lever was raised,

Figure 3
View uphill to shed from path.

Figure 4
Final position of tractor with engine running.

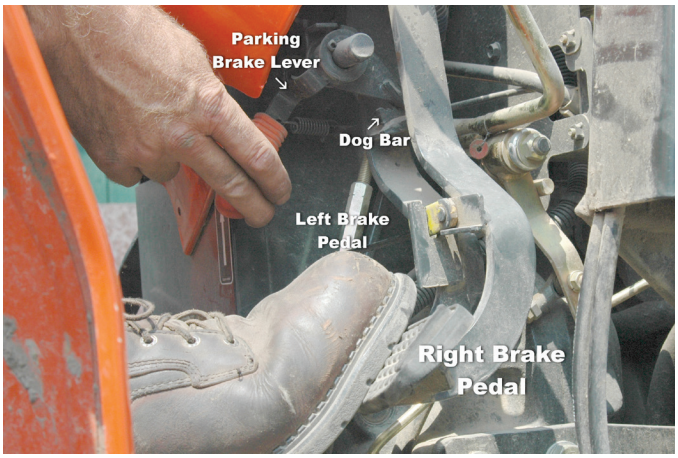

Figure 5
Parking brake configuration.

the end tip of this bar dropped at an acute angle into one of a series of transverse tooth-shaped slots (**Figure 6**) cut across another bar ("dog bar") welded horizontally to the upper side of the inboard pedal.

The dog bar grooves were shaped such that the pedal return action engaged the flat bar tip edge, catching it and locking the brake pedal at that position. There were eight slots in the dog bar over its length from leading to trailing ends. The dog bar and the flat bar were composed of steel, and appeared to have been painted dark grey originally. The paint on the front leading edge of the flat bar had been worn away, and the underlying metal had rusted.

Parking Brake Operation Test

The parking brake on the W tractor was operated at idle. When throttling up the engine, the following characteristics were observed:

a) The flat bar tip in the first slot position at the leading tooth of the dog bar would not hold the brake pedal, and the parking brake would disengage immediately at idle;

b) The flat bar tip in the second slot position would not hold the brake pedal in locked position, when the engine was throttled up with a person sitting on the seat;

c) The brake held with the flat bar tip in the third slot position;

d) The brake pedal remained depressed, and the parking brake remained fully engaged while the flat bar tip was in the fourth slot position of the dog bar, at idle and when the engine was throttled up.

During the interaction between the flat bar and the grooves, it could be seen that the shape of the upper portion of the dog bar at the first and second slots was rounded, rather than sharp. Furthermore, the depth of the grooves appeared insufficient to provide contact forces to reliably engage the brake pedal and hold it depressed.

Testing the W Tractor Roll under Local Conditions

The tractor transmission was set in neutral with the engine running, without the parking brake engaged, at the edge of the shed, as shown in **Figure 7**. With the rear tires on a projected line on the ground below the eaves, the tractor was witnessed creeping backward out of the shed into the driveway. The 3.5-meter-long tractor backed out, gradually increasing in speed, and exited the shed in about 15 seconds. Further tests demonstrated that creeping would occur even with the engine stopped and the transmission in neutral.

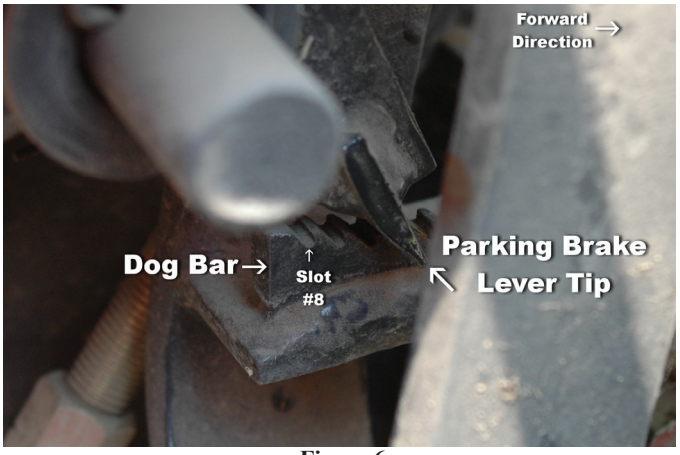

Figure 6
Dog bar and tip interaction.

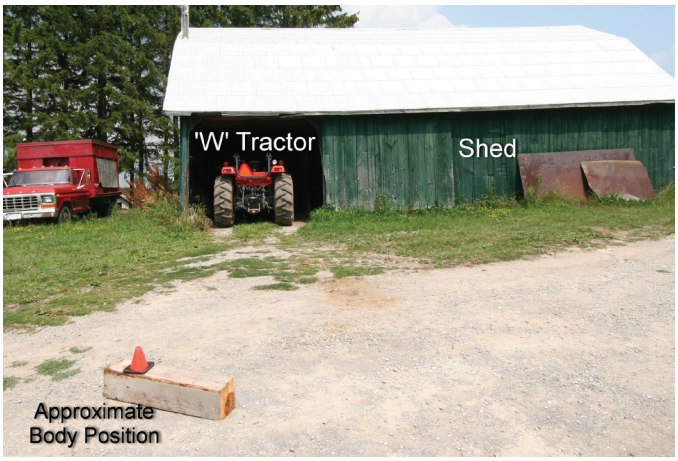

Figure 7
Position of the tractor for neutral drifting test.

The R Exemplar Tractor and Parking Brake

The authors compared notes with observations made on an identical model tractor of similar age owned by Mr. R, which had about 750 hours on its operating clock. The R tractor parking brake comprised the identical components. When tested, the brake handle remained engaged, even on the first slot of the leading edge of the dog bar. The parking brake could not be made to disengage, even when the engine was throttled up. It was tested in the R barn where it was parked.

Summary of First-Phase Findings

These results generated immediate concerns about the variation of performance between the parking brakes of these two tractors with identical model and similar manufacturing dates. The service hours could not account for the disengagement issue, since the newer one did not work — but the older one worked correctly.

The first two positions on the W tractor would not hold the parking brake engaged when parked with the transmission in neutral and the engine running. This would have presented an operating hazard, since an operator could move the hand lever, and may have falsely perceived that the parking brake was engaged when it was not.

Recalling that the tractor transmission was found after the incident in neutral (with the engine running), it was inferred to have been that way at the time of the incident. With the local slope conditions contributing to creep of the tractor backward, the tractor parking brake was either not engaged at the time of the incident involving Mr. W, or it was engaged and had become disengaged. The possibility of the latter provided the impetus to continue the second phase of the investigation.

Second-Phase Elements and Observations

Further detailed analysis of the involved components was warranted in order to reveal whether they fell within the specified range in the manufacturer's guidelines. The authors wrote to the manufacturer in January 2007, disclosing the potential issue with the parking brake and requesting that a detailed physical inspection be arranged.

A field inspection was proposed to be carried out in the presence of representatives of the tractor manufacturer and other parties. The inboard brake pedal and hand-release lever would be removed for detailed inspection by all parties. A further suggestion was that exemplar parts be obtained from stock — and that they be used to compare the surface geometry and slot morphology of the dog bar. The suggestions were accepted by the other parties.

The second inspection and testing of the tractor was arranged at the W farm in July 2007. The second phase incorporated the following elements:

- An inspection protocol was discussed prior to the activities, and proceeded after agreement on the suggested steps;
- The parking brake lever operation was demonstrated by AW;
- The tractor was placed in neutral with the engine running, and allowed to travel from the tool shed down the path to the fence;
- The tractor's brake system was tested by a manufacturer's technical service supervisor;
- The cover on the right side of the tractor was removed for closer inspection of the operation of the parking brake lever and pedal combination;
- The involved parking brake mechanism was removed from the W tractor; and
- The involved and exemplar components were retained in the author's secure evidence facility to maintain the chain of custody.

Total Station Survey of the Site

A Total Station Survey of the site identified the slope at the south entrance to the tool shed, where the tractor had allegedly been prior to the collision, as between 5.6% and 6.1% downward to the west. The slopes were independently confirmed as being between 6% and 10% with a 24-inch-long (60-cm-long) smart level.

Brake System Component Observations

The tractor's brakes were properly adjusted and functioned correctly, according to the technical service representative who test drove the tractor around the site. The range of free movement of the brake pedals was about 50 mm (2 inches), and another expert report cited 36 mm as the norm, although the workshop manual contains a value of 40 to 45 mm. The range of movement is shown in **Figure 8** and **Figure 9**. The parking brake adjustment turnbuckle had not been altered by servicing since the incident.

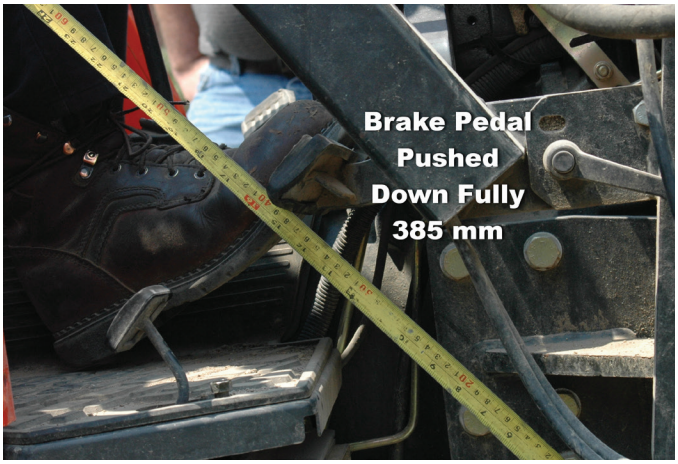

Figure 8
Brake pedal pushed down fully.

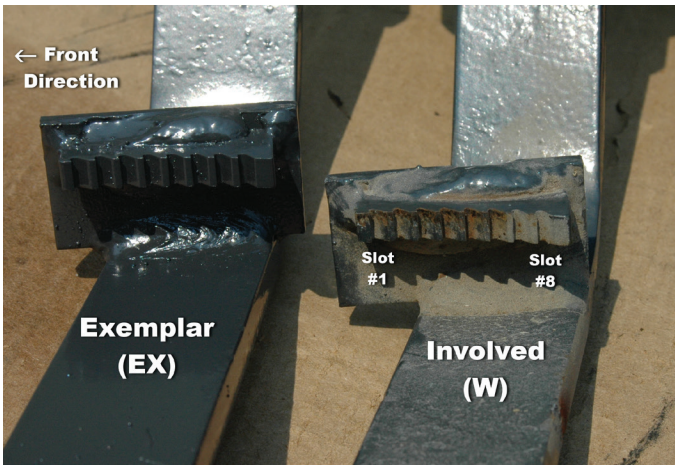

Figure 10
Exemplar (EX) and involved (W) dog bars.

The exemplar and the W (hence forward referred to as "EX" and "W," respectively) brake pedal dog bar welded positions were visibly different (**Figure 10**), when the front edge of the brake pedal was used as a reference point. On the W dog bar, the wear pattern was concentrated on one side — and on the first six teeth only — as shown in **Figure 11**.

As shown in **Figures 12** and **13**, there was a trapezoidal shape of the wear pattern to the paint on the W parking brake lever tip, while on the obverse the paint coating was missing on the W lever tip, covering about three quarters of the width to a depth of 1.5 mm. The uneven wear pattern seen in **Figures 12** and **13** at the tip was suggestive of a lateral offset between the tip and the teeth, matching the uneven pattern as seen in **Figure 11**, possibly indicating incorrect fit.

The uneven wear pattern seen at the tip was suggestive of a lateral offset between the tip and the teeth of the dog bar, as seen in **Figure 10**.

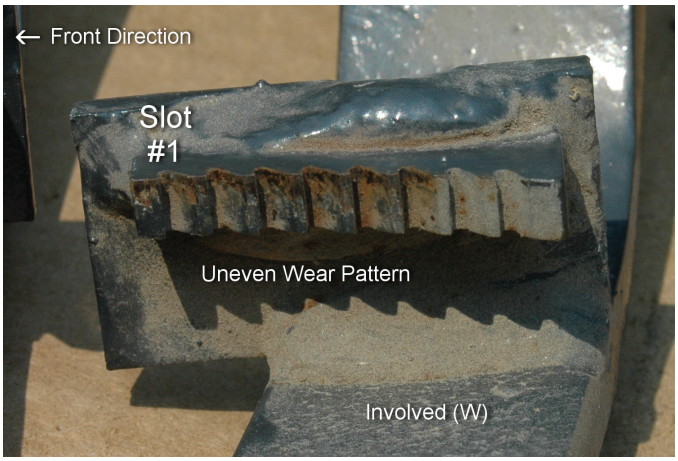

Figure 11
The wear pattern on the involved dog bar was uneven.

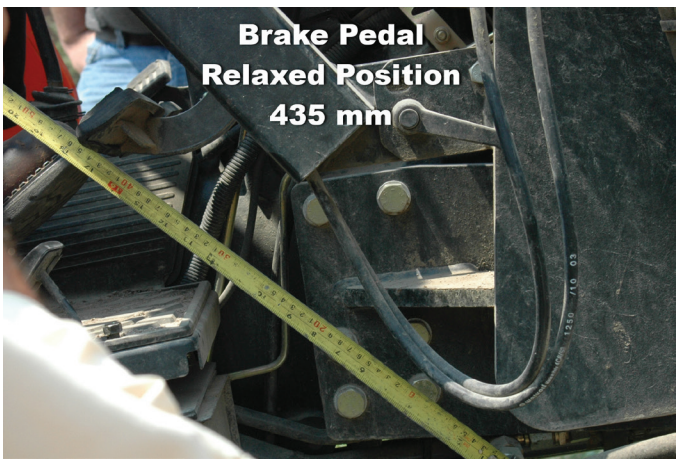

Figure 9
Brake pedal in relaxed position.

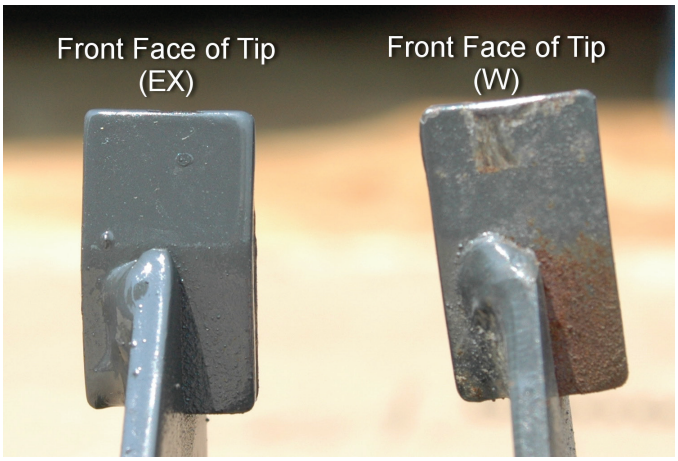

Figure 12
Front faces of the tips of the exemplar (EX) and involved (W).

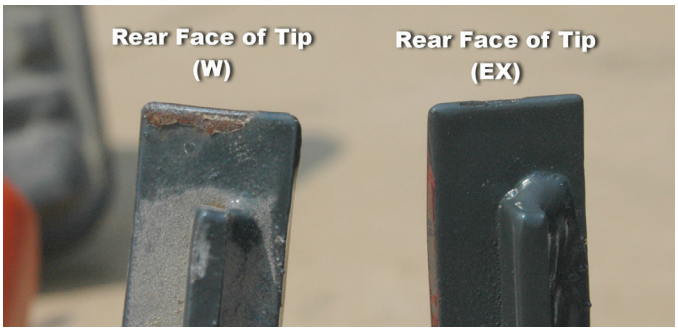

Figure 13
Rear faces of the tips.

Demonstration of Disengagement of the Lever

During the second inspection, the operation was tested in front of the assembled group. The videograph* of the operation of the parking brake lever and dog bar combination demonstrated that the lever would not stay safely engaged in the first three slots, which confirmed the findings of the first parking brake operation test.

Third-Phase Elements and Observations

The third phase of the investigation was designed to gather specific characteristics of the components, and included:

- Laser scanning of the exemplar and involved components at a specialty contractor;

- Analyzing the resulting data with modelling software to determine relevant similarities and differences; and

- Presenting the data and comparisons in 2-D and 3-D formats.

Geometric Evaluation of Involved and Exemplar Assemblies

The forensic engineers evaluated the geometric issues associated with the brake assembly. Two assemblies were made available — one specimen from the involved W tractor and the exemplar from the manufacturer's stock (EX). The assembly consisted of two parts: 1) brake-lever with the integrated chisel-like flat bar and 2) a brake-arm with an integral foot pedal and a slotted teeth set machined out of a block (dog bar). Both parts were designed to rotate about different axes of rotation. The flat bar tip was designed to engage the separate teeth of the dog bar in eight successive positions.

Tooth-Profile Examination

The tooth profiles of the dog bar(s) were assessed for differences. Close-up digital SLR photographs of each profile were performed using a 50-mm macro lens (**Figure 14**). In Adobe Photoshop, the photographs were superimposed by overlaying a transparency of EX over top of W — the EX profile was uniformly scaled until both EX and W dog bar lengths were equal. The profiles were subjectively assessed and found to be identical.

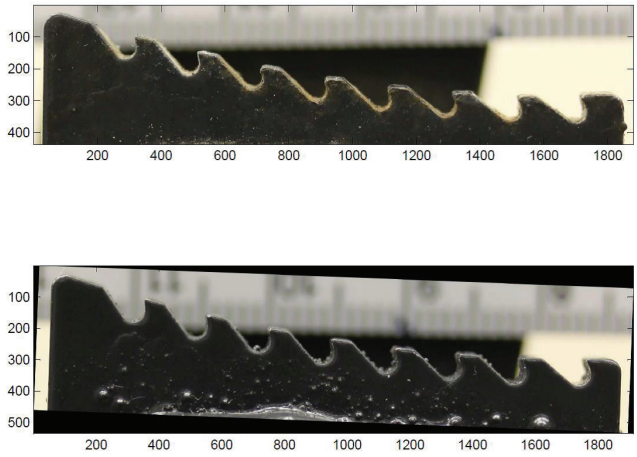

Figure 14
Tooth profiles for W (top) and EX (bottom) dog bars.

3-D Scans and Model Development in Rhino Software

The local service provider performed 3-D scans (high-resolution 175 microns, lower resolution 520 microns) of both EX and W brake-arm specimens using a laser scanner. The 3-D data of these scans were supplied in IGES format.

Rhino 3D software (v3.0, Robert McNeal & Associates) was used under license to create 3-D models of the brake-lever and brake-arm parts. Using the 3-D scans, the solid IGES brake-arm parts were imported into a 3-D workspace. Blueprints (scaled engineering drawings disclosed in the affidavit of documents of the manufacturer) of the brake-lever and brake-arm components were transferred to digital format. As scans were only performed on the brake-arm parts, the blueprints were used to create a 3-D model of the brake-lever in Rhino. From the blueprint, the relative position of the two rotation axes was calculated to accurately place the two parts in 3-D space.

Three brake assemblies were then constructed in Rhino to geometrically analyze brake engagement and sub-assembly (dog bar) placement: EX (exemplar); W (involved); and Y (blueprint).

* A videograph is the physical record made by a video device that describes movement captured in a scene over time. It is derived from Latin videre "to see" and Greek grapho "to describe."

Brake Engagement Assessment

For each of the three brake assemblies, 2-D flat-bar tooth engagement was quantified for the eight different gear engagement positions. The amount of tooth engagement (i.e., locking) was related to both the relative positions and orientations of the flat bar and dog bar. Eight locking positions were made possible by the eight slots in the dog bar. For example, Position 1 for EX is shown in **Figure 15**.

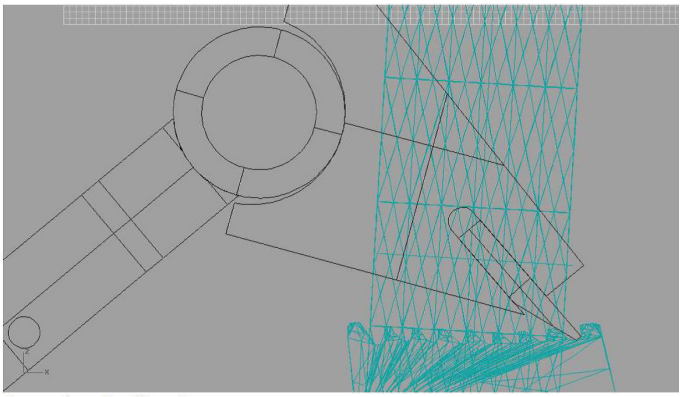

Figure 15
Position 1 for EX in two dimensions.

Comparison of Tooth Contact Depth and Tooth Contact Angle at Brake Lever Positions							
	Blueprint (Y); Involved (W); Exemplar (EX)						
	Tooth Contact-Depth mm				Tooth Contact Angle		
Position	Y	EX	Delta mm	Position	Y	EX	Delta degrees
1	1.4	1.8	-0.4	1	9.7	29.5	-19.8
2	1.2	1.2	0.0	2	9.6	28.6	-19.0
3	1.3	1.1	0.2	3	9.2	29.8	-20.5
4	1.4	1.1	0.3	4	7.8	30.7	-22.9
5	1.5	1.4	0.1	5	8.5	23.9	-15.4
6	1.5	1.3	0.2	6	8.2	31.3	-23.0
7	1.4	1.2	0.1	7	8.0	33.7	-25.7
8	1.3	2.2	-0.8	8	7.7	22.0	-14.3
mean	1.4	1.4	0.0	mean	8.6	28.7	-20.1
std dev	0.1	0.4	0.4	std dev	0.8	3.9	3.9
Position	Y	W	Delta mm	Position	Y	W	Delta degrees
1	1.4	1.5	-0.2	1	9.7	30.5	-20.8
2	1.2	1.2	0.0	2	9.6	29.8	-20.2
3	1.3	1.0	0.3	3	9.2	32.7	-23.5
4	1.4	0.7	0.8	4	7.8	30.4	-22.5
5	1.5	1.2	0.3	5	8.5	25.5	-17.0
6	1.5	1.0	0.5	6	8.2	31.6	-23.4
7	1.4	1.0	0.4	7	8.0	33.3	-25.3
8	1.3	1.9	-0.6	8	7.7	23.3	-15.6
mean	1.4	1.2	0.2	mean	8.6	29.6	-21.0
std dev	0.1	0.4	0.4	std dev	0.8	3.5	3.3
Position	EX	W	Delta mm	Position	EX	W	Delta degrees
1	1.8	1.5	0.2	1	29.5	30.5	-0.9
2	1.2	1.2	0.0	2	28.6	29.8	-1.2
3	1.1	1.0	0.1	3	29.8	32.7	-2.9
4	1.1	0.7	0.4	4	30.7	30.4	0.4
5	1.4	1.2	0.2	5	23.9	25.5	-1.6
6	1.3	1.0	0.3	6	31.3	31.6	-0.4
7	1.2	1.0	0.2	7	33.7	33.3	0.4
8	2.2	1.9	0.3	8	22.0	23.3	-1.4
mean	1.4	1.2	0.2	mean	28.7	29.6	-1.0
std dev	0.4	0.4	0.1	std dev	3.9	3.5	1.1

Figure 16
Comparison of tooth contact depth and contact angle for Y, W, and EX.

Two measures of tooth engagement were established to indicate the amount of potential interference contributing to locking: the angle between the flat bar top surface and the dog bar slot top surface and the engagement depth between the tip of the flat bar tooth and the top surface of the dog bar. These measures were calculated for all three assemblies in all eight positions (**Figure 16** and **Figure 17**).

Comparison of Relative Positions and Angles of the Brake Lever Sub-Assemblies					
Blueprint (Y); Involved (W); Exemplar (EX)					
W to Y	value	units	EX to Y	value	units
offset	6.3	mm	offset	4.2	mm
rotation (side)	1.8	deg	rotation (side)	0.2	deg
rotation (top)	2.6	deg	rotation (top)	0.4	deg
rotation (front)	5.8	deg	rotation (front)	0.2	deg

Figure 17
Comparison of relative positions and angles for Y, W, and EX.

3-D Dog Bar Position Comparison and Assessment

The relative positions of the dog bar with respect to the blueprint position and orientation were computed in both side- and top-planes. The accompanying **Figures 18** through **23** for Y, EX, and W depict the positions in 2D snapshots — a more convenient form for viewing. The 3-D versions were distributed on a DVD included with report to counsel, and could be opened with the accompanying MYRIAD viewing software.

Analysis

The data scans of the components were compared and contrasted in the plane of action in 2-D and 3-D space.

When compared in three dimensions, using a common reference origin with respect to the blueprint dog bar orientation and dimensions, it was determined that W dog bar had an offset of 6.3 mm, and rotation of its side, top and front by 1.8, 2.6 and 5.8 degrees, respectively. The

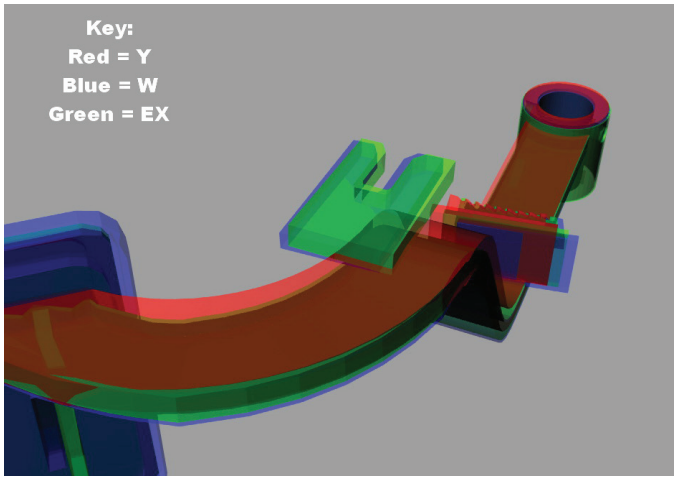

Figure 18
3D color overlay comparison #1.

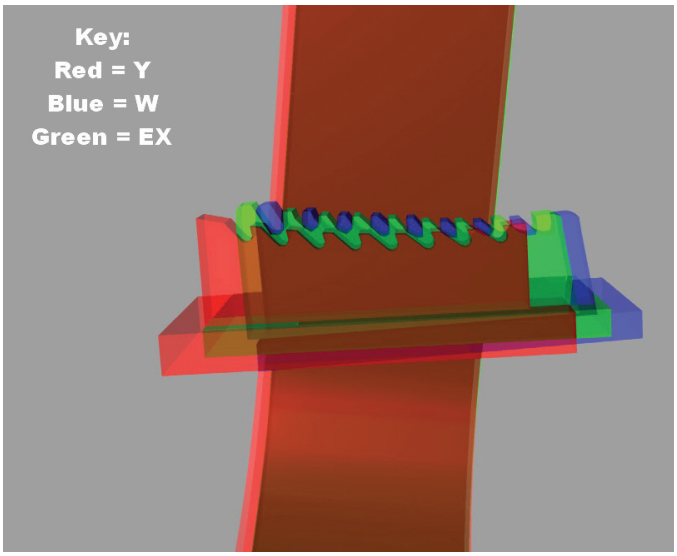

Figure 19
3D color overlay comparison #2.

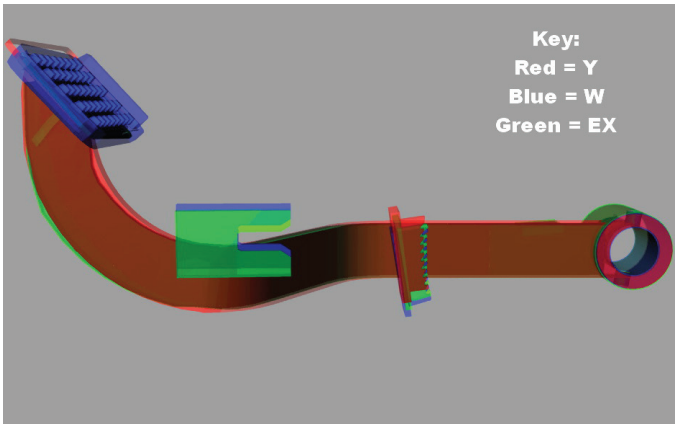

Figure 20
3D color overlay comparison #3.

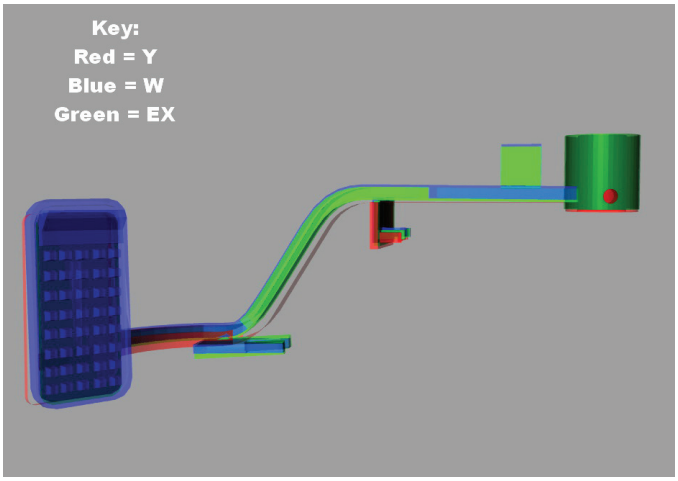

Figure 21
3D color overlay comparison #4.

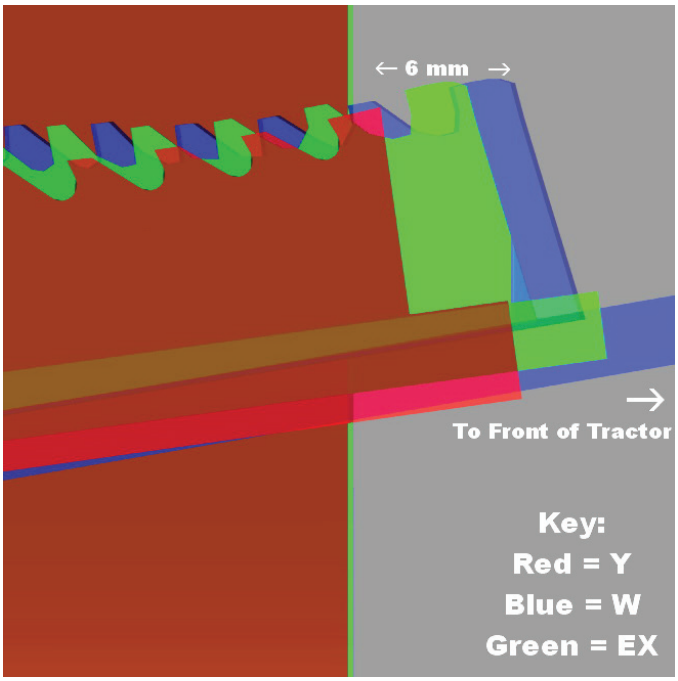

Figure 22
3D color overlay comparison #5.

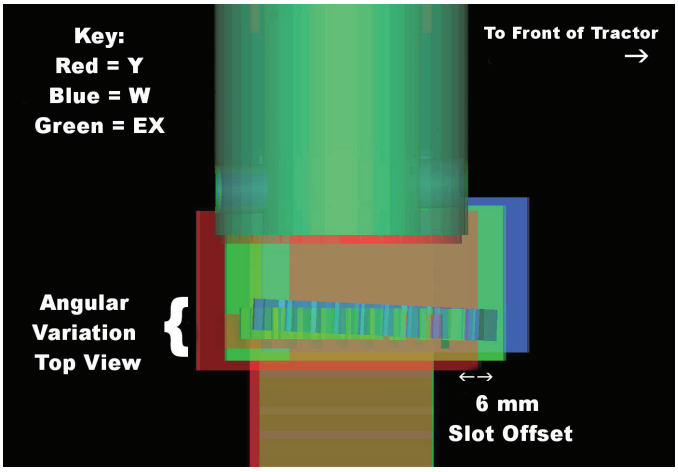

Figure 23
3D color overlay comparison #6.

EX dog bar had an offset of 4.2 mm, and rotation of its side, top and front by 0.2, 0.4, and 0.2 degrees, respectively.

When the three are set at the common center of rotation and overlaid in color (red for Y, blue for W, and green for EX), the positions and orientations are very different, as depicted in **Figure 22** and **Figure 23**. The blue portion lies at an angle to the red, and at the forward edge, the separation between the supposed position of the first tooth on Y and that of the W is about 6 mm (about $^{1}/_{4}$ inch). This offset is 133% of the 4.5-mm slot center-to-center

distance on the dog bar toward the front of the tractor.

In summary, the tooth contact-angle was much smaller for the blueprint (Y) than both EX and W. The tooth contact-depth was slightly larger and more consistent across all positions for Y than found in both EX and the W parts. These characteristics indicated that for the manufactured parts the amount of engagement varies significantly across all eight positions. Parking brake locking was less consistent than that shown on the blueprint.

Discussion

Tractor Starting and Final Positions

The starting position of the tractor was assumed to be within the tool shed, at the south edge of the door, with its engine running and the transmission in neutral. The tractor could not have been driven backward and down the hill to its final position 60 meters away. If the engine had been off at the time of the incident, it would not have restarted on the way down the hill. In police photographs, the parking brake lever was in the relaxed state on the tractor at the position of rest.

Contact Mismatch Between Dog Bar Tooth and Flat Bar Tip

The software models and part imaging showed that there were measurable differences between the master blueprint directing production of the parts on one hand and the unused exemplar and the involved component on the other.

In a 2-D analysis, which did not take into account out-of-plane orientation, the differences appeared to be minor. In a 3-D analysis, which did account for out-of-plane orientation, the variations would change the interaction between the dog bar and the slot bar edge because the dog bars lay in different positions on the expected arc of travel of the brake pedal. The slot bar edge tip should have met and engaged each of the eight teeth independently and firmly, transferring the force from the return spring through the dog bar against the slot bar of the handle.

The tip-to-tooth engagement went from a defined area (the width of the tip times its thickness held against the inner surface of a tooth in the dog bar) to a fraction of this area because the faces of the tooth and tip were no longer parallel.

The angular variations affected the interaction of the edge of the bar and the tooth, in particular at positions 1, 2, and 3 of the W, which were displaced forward by 6 mm. The intersection of the arc of travel of the lever tip and the dog bar no longer lay at the expected location in space after assembly, as shown in **Figure 24**.

The direct observations during the first phase provided the impetus for the detailed investigation; to wit, that the parking brake lever edge would not catch in the dog bar's teeth in the first two and possibly three positions on the W tractor, whereas it fit and held correctly on the neighbor's similar tractor.

Efforts were taken to explain the different behavior, by evaluating brake setting, parking brake adjustment, and field performance of the brakes during a dynamic test during the second instance of examination. No performance variations from the specified parameters for the brake system were noted except for the parking brake lever disengagement as captured in the videographs.

More detailed scrutiny of the components in the third stage, using (newly) available laser-scanning technology was judged to be the most effective route to quantify the existence of variations between the drawings for making the parts (the blueprint, Y) and the two components (EX and W).

The 6 mm ($^1/_4$ inch) displacement and relative rotation of the W components accounted for the change of behavior noted during the first and second phases of the investigation, in which the slot bar edge tip would not remain within the teeth of the dog bar. As mentioned, this distance was 133% of the slot center-to-center distance on the dog bar — a misalignment of more than one tooth.

Specifically, this safety component — the parking brake — had been intended to lock with the lever tip in each and every tooth of the dog bar, per the service

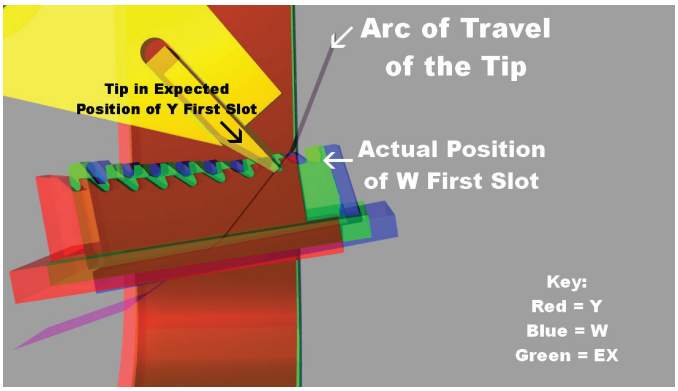

Figure 24
Expected and actual positions of the tip at dog bar first slot.

instructions. In the small tractor's Workshop Manual, under the heading "Parking Brake Lever Free Play," it states, "Pull the parking brake one notch and make sure the parking brake shaft is activated." The parking brake lever did not lock in the first notch on the W tractor.

The positional variations were found in an area of critical safety to the operator of the tractor, and for which he would rely intuitively to function each and every time it was deployed.

The parking brake malfunction was a plausible root cause of the fatal farm tractor incident, given the reported circumstances. The tractor began moving away from the shed, and the incident was consistent with Mr. W falling beneath the bale spear attachment. This explanation of the sequence of events was accepted by Mr. AW.

Conclusions

The proven hypothesis was that, due to the welded orientation of the W dog bar on the pedal, the first, and second slots could not have met the lever edge tip, and therefore could not have acted to distribute the load across sufficient area to develop the required binding force. On the third slot, the binding force was shown to be inadequate to secure the engagement during local vibration caused by the running engine. This had the potential to allow a sudden unexpected release of the parking brake lever, which would disengage the brake.

The comparison illustration set in color, highlights the difference when the parts (red = Y; blue = W; green = EX) are placed in a common reference orientation.

These variations formed the basis of a reasonable explanation for the symptoms observed in the first instance, as well as reported by AW when he had operated the tractor on several prior occasions, when the lever tip failed to stay engaged in the dog bar on the W tractor. The author's analysis showed that the mating position of the first slot lay beyond the circle of contact for the lever bar tip, such that it could have never correctly met and sat within the first tooth.

Given that the design appears intended to facilitate reliable engagement between the lever edge tip and all slots of the dog bar, the fact that the subject parts did not adequately engage in three of the eight positions reveals that there were design and/or manufacturing errors that could foreseeably have led to unreliable engagement of the parking brake. The subject parts were undamaged compared to new condition, did not have appreciable amounts of wear on the contacting surfaces (see **Figures 10** to **13**), and had been maintained by the owner.

Acknowledgements

The author is pleased to acknowledge the substantial detailed analysis performed by Dr. Alan R. Morris, PEng on the 3D software programs, the assistance of Mr. Adam L. King during the field operations and measurement process, and Dr. Taian Chen during the model development.

Engineering Analysis of Cost to Protect Workers from Diacetyl Exposure and the Economic Benefit of Noncompliance

By Drew Peake, PE (NAFE 460F) and Greg Haitz

Abstract

Large commercial bakeries use artificial butter flavor (containing diacetyl) in its recipes, and have for more than 40 years. In 2012, a health-based exposure threshold was published for diacetyl by the American Conference of Governmental Industrial Hygienists (ACGIH). Bakery managers typically knew what was necessary to protect workers from exposure. However, for a variety of reasons, most did little to control exposure: The Food and Drug Administration said diacetyl was generally recognized as safe; substitute products had not been demonstrated as less harmful; and no regulatory standard had been established. This study develops the costs that would have been necessary to protect workers, using the U.S. EPA model (known as BEN) to calculate the economic benefit of noncompliance, and offers a characterization of the profit incentive to place workers at risk.

Keywords

Diacetyl, butter, bakery, noncompliance, bronchiolitis obliterans, respirators, ventilation, capital expense, return on investment, BEN, PEL, REL, TLV, STEL, forensic engineering

Introduction

Diacetyl (IUPAC* name butanedione or butane-2,3-dione) is a natural component of butter that can be artificially manufactured. Used in flavorings to add butter taste to popcorn, bakery products, and other consumer goods, it can also be found in coffee, beer, cigarettes, and other common consumer items. It has been shown to cause harm to workers who inhale diacetyl. In 2016, the National Institute of Occupational Safety and Health (NIOSH) published a Recommended Exposure Limit (REL)[1]. As of this writing, the Occupational Safety and Health Administration (OSHA) has not finalized a Permissible Exposure Limit (PEL). Litigation is not the topic of this paper. Instead, information learned will be used to develop what a company could have done, how much that would have cost, and (using one of U.S. Environmental Protection Agency's financial models, specifically BEN) calculate the economic benefit derived by not implementing controls.

While not a topic of this paper, the financial measures discussed may prompt other researchers to examine the ethical dilemma managers face when dealing with seemingly competing obligations to workers and owners.

The Hazard

In 1985, NIOSH published the results/conclusions of an investigation regarding two bakers who developed symptoms[2] suggestive of bronchiolitis obliterans (BO) disease. The report stated: "None of the chemical ingredients used in the mixes are known causes of bronchiolitis obliterans or emphysema"[2]. Diacetyl was used as an ingredient at that bakery; however, no specific etiology of the workers' disease was identified[2].

Popcorn plants came under scrutiny first, and much was learned about how to reduce exposure using engineering controls, administrative controls, and personal protective equipment. In 2000, employees at Gilster-Mary Lee popcorn plant in Jasper, Missouri became sick with a disease that was subsequently identified as BO, prompting the term "popcorn lung." As a result, the Missouri Department of Health and Senior Services requested a Health Hazard Assessment (HHA) in 2000 by NIOSH at the Gilster-Mary Lee plant[3]. While it took only a few months for NIOSH to begin work, it did not publish the

Drew Peake, PE, PO Box 669834, Marietta, GA 30066, dpeake@peakeeng.com

* International Union of Pure and Applied Chemistry (https://iupac.org/)

HHA until completing the study in 2006. The NIOSH HHA sampled for diacetyl in the air at numerous popcorn plants. Subsequently, they found that workers with obstructive lung disease had been exposed to 3.3 times the national average workplace exposure to diacetyl. In 2000, NIOSH recommended a series of controls, including engineering controls, administrative controls, and personal protection equipment, that by 2006 (based on additional air monitoring) had significantly reduced exposure from butter flavor. While diacetyl was sampled, it was not identified as a chemical of concern in 2006.

In 2004, NIOSH published and widely distributed "ALERT: Preventing Lung Disease in Workers Who Use or Make Flavorings"[4]. NIOSH recommended:

1. Engineering controls:

a. Pollution prevention through substitution[¥].

b. Cover open containers of flavors and ingredients.

c. Use local and general ventilation to remove vapors from the workplace.

d. Isolate high-exposure process from the workers, and keep those spaces under negative pressure.

e. Maintain the temperature as low as practicable for the process.

2. Administrative controls:

a. Develop work practices and ensure compliance to limit vapor and dust emissions.

b. Monitor air concentrations and track progress to lowest level possible.

c. Keep Material Safety Data Sheets (MSDSs) up to date, and make sure containers are properly labeled.

d. Train employees regarding the potential hazards and how to protect themselves.

e. Use medical monitoring to evaluate employees when they are hired and follow up with routine monitoring to track employee health.

3. Personal protective equipment (PPE):

a. Provide respiratory protection when there is risk of exposure[£].

b. Provide other PPE such as gloves, masks, and goggles when there is risk of dermal exposure.

Soon thereafter, flavor manufacturers, especially those making butter flavor, became an industry of concern. In 2008, the International Brotherhood of Teamsters requested NIOSH perform a Health Hazard Evaluation (HHE)[¤] at a flavor manufacturing plant in Indiana because of its concern about flavor manufacturing, especially butter flavor. At that plant, the NIOSH HHE[5] found 3.8 times the number of workers with restricted lung function based on the most recent spirometry tests when compared to the general population of the United States. Again, engineering controls, administrative controls, and personal protective equipment were recommended to reduce exposure.

In response to a confidential employee request in 2005, NIOSH performed an HHE at a commercial bakery in Sacramento, California[6]. There was concern about skin rashes, dermatitis, coughing, and eye irritation. One employee had been diagnosed with Bakers' Asthma. Workers were exposed to flour dust and other allergens; some were exposed to more than the ACGIH threshold limit value (TLV[§]) for inhalable flour dust. The Occupational Safety and Health Administration (OSHA) did not specify a permissible exposure limit (PEL), nor did NIOSH specify a recommended exposure limit (REL) for flour dust. However, the OSHA limit for particulate not otherwise classified (PNOC) and the NIOSH REL for grain dust were both exceeded. Recommendations to control exposure were like those offered for control of diacetyl: engineering controls, administrative controls, and personal protective equipment. Note that the test for health effects from exposure to both diacetyl and flour dust is the same spirometry evaluation of lung capacity.

[¥] The health effects of known substitutes were not known. Caution was recommended because the state of science was such that these were unknowable at the time.

[£] Because there was no health-based threshold for safe exposure in 2006, proper respiratory protection could not be determined.

[¤] Health Hazard Evaluation (HHE) and Health Hazard Assessment (HHA) are terms with subtle differences that are not relevant for this discussion.

[§] A TLV is that concentration expected to be safe for workers to be exposed for an 8-hour work day and 40-hour work week. A PEL is a regulatory standard that is not be exceeded. The REL is a recommendation that is expected to keep workers safe over the workday and workweek.

Health-Based Standards

The Food and Drug Administration evaluated diacetyl in 1980, and determined that it was Generally Recognized as Safe (GRAS)[7]. The report evaluated ingestion as the route of exposure. Based on this federal regulation and the business confidential nature of flavor formulas, diacetyl was not normally listed as an ingredient on Material Safety Data Sheets (MSDSs). Therefore, this gave manufacturers and users of diacetyl a scientifically based reason to think this chemical was safe.

When a link was established between BO and butter flavor, industry, regulatory agencies, and scientific organizations rushed to establish a safe exposure concentration. Efforts by ACGIH, OSHA, and NIOSH are briefly discussed below. NIOSH is basically a research organization, and OSHA often accepts the REL for the PEL.

The ACGIH is a non-profit scientific organization that publishes TLVs as guidance. Since the ACGIH is not a regulatory agency, it can set "standards" more quickly, though ACGIH is also not a formal voluntary consensus standards developer. ACGIH uses a diverse committee of about 25 scientists who develop a list of chemicals under study. Each February 1, that list is published in two tiers: Tier 1 are chemicals likely to progress through standard development; Tier 2 chemicals are those not likely to progress. One or more of the committee members reviews the available literature focusing on concentrations that are at or near the "no effect" level, including a suggested TLV. This literature review is further reviewed by more members of the committee. When they reach a consensus, the review is presented to the full committee. Then it is presented to the Board of Directors. If approved, it is published as a Notice of Intended Change (NIC) on a subsequent February 1. The review period is strictly limited to four months, and ends on May 31. Absent substantial additional information, it is published along with the adopted documentation the following year. Diacetyl was published as a NIC in 2011. In 2012, a TLV for diacetyl was adopted and set at 0.01 ppm (0.04 mg/m^3)[8]. ACGIH also set a Short-Term Exposure Limit[$] (STEL) at 0.02 ppm (0.07 mg/m^3).

Perhaps due to political pressure, OSHA moved to regulate prior to NIOSH completing its work on diacetyl. On January 21, 2009, OSHA published an Advanced Notice of Proposed Rulemaking[9], setting a threshold for safe exposure. It was withdrawn three months later[10], when it was decided scientific peer review was necessary. It is interesting this was withdrawn before the comment period ended on April 21, 2009. In October 2009, OSHA initiated peer review of health effects and risk assessment. OSHA has not set a PEL for diacetyl to date. A NIOSH REL for diacetyl was not published until October 2016[1].

Unless and until there is a regulatory standard (PEL), the only enforcement action available to OSHA is the General Duty Clause of the Occupational Safety and Health Act, which reads:

"Each employer shall furnish to each of his employees employment and a place of employment which are free from recognized hazards that are causing or are likely to cause death or serious physical harm to his employees."[11]

This law charged the Administrator of the Occupational Safety and Health Administration with the authority and responsibility to enforce violations of this general duty in cases where a specific standard was not established.

Commercial Bakery

A particular large commercial bakery used flavors on two product lines to manufacture refrigerated dough. Some of the flavors contained diacetyl in varying concentrations, ranging from 0.002% to as high as 11%. The flavorings represented a very small amount in each product. Very little of the diacetyl-containing butter flavoring was mixed with the flavor mix, which made up a small portion of the dough. The amount of diacetyl in the final dough mix was on the order of 9.5 x 10^{-6} pound diacetyl/pound of dough.

As demonstrated by Dr. Rigler[12], diacetyl evaporates from any particular butter flavoring. Henry's Law shows that evaporation varies directly with temperature. Diacetyl emissions were reduced by cooler temperature in this refrigerated dough plant. Nonetheless, workers at this bakery were exposed and reported health consequences as a result.

Estimated Cost to Protect Workers

The necessary controls were well defined through the NIOSH publications cited above. They have been incorporated to reflect a typical large commercial bakery for the purposes of calculations in this paper. These companies are large, with average sales per plant of $12,857,153[13]. A large commercial bakery is defined as having more than 100 employees.

[$] A STEL is not to be exceeded for more than 15 minutes.

Cost of controls for this analysis were drawn from a report from Eastern Research Group (ERG) commissioned by OSHA in anticipation of regulatory action setting a PEL for diacetyl[14]. The author has calculated cost of controls numerous times, and the costs presented in the report are reasonable — however dated[15] – and sufficient for demonstrating the BEN model discussed later.

Following the link in the citation[14], the ERG report is available at www.regulations.gov. This website is a significantly expanded resource that makes available background and supporting documents for government regulations. The ERG Report has completed significant internal review by OSHA. However, it is marked "Draft Final Report" and cautions "Do Not Quote or Cite." The author understands OSHA does not intend to finalize this report. As briefly discussed above, OSHA has not published health-based thresholds for diacetyl. Supporting documentation for the NIOSH proposed recommended exposure level is, in the author's opinion, flawed. That may be a topic for another paper, but it is not within the scope of this paper.

Costs will be presented in the three control classifications: engineering controls, administrative controls, and personal protective equipment. Engineering controls include local exhaust and general ventilation and isolating equipment or processes.

Engineering Controls

Engineering controls are itemized in **Figures 1** and **2. Figure 1** includes a line item with equivalent annual costs (EAC) for all engineering controls. EAC is calculated using the following formula:

Some of the controls listed in the ERG Report were not included in the Figures. For example, converting mixers to mechanical systems had long since been completed for operational efficiency in most commercial bakeries. Therefore, it is not considered a cost of compliance.

$$EAC = \frac{NPV}{A}$$

Where; NPV = net present value

$$A = \frac{1 - \left[\frac{1}{(1+r)^t}\right]}{r}$$

Where; r = cost annualized at 7%

t = economic life

$A_{7\%,10y} = 7.02$

$A_{7\%,5y} = 4.10$

The additional equipment costs are process changes implemented to improve production, not control costs. Therefore, they are not included in the BEN analysis. They are included here for information and completeness.

Administrative Controls

For this discussion, administrative controls are used when engineering controls are not fully protective of workers. If the combination of engineering and administrative controls does not provide a sufficient margin of safety, personal protective equipment (PPE) is necessary.

The regulation envisioned by ERG as it prepared this report was developed through direct conversations with OSHA staff and review of an October 2007 internal draft of the proposed regulations of the final rule. These administrative controls included: exposure monitoring, medical surveillance, training, delineation of regulated areas, and an exposure control plan.

ERG developed annualized unit costs for each administrative requirement. These are identified in the Figures. Admittedly, some of the detail seems low. Data from 2006[16] and 2007[17, 18] were the basis for outdated wage and benefits ratios.

Exposure Monitoring

The draft regulation required establishing a baseline for exposure by monitoring if 50 workers are at risk of exposure for diacetyl and acetoin. The individual costs for this sampling are detailed in **Figure 3**.

Medical Surveillance

The draft regulation specifies medical surveillance for each at-risk employee. This would include a complete work history and respiratory questionnaire followed by a medical exam with spirometry test pre-employment and every six months. These costs are tabulated in **Figure 4**.

Training

The draft regulation required training to familiarize workers with the diacetyl standard, employers' exposure control plan, and medical surveillance plans. The estimated costs are tabulated in **Figure 5**.

Regulated Areas

This requirement of the draft regulation seems overly restrictive. It specified delineating areas wherever "a source of emission or potential employee exposure to

diacetyl, acetoin, or food flavorings or fragrances containing diacetyl or acetoin is reasonably expected." Details anticipated by ERG are tabulated in **Figure 6.**

Exposure Control Plan

The exposure control plan combines the other program costs, details the engineering controls, and incorporates the personal protective equipment in one plan and management effort. Becoming familiar with the program, developing the program, and writing it down are one-time costs. Administering the program and revising the program for process changes are a continuing effort. These are tabulated in **Figure 7**.

Annualized Costs for Administrative Controls

Annualized costs for administrative control are tabulated and totaled in **Figure 8**.

Personal Protective Equipment

ERG recommended full-face air-purifying respirators

Item	Reference	Number	Cubic Feet/Minute	Cost/Element	Total CFM	Costs
Drum Measuring/Mix Station	NIOSH, 2007[a]	8	1,200	$20,400	9,600	$163,200
Ventilated Small Batch Mixing Station	NIOSH, 2007[a]	8	800	$13,600	6,400	$108,800
Moveable Exhaust Hood	VS-90-02	8	1,050	$17,850	8,400	$142,800
Total					24,400	$414,800
Makeup Air ($3/CFM)						$58,560
Ventilation Capital Costs						$473,360
Engineering Design Costs						$33,135
Total Capital Costs						$506,495
Hours of Operation Factor						75%
Operating Costs				$2.43/CFM		$44,469
Maintenance (10% of capital costs)						$37,987
EAC (r =7%, n = 10)						$153,072
Other EAC (r = 7%; n = 5 or 10)						$15,432
Total EAC						$168,504

Figure 1
Enhanced ventilation costs.

with both an organic vapor cartridge and a particulate filter. Although NIOSH recommended gloves and goggles[4], ACGIH later published documentation for a diacetyl TLV[8] in which they cited only one study that referenced dermal exposure, with the comment that there were conflicting reports. Respirator costs are tabulated in **Figure 9**. A cost summary is shown in **Figure 10.**

Economic Benefit of Noncompliance

One of EPA's financial analysis models is BEN[19], which calculates the economic benefit of noncompliance for the various laws EPA administers. Others are:

° ABEL, which evaluates a corporation's or partnership's ability to afford compliance costs, cleanup costs, or civil penalties;

° INDIPAY, which evaluates an individual's ability to afford compliance costs, cleanup costs or civil penalties;

° MUNIPAY, which evaluates a municipality's or regional utility's ability to afford compliance costs, cleanup costs or civil penalties; and,

° PROJECT, which calculates the full cost to a

Other Control Equipment	Description	Equipment Cost	Operating Cost	Number of Units	Equipment Life	Capital Cost	Specifications
Covered Bucket	Stainless Steel Buckets	$110	$11	8	5	$880	13-quart Bucket and Lid
Tank Covers Small	Stainless Steel Cover for Tank, Custom Designed	$500	$50	8	5	$4,000	Approximate Costs Smaller Tanks
Tank covers Large	Stainless Steel Cover for Tank, Custom Designed	$2,000	$200	8	5	$16,000	Approximate Cost Larger Tanks
Spill Clean-up Kits	Spill Control Station	$350	$35	4	5	$1400	Quoted Price Suppler
Separate Mixing Rooms	1,000 ft^2 of 10 x 10 ft. wall and Industrial Door	$6,790	$679	4	10	$27,160	$4.89/$ft^2$ and $1,900/door
Reduce Water Pressure in Some Cleaning	Purchase Water Pressure Limiting Devices	$12	Negligible	8	5	$96	
Dopak® Closed Vent Sampler	3-Way Valve	$1,200	$120	4	10	$4,800	Needle Assembly and Valve

Figure 2
Additional equipment costs.

Item	Unit Costs	Detail
IH fees/8-hour PBZ[i] sample	$250.00	Consulting IH Technician, Daily rate $500
Lab Fees	$90.00	Per Sample
Samples Per 8-hour shift	4	Each for diacetyl and acetoin
Fee for blank	$90.00	1 blank for each set of samples
Sub-total Cost per sample	**$1,060.00**	Costs for both diacetyl and acetoin
Workers per sample	4	
Samples/year/worker for process change	0.1	
Time Requirements		
Worker productivity lost while sample pump is attached (hours)	0.5	
Manager Time per sample (h)	0.25	
Unit Cost per 8-hour sample	$1,080.00	
Initial Monitoring/worker annualized[ii]	$38.00	
Monitoring for process changes/worker annualized[iii]	$108.00	
If half of 100 employees are at- risk the annualized cost are	**$1,015.00**	(50 workers * 25% * $38) + (5 workers * $108) = $1015 (N = 10 years)

Figure 3
Exposure monitoring costs.

[i] Personal Breathing Zone (PBZ)
[ii] The underlying assumption is that 25% of at-risk employees would be monitored initially.
[iii] This assumes that 10% of the at-risk employees would be monitored each year for process changes.

Item	Cost	Detail
Spirometry test	$100.00	
Checkup	$80.00	
Medical History	0.75	Hours; first year only
Worker Time for test	1.00	Hours
Recordkeeping	0.25	Hours per worker tested
Initial exam per person	$222.70	
Subsequent exam per worker	$207.13	
Frequency (months)	6	
Annual Cost/worker	$416.33	
Average turn per year	30.1%	Percent of total employment (Bureau of Labor Statistics 2007)
Annual cost per worker adjusted for turnover	$514.53	
All 50 At-risk employees annual cost	**$25,726.50**	N = 10 years

Figure 4
Medical surveillance costs.

defendant of a proposed supplemental project in lieu of civil penalties.

These other models can be used to argue against the results of a BEN analysis. If there is sufficient interest, these will be presented in a subsequent paper.

As described by EPA:

"The U.S. Environmental Protection Agency developed the BEN computer model to calculate the economic benefit a violator derives from delaying and/or avoiding compliance with environmental statutes. In general, EPA uses the model to assist its own staff in developing

Item	Cost	Detail
Class Size	4	Employees
Training Time per session	0.5	hours
Materials	$2.00	Per employee per session
Instructors	1	Per class
Record keeping	0.02	Hours per worker trained
Training Frequency	1	Per year
Costs per worker	$17.69	
Annual cost for 50 workers	**$884.50**	N = 10 years

Figure 5
Training costs.

Item	Cost	Detail
Identify and establish regulated areas	16	Hours
Costs for hazard marking	$500	
Recurring admin requirements	32	Hours
Annual costs	**$2,244.00**	N = 10 years

Figure 6
Regulated areas cost.

Item	Cost	Detail
Rule familiarization	1	Hour
Develop program	16	Hour
Written program	8	Hour
Administer program	32	Hour
Revisions for process changes	16	Hour
Annualized costs	**$2,503**	N = 10 years

Figure 7
Exposure control plan costs.

Item	Annualized Cost	Detail
Exposure Monitoring	$1,015.00	
Medical Surveillance	$25,726.50	
Training	$884.50	
Regulated Areas	$2,244.00	
Exposure Control Plan	$2,503.00	
Annualized Cost for Administrative Controls	**$32,373.00**	**Non-Depreciable**

Figure 8
Annualized cost for administrative control.

settlement penalty figures. (For trial or hearing, an expert in financial economics must present the analysis of economic benefit, using whatever analytical tools — possibly including BEN, or maybe instead customized computer spreadsheets — are appropriate to the case's particular compliance scenarios.)

Calculating economic benefit using the BEN model is generally the first step in developing a civil penalty figure under EPA's February 16, 1984, generic penalty policy. This two- part document was codified in the General Enforcement Policy Compendium as P.T. 1-1 and P.T. 1-2. Related medium-specific policies have been developed since then to implement the 1984 policy. The BEN model assists in fulfilling one of the main goals of the generic policy. That goal is that civil penalties should at least recover the economic benefit from noncompliance to ensure that members of the regulated community have a strong economic incentive to comply with environmental laws on time."[19]

For civil litigation, the documented financial benefits of this model could certainly help attorneys and judges

Item	Cost	Detail
Equipment Cost	$237.50	Full-face air purifying respirator
Equipment Service Life	2	Years
Annualized Equipment Cost	$131.36	
Accessory Cost	$278.00	Includes organic vapor cartridge and particulate filter
Accessory Service Life	1	Year
Annualized Accessory Cost	$278.00	
Total Annualized Cost	$409.36	Equipment only
Training hours	2	Hours
Training Frequencies	1	Yearly
Annualized Training Costs	$61.08	
Fit Test Costs	$80.63	
Fit Test Frequency	1	Yearly
Annualized Fit Test Costs	$80.63	
Respirator Cleaning	$86.50	Five minutes for cleaning, fifty times per year
Total Annual Costs (each)	**$637.57**	Per at-risk employee
Total Annual Costs	**$31,878.50**	50 at-risk employees

Figure 9
Personal protective equipment cost.

Item	Cost	Detail
Capital Cost[i]	**$506,495**	Depreciable
Annual Operating & Maintenance Cost for Ventilation[ii]	**$83,551**	Includes some operating cost
Annualized Administrative Controls	**$32.373**	Non-depreciable
Annualized PPE	**$31,879**	Non-depreciable

Figure 10
Cost summary.

[i] Capital costs are adjusted for inflation and listed in the BEN model as Capital Costs.
[ii] The sum of Annual Operating & Maintenance Costs for Ventilation, Annualized Administrative Controls, and Annualized PPE are listed in the BEN model as non-depreciable expenses.

determine what amount of compensatory damages should be rewarded.

"You can use BEN in all cases to measure benefit from delayed and/or avoided compliance, except for Clean Air Act Section 120 actions, which require the application of a Section 120 specific computer model. BEN can calculate economic benefit for many types of organizations: corporations, partnerships, sole proprietorships, not-for-profit organizations, municipalities, and so forth. BEN is easy to use, even for people with no background in financial economics. Because the program contains standard values for many of the variables needed to calculate economic benefit, BEN requires only a small number of user inputs. BEN also allows the user to modify all of its standard values." [19]

Using the BEN model with this example calculates the following outputs, as shown in the printouts of the BEN model in the **Appendix**, are:

• For the delayed compliance[δ] from the date compliance was required to the date of penalty calculation: $1,224,258.

• For avoiding compliance altogether: $1,526,535.

The Opportunity Gain from noncompliance could be distributed in three separate ways:

• Paid out in management bonuses.

• Increased dividends to stockholders.

• Invested in additional production & automation equipment.

In conjunction with the BEN model (to determine the economic benefit of putting workers at risk), it would seem appropriate to determine the At Fault Company's return on investment (ROI) and factor that value (Opportunity Gain) on the economic benefit received for ignoring or delaying worker safety and health concerns.

The assumption here is that the company would alternatively invest those dollars into production and automation equipment and expect their normal or the industry standard return. The hurdle rate, which is also known as minimum acceptable rate of return (MARR), is the minimum required rate of return or target rate that companies are expecting to receive on an investment.

The following scenario uses a MARR of 10.41%, compounded over seven years (expected life of the equipment) which would be a conservative expected return for this industry.

In reality, rate of return (ROR) can easily be two to three times this percentage amount. The actual ROR of a Company in question would need to be assessed through a thorough financial analysis of their internal investment calculation model, and its corresponding ROR goal.

ROI (return on investment) is a common measure of profitability.[20]

$$\text{ROI} = \frac{\text{investment gain - investment cost}}{\text{investment cost}} \times 100\%$$

Annualized ROR using exact dates is typically more meaningful. Converting from ROI to ROR is most easily accomplished using one of the web-based calculators (IT Professionals 2008). For example, assuming a doubling of money over seven years;

$$\text{ROI delayed} = \frac{\$2,448,516 - \$1,224,258}{\$1,224,258} \times 100\%$$

$$= 100\% \text{ over 7 yrs. yields an ROR} = 10.41\%$$

In this scenario, you could either present the $1,224,258 gain made as an additional economic benefit or use a 1.1041 multiplier, compounded over seven years, on the resulting BEN output.

$$\text{ROI avoided} = \frac{\$3,053,070 - \$1,526,535}{\$1,526,535} \times 100\%$$

$$= 100\% \text{ over 7 yrs. yields an ROR} = 10.41\%$$

In this scenario, you could either present the $1,526,535 gain made as an additional economic benefit or use a 1.1041 multiplier, compounded over seven years, on the resulting BEN output.

Assuming these funds were invested in production equipment and automation, it is reasonable to expect a return on investment at an ROR OF 10.41%, would double the economic benefit amount calculated by the BEN model.

Conclusion

It costs time and money to implement effective environmental controls. This should be considered overhead; a necessary expense of production. Of course, funding such controls diminishes profits that can be distributed to

[δ]Delayed compliance was calculated from 01 May 2011 (date regulations effective) to 01 July 2017 (date selected arbitrarily to demonstrate delayed compliance).

owners. This paper shows how to calculate the real economic benefit that can result from not fully protecting workers.

Broader applications of this methodology may be useful to quantify the egregiousness of a harm that should have been prevented, or as a measure of unreasonableness of proactive efforts. These economic models have been effective in negotiating resolution of non-compliance with environmental regulations. This is a service engineers can offer attorneys.

References

1. NIOSH (2016). Criteria for a recommended standard: occupational exposure to diacetyl and 2,3-pentanedione. By McKernan LT, Niemeier RT, Kreiss K, Hubbs A, Park R, Dankovic D, Dunn KH, Parker J, Fedan K, Streicher R, Fedan J, Garcia A, Whittaker C, Gilbert S, Nourian F, Galloway E, Smith R, Lentz TJ, Hirst D, Topmiller J, Curwin B. Cincinnati, OH: U.S. Department of Health and Human Services, Centers for Disease Control and Prevention, National Institute for Occupational Safety and Health, DHHS (NIOSH) Publication No. 2016-111.

2. Centers for Disease Control. HHE Report No. HETA-1985-0171-1710, International Bakers Services, Inc., South Bend, Indiana. 1985 [accessed 2019 Apr 25]. https://bit.ly/2Vs6gWL.

3. Kanwal R, Kullman G, Fedan KB, Kreiss K. Health hazard evaluation report: Gilster-Mary Lee Corporation; Jasper, Missouri. HETA 2000-0401-2991. Centers for Disease Control, NIOSH. 2006.

4. NIOSH Alert: Preventing lung disease in workers who use or make flavorings. NIOSH Publication No. 2004-110. 2003 [accessed 2019 Apr 25]. https://bit.ly/2VgK5Oh.

5. Kreiss KM, Piacitelli C, Cox-Ganser J. Lung Function (Spirometry) Testing in Employees at a Flavorings Manufacturing Plant --- Indiana. Health Hazard Evaluation Report HETA 2008-0155-3131. Cincinnati, OH: Centers for Disease Control, NIOSH; 2011.

6. Page EH, Dowell CH, Mueller CA, Biagini RE. Exposure to flour dust and sensitization among bakery employees: Am J Ind Med. 2010 Dec;53(12):1225-32.

7. Code of Federal Regulations. Select committee on GRAS substances (SCOGS) opinion: diacetyl. Washington, DC; 1980.

8. Documentation for Diacetyl Threshold Limit Value. Cincinnati: American Conference of Governmental Industrial Hygienists; 2012.

9. Federal Register (US Government Printing Office) 74 (12): 3937-3947. Occupational exposure to diacetyl and food flavorings containing diacetyl. Washington DC; Occupational Safety and Health Administration, 2009.

10. Federal Register (US Government Printing Office) 74 (50): 11329-11330. Occupational exposure to diacetyl and food flavorings containing diacetyl. Washington DC; Occupational Safety and Health Administration, 2009.

11. Occupational Safety and Health Act of 1970, Public Law 91-596. Washington DC, US Congress. 1970 [accessed 2019 Apr 25]. https://bit.ly/2WyKkFZ.

12. Rigler M, Longo W. Emissions of diacetyl (2,3, butenedion) from natural butter, microwave butter flavor powder, paste and liquid. Int J Occup Environ Health. 2010 Jul-Sep;16(3):291-302.

13. Bakery business 2017. San Antonio (TX): The Small Business Development Center National Information Clearinghouse [accessed 2019 Apr 25]. https://bit.ly/2PZjowS.

14. Eastern Research Group. 2008. Technological and economic feasibility analysis for proposed OSHA standard for diacetyl and acetoin: draft final report. OSHA document 2008-0046-0052. [accessed 2019 May 11] https://bit.ly/2LMMuRk.

15. Knutson G. Industrial ventilation systems: energy savings and cost estimation. ACGIH Webinar; 2007 November 17; Cincinnati, OH: American Conference of Governmental Industrial Hygienists.

16. Bureau of Labor Statistics. Washington DC:

Economic News Release [accessed 2017 May 21]. https://bit.ly/2HkRZCN

17. Bureau of Labor Statistics. Washington DC: 2007 Job Openings and Labor Turnover Survey [accessed 2017 May 21]. https://www.bls.gov/jlt/

18. Bureau of Labor Statistics. Washington DC: 2007 Occupational Employment Statistics [accessed 2017 May 21]. https://bit.ly/2WyYdnN

19. Penalty and financial models, vers. 5.7.0. EPA Enforcement. Edited by EPA [accessed 2019 Apr 25]. https://bit.ly/2HijgnY.

20. ROI Calculator. IT Professionals. 2008. [accessed April 15, 2017]. https://bit.ly/2gOSp6s.

Appendix

Note: The inputs to the tables below have been modified by the program to reflect Discount/Compound rates calculations based on the values tabulated below the BEN runs. The model performs these calculations. Therefore, the inputs listed below do not copy the inputs discussed above.

	Run Name = NAFE3 Delayed
Present Values as of Noncompliance Date (NCO)	01-May-2011
A) On-Time Capital & One-Time Costs	$640,478
B) Delay Capital & One-Time Costs	$276,167
C) Avoided Annually Recurring Costs	$461,743
D) Initial Economic Benefit (A-B+C)	$826,055
E) Final Econ. Ben. at Penalty Payment Date,	
01-Jul-2017	$1,283,471

C-Corporation wl GA tax rates	
Discount/Compound Rate	7.4%
Discount/Compound Rate Calculated By:	BEN
Compliance Date	01-Jul-2017
Capital Investment:	
Cost Estimate	$560,831
Cost Estimate Date	01-May-2011
Cost Index for Inflation	PCI
Consider Future Replacement (Useful Life)	y (7)
One-Time. Nondepreciable Expenditure:	
Cost Estimate	$147,804
Cost Estimate Date	01-Nov-2011
Cost Index for Inflation	PCI
Tax Deductible?	y
Annually Recurring Costs:	
Cost Estimate	$147,804
Cost Estimate Date	01-Nov-2017
Cost Index for Inflation	PCI
User-Customized Specific Cost Estimates·	N/A
On-Time Capital Investment	
Delay Capital Investment	
On-Time Nondepreciable Expenditure	
Delay Nondepreciable Expenditure	

Discount/Compound Rate Calculation

Notes : (1) Corporate bond rates averaged across all industries (average of Aaa & Baa); Federal Reserve Statistical Release H.15.
(2) Combined state/federal marginal tax rates: federal+(state*(1-federal)); Federation of Tax Administrators.
(3) Calculated as: (1) * (100%-(2)). [Adjusts for tax-deductibility of interest payments.]
(4) Average corporate debt weight; Standard & Poor's Analysts' Handbook, S&P Industrials Sample Balance Sheet.
(5) Federal Reserve Statistical Release H.15. [Used as a proxy for the risk-free rate in the Capital Asset Pricing Model (CAPM)].
(6) Beta measures risk relative to overall stock market, with a value of 1.00 therefore setting risk at overall market.
(7) Differences of average returns between stock market vs. long-term Treasuries, 1926 - prior yr; Ibbotson then Duff & Phelps.
(8) Calculated as (6) * (7). [Also equal to (7), since (6) is equal to 1.00 for a company of average risk.]
(9) Calculated as (5) + (8). [Reflects risk-free rate of return plus the company risk premium.]
(10) Calculated as 100% - (4). [Reflects: total financing - debt = equity financing.]
(11) Calculated as (3) * (4) + (9) * (10). [Reflects: (debt cost x debt weight) + (equity cost x equity weight).]

Final rate:

						average from:		to:		=	
	(1)	(2)	(3)	(4)	(5)	(6)	(7)	(8)	(9)	(10)	(11)
YEAR	Cost of Debt	Tax Rate	After-Tax Debt Cost	Debt Weight	Long-Term Treasury Notes	Beta	Long-Horizon Risk Prem	Company Risk Premium	Equity Cost	Equity Weight	Rate
1987					8.49%	1.00	7.4%	7.4%	15.9%		
1988					8.91%	1.00	7.2%	7.2%	16.1%		
1989					8.47%	1.00	7.2%	7.2%	15.7%		
1990					8.58%	1.00	7.5%	7.5%	16.1%		
1991					8.00%	1.00	7.2%	7.2%	15.2%		
1992					7.34%	1.00	7.4%	7.4%	14.7%		
1993					6.29%	1.00	7.3%	7.3%	13.6%		
1994					7.49%	1.00	7.2%	7.2%	14.7%		
1995					6.95%	1.00	7.0%	7.0%	14.0%		
1996					6.83%	1.00	7.4%	7.4%	14.2%		
1997					6.69%	1.00	7.5%	7.5%	14.2%		
1998					5.72%	1.00	7.8%	7.8%	13.5%		
1999					6.20%	1.00	8.0%	8.0%	14.2%		
2000					6.23%	1.00	8.1%	8.1%	14.3%		
2001					5.63%	1.00	7.8%	7.8%	13.4%		
2002					5.43%	1.00	7.4%	7.4%	12.8%		
2003					4.96%	1.00	7.0%	7.0%	12.0%		
2004					5.04%	1.00	7.2%	7.2%	12.2%		

2005	4.64%	1.00	7.2%	7.2%	11.8%
2006	5.00%	1.00	7.1%	7.1%	12.1%
2007	4.91%	1.00	7.1%	7.1%	12.0%
2008	4.36%	1.00	7.1%	7.1%	11.5%
2009	4.11%	1.00	6.5%	6.5%	10.6%
2010	4.03%	1.00	6.7%	6.7%	10.7%
2011	3.62%	1.00	6.7%	6.7%	10.3%
2012	2.54%	1.00	6.6%	6.6%	9.1%
2013	3.12%	1.00	6.7%	6.7%	9.8%
2014	3.07%	1.00	6.96%	7.0%	10.1%
2015	2.55%	1.00	7.00%	7.0%	9.6%
2016	2.22%	1.00	6.90%	6.9%	9.1%

Calculations for Specific Cost Estimates

	On-Time	Delay
Date:	01-May-2011	01-Jul-2017
Capital Investment:		
Original Cost Estimate	$560,831	$560,831
	÷	÷
PCI Value as *of Cost Estimate Date, 01-May-2011*	581.900	581.900
	x	x
PCI Value as *of Specific Estimate Date*	581.900	551.517
	=	=
Specific Cost Estimate,	**$560,831**	**$531,548**
reflecting implicit annualized inflation rate of:	N/A	-0.9%
One-Time, Nondepreciable Expenditure:		
Original Cost Estimate	$147,804	$147,804
	÷	÷
PCI Value as *of Cost Estimate Date, 01-Nov-2011*	590.800	590.800
	x	x
PCI Value as *of Specific Estimate Date*	581.900	551.517
	=	=
Specific Cost Estimate,	**$145,577**	**$137,976**
reflecting implicit annualized inflation rate of:	3.1%	-1.2%

A) On-Time Capital & One-Time Costs	01-May 2011	01 – Nov 2011	01 – Nov 2012	01-Nov-2013	01-Nov-2014	01-Nov-2015	01-Nov-2016	01-Nov-2017	01-Nov 2018
One-Time, Nondepreciable Expenditure	(145,577)								
Capital Investment- Initial Installation	(560,831)								
Depreciation - Federal	0	(336,499)	(89,733)	(53,840)	(32,304)	(32,304)	(16,152)	0	0
Marginal Tax Rate (MTR)- Federal	35.0%	35.0%	35.0%	35.0%	35.0%	35.0%	35.0%	35.0%	35.0%
Tax Liability Offset- Federal	50,952	117,775	31,407	18,844	11,306	11,306	5,653	0	0
Depreciation- State (GA)	0	(112,166)	(179,466)	(107,680)	(64,608)	(64,608)	(32,304)	0	0
MTR- State (GA), adj. for fed. deductibility	3.9%	3.9%	3.9%	3.9%	3.9%	3.9%	3.9%	3.9%	3.9%
Tax li ability Offset- State (GA)	5,678	4,374	6,999	4,200	2,520	2,520	1,260	0	0
Net After-Tax Cash Flow	(649,779)	122,149	38,406	23,043	13,826	13,826	6,913	0	0
PV Factor: Adjusts Cash Flow to NCO	1.0000	0.9647	0.8980	0.8361	0.7785	0.7249	0.6748	0.6283	0.5850
PV Cash Flow as of NCO	{649,779)	117,831	34,489	19,267	10,764	10,022	4,665	0	0
Federal Utilized Depreciation Schedule:		60.00%	16.00%	9.60%	5.76%	5.76%	2.88%	0.00%	0.00%
State Utilized Depreciation Schedule:		20.00%	32.00%	19.20%	11.52%	11.52%	5.76%	0.00%	0.00%
Bonus schedules/dates (&'08 forward): MACRS:		20.00%	32.00%	19.20%	11.52%	11.52%	5.76%	0.00%	0.00%
10-Sep-01 6-May-03		*44.00%*	*22.40%*	*13.44%*	*8.06%*	*8.06%*	*4.03%*	*0.00%*	*0.00%*
5-May-03 1-Jan-05		*60.00%*	*16.00%*	*9.60%*	*5.76%*	*5.76%*	*288%*	*0.00%*	*0.00%*

Imputed Lease Cost for Interim Period When On-Time (But Not Delay) Equipment Would Need Replacement				Start Date:	End Date:	Years:	Capital Cost:	Annual Lease:
Applicable Only wl Default Value s of Delayed (Not Avoided) Capital and Considered Future Replacement				01-May-2018	01-Jul-2024	6.2	(541,386)	(101 ,861)
Total Imputed Lease Cost:	(631,539)	x	MTR- Federal/State Combined:	38.9%	=	Net After-Tax Cash Flow:		(385,870)
PV Factor: Adjusts Cash Flow to NCD:	0.4865							
PVCash Flow as QfNCD· (187,738)		+	Initial Install. NPV (see above}: (452 740)		=	On-TimeTotal NPV Install+Lease: **(640,478)**		

B) Delay Capital & One-Time Costs	01-Jul-2017	01-Jan-2018	01-Jan-2019	01-Jan-2020	01-Jan-2021	01-Jan-2022	01-Jan-2023	01-Jan-2024	01-Jan -2025
One -Time, Nondepreciable Expenditure	(137,976)								
Capital Investment	(531,548)								
Depreciation- Federal	0	(318,929)	(85,048)	(51,029)	(30,617)	(30,617)	(15,309)	0	0
Marginal Tax Rate (MTR)- Federal	35.0%	35.0%	35.0%	35.0%	35.0%	35.0%	35.0%	35.0%	35.0%
Tax Liability Offset- Federal	48,292	111,625	29,767	17,860	10,716	10,716	5,358	0	0
Depreciation - State (GA)	0	(106,310)	(170,095)	(102,057)	(61,234)	(61,234)	(30,617)	0	0
MTR- State (GA), adj. for fed. deductibility	3.9%	3.9%	3.9%	3.9%	3.9%	3.9%	3.9%	3.9%	3.9%
Tax Liability Offset- State (GA)	5,381	4,146	6,634	3,980	2,388	2,388	1,194	0	0
Net After-Tax Cash Flow	(615,851)	115,771	36,400	21,840	13,104	13,104	6,552	0	0
PV Factor: Adjusts Cash Flow to NCO	0.6436	0.6209	0.5781	0.5383	0.5011	0.4665	0.4344	0.4045	0.3765
PV Cash Flow as of NCO	(396,368)	71,878	21,042	11,756	6,566	6,114	2,846	0	0
PV Cash FIQW as of NCO: (276,167)									
Federal Utilized Depreciation Schedule:		60.00%	16.00%	9.60%	5.76%	5.76%	2.88%	0.00%	0.00%
State Utilized Depreciation Schedule:·		20.00%	32.00%	19.20%	11.52%	11.52%	5.76%	0.00%	0.00%

C) Avoided Annually Recurring Costs

PCI value as of cost estimate date = 590,800

PCI mid-point value:	596.100	582.200	564.000	576.900	556.300	544.900	548.525
Period of Avoided Annual Costs; From:	01-May-2011	01-Jan-2012	01-Jan-2013	01-Jan-2014	01-Jan-2015	01-Jan-2016	01-Jan-2017
To:	31-Dec-2011	31-Dec-2012	31-Dec-2013	31-Dec-2014	31-Dec-2015	31-Dec-2016	01-Jul-2017
Annual Costs Avoided	(100,101)	(146,052)	(141,099)	(144,327)	(139,173)	(139,694)	(68,426)
Marginal Tax Rate	38.9%	38.9%	38.9%	38.9%	38.9%	38.9%	38.9%
Net After-Tax Cash Flow	(61,162)	(89,237)	(86,212)	(88,184)	(85,035)	(83,520)	(41,808)
PV Factor: Adjusts Cash Flow to NCD	0.9764	0.9198	0.8563	0.7973	0.7424	0.6912	0.6551
PV Cash Flow as of NCD	(59,720)	(82,079)	(73,825)	(70,311)	(63,129)	(57,727)	(27,389)

NPV of Avoided Annual Costs as of NCD **($434,180)**

Run Name= NAFE4 Avoided

Present Values as of Noncompliance Date (NCD)	01-May-2011
A) On-Time Capital & One-Time Costs	$640,478
B) Delay Capital & One-Time Costs	$0
C) Avoided Annually Recurring Costs	$434,180
D) Initial Economic Benefit (A-B+C)	$1,074,658
E) Final Econ. Ben. at Penalty Payment Date, *01-Jul-2017*	**$1,669.734**

C-Corporation w/ GA tax rates	
Discount/Compound Rate	7.4%
Discount/Compound Rate Calculated By:	BEN
Compliance Date	01-Jul-2017
Capital Investment:	avoided
Cost Estimate	$560,831
Cost Estimate Date	01-May-2011
Cost Index for Inflation	PCI
Consider Future Replacement (Useful Life)	*y* (7)
One-Time, Nondepreciable Expenditure:	avoided
Cost Estimate	$147,804
Cost Estimate Date	01-Nov-2011
Cost Index for Inflation	PCI
Tax Deductible?	y
Annually Recurring Costs:	
Cost Estimate	$147,804
Cost Estimate Date	01-Nov-2011
Cost Index for Inflation	PCI
User-Customized Specific Cost Estimates·	N/A
On-Time Capital Investment	
Delay Capital Investment	
On-Time Nondepreciable Expenditure	
Delay Nondepreciable Expenditure	

Discount/Compound Rate Calculation

Notes : (1) Corporate bond rates averaged across all industries (average of Aaa & Baa); Federal Reserve Statistical Release H.15.
(2) Combined state/federal marginal tax rates: federal+(state*(1-federal)); Federation of Tax Administrators.
(3) Calculated as: (1) * (100%-(2)). [Adjusts for tax-deductibility of interest payments.]
(4) Average corporate debt weight; Standard & Poor's Analysts' Handbook, S&P Industrials Sample Balance Sheet.
(5) Federal Reserve Statistical Release H.15. [Used as a proxy for the risk-free rate in the Capital Asset Pricing Model (CAPM)].
(6) Beta measures risk relative to overall stock market, with a value of 1.00 therefore setting risk at overall market.
(7) Differences of average returns between stock market vs. long-term Treasuries, 1926 - prior yr; Ibbotson then Duff & Phelps.
(8) Calculated as (6) * (7). [Also equal to (7), since (6) is equal to 1.00 for a company of average risk.]
(9) Calculated as (5) + (8). [Reflects risk-free rate of return plus the company risk premium.]
(10) Calculated as 100% - (4). [Reflects: total financing - debt = equity financing.]
(11) Calculated as (3) * (4) + (9) * (10). [Reflects: (debt cost x debt weight) + (equity cost x equity weight).]

Final rate:

					average from:			to:		=	
	(1)	(2)	(3)	(4)	(5)	(6)	(7)	(8)	(9)	(10)	(11)
YEAR	Cost of Debt	Tax Rate	After-Tax Debt Cost	Debt Weight	Long-Term Treasury Notes	Beta	Long-Horizon Risk Prem	Company Risk Premium	Equity Cost	Equity Weight	Rate
1987					8.49%	1.00	7.4%	7.4%	15.9%		
1988					8.91%	1.00	7.2%	7.2%	16.1%		
1989					8.47%	1.00	7.2%	7.2%	15.7%		
1990					8.58%	1.00	7.5%	7.5%	16.1%		
1991					8.00%	1.00	7.2%	7.2%	15.2%		
1992					7.34%	1.00	7.4%	7.4%	14.7%		
1993					6.29%	1.00	7.3%	7.3%	13.6%		
1994					7.49%	1.00	7.2%	7.2%	14.7%		
1995					6.95%	1.00	7.0%	7.0%	14.0%		
1996					6.83%	1.00	7.4%	7.4%	14.2%		
1997					6.69%	1.00	7.5%	7.5%	14.2%		
1998					5.72%	1.00	7.8%	7.8%	13.5%		
1999					6.20%	1.00	8.0%	8.0%	14.2%		
2000					6.23%	1.00	8.1%	8.1%	14.3%		
2001					5.63%	1.00	7.8%	7.8%	13.4%		
2002					5.43%	1.00	7.4%	7.4%	12.8%		
2003					4.96%	1.00	7.0%	7.0%	12.0%		
2004					5.04%	1.00	7.2%	7.2%	12.2%		

2005	5.65%	38.9%	3.45%	35.9%	4.64%	1.00	7.2%	7.2%	11.8%	64%	
2006	6.04%	38.9%	3.69%	32.8%	5.00%	1.00	7.1%	7.1%	12.1%	67%	
2007	6.02%	38.9%	3.68%	33.7%	4.91%	1.00	7.1%	7.1%	12.0%	66%	
2008	6.54%	38.9%	4.00%	45.0%	4.36%	1.00	7.1%	7.1%	11.5%	55%	
2009	6.30%	38.9%	3.85%	38.6%	4.11%	1.00	6.5%	6.5%	10.6%	61%	
2010	5.49%	38.9%	3.35%	36.7%	4.03%	1.00	6.7%	6.7%	10.7%	63%	
2011	5.15%	38.9%	3.15%	37.0%	3.62%	1.00	6.7%	6.7%	10.3%	63%	**7.7%**
2012	4.31%	38.9%	2.63%	35.9%	2.54%	1.00	6.6%	6.6%	9.1%	64%	**6.8%**
2013	4.67%	38.9%	2.85%	30.9%	3.12%	1.00	6.7%	6.7%	9.8%	69%	**7.7%**
2014	4.51%	38.9%	2.76%	30.9%	3.07%	1.00	6.96%	7.0%	10.1%	69%	**7.8%**
2015	4.45%	38.9%	2.72%	32.2%	2.55%	1.00	7.00%	7.0%	9.6%	68%	**7.4%**
2016	4.15%	38.9%	2.54%	32.2%	2.22%	1.00	6.90%	6.9%	9.1%	68%	**7.0%**

Calculations for Specific Cost Estimates

	On-Time	Delay
Date:	01-May-2011	01-Jul-2017
Capital Investment:		
Original Cost Estimate	$560,831	N/A
	÷	÷
PCI Value as of Cost Estimate Date,	581.900	N/A
01-May-2011	x	x
PCI Value as of Specific Estimate Date	581.900	N/A
	=	=
Specific Cost Estimate,	**$560,831**	**NIA**
reflecting implicit annualized inflation rate of:	N/A	N/A
One-Time, Nondepreciable Expenditure·		
Original Cost Estimate	$147,804	N/A
	÷	÷.
PCI Value as of Cost *Estimate Date,*	590.800	N/A
01-Nov-2011	**X**	**X**
PCI Value as of Specific Estimate Date	581.900	N/A
	=	=
Specific Cost Estimate,	**$145,577**	N/A
reflecting implicit annualized inflation rate:	3.1%	N/A

A) On-Time Capital & One - Time Costs	01-May-2011	01-Nov-2011	01-Nov-2012	01-Nov-2013	01-Nov-2014	01-Nov-2015	01-Nov-2016	01-Nov-2017	01-Nov -2018
One-Time, Nondepreciable Expenditure	(145,577)								
Capital Investment- Initial Installation	(560,831)								
Depreciation- Federal	0	(336,499)	(89,733)	(53,840)	(32,304)	(32,304)	(16,152}	0	0
Marginal Tax Rate (MTR)- Federal	35.0%	35.0%	35.0%	35.0%	35.0%	35.0%	35.0%	35.0%	35.0%
Tax Liability Offset- Federal	50,952	117,775	31,407	18,844	11,306	11,306	5,653	0	0
Depreciation- State (GA}	0	(112,166}	(179,466}	(107,680)	(64,608)	(64,608)	(32,304)	0	0
MTR- State (GA), adj. for fed. deductibility	3.9%	3.9%	3.9%	3.9%	3.9%	3.9%	3.9%	3.9%	3.9%
Tax Liability Offset- State (GA)	5,678	4,374	6,999	4,200	2,520	2,520	1,260	0	0
Net After-Tax Cash Flow	(649,779)	122,149	38,406	23,043	13,826	13,826	6,913	0	0
PV Factor: Adjusts Cash Flow to NCO	1.0000	0.9647	0.8980	0.8361	0.7785	0.7249	0.6748	0.6283	0.5850
PV Cash Flow as of NCO	(649,779)	117,831	34,489	19,267	10,764	10,022	4,665	0	0
Federal Utilized Depreciation Schedule:		60.00%	16.00%	9.60%	5.76%	5.76%	2.88%	0.00%	0.00%
State Utilized Depreciation Schedule:		20.00%	32.00%	19.20%	11.52%	11.52%	5.76%	0.00%	0.00%
Bonus schedules/dates (& '08 forward): MACRS:		20.00%	32.00%	19.20%	11.52%	11.52%	5.76%	0.00%	0.00%
10-Sep-01 6-May-03		*44.00%*	*22.40%*	*13.44%*	*8.06%*	*8.06%*	*4.03%*	*0.00%*	*0.00%*
5-May-03 1-Jan-05		*60.00%*	*16.00%*	*9.60%*	*5.76%*	*5.76%*	*2.88%*	*0.00%*	*0.00%*

Imputed Lease Cost for Interim Period When On-Time (But Not Delay) Equipment Would Need Replacement				Start Date:	End Date:	Years:	Capital Cost:	Annual Lease:
Applicable Only w/ Default Values of Delayed (Not Avoided) Capital and Considered Future Replacement				01-May-2018	01-Jul-2024	6.2	(541,386)	(101,861) Total
Imputed Lease Cost:	(631,539)	X	MTR- Federal/State Combined:	38.9%	=	Net After-Tax Cash Flow:		(385,870)
PV Factor: Adjusts Cash Flow to NCD:	0.4865							
PY Cash Flow as of NCD· (187,738)		+	Initial Install, NPV (see above): (452,740)		=	On-Time Total NPV. Install+Lease: **(640,478)**		

B} Delay Capital & One-Time Costs	01-Jul-2017	01-Jan-2018	01-Jan-2019	01-Jan-2020	01-Jan-2021	01-Jan-2022	01-Jan-2023	01-Jan-2024	01-Jan-2025
One-Time, Nondepreciable Expenditure	0								
Capital Investment	0								
Depreciation- Federal	0	0	0	0	0	0	0	0	0
Marginal Tax Rate (MTR)- Federal	35.0%	35.0%	35.0%	35.0%	35.0%	35.0%	35.0%	35.0%	35.0%
Tax Liability Offset- Federal	0	0	0	0	0	0	0	0	0
Depreciation- State (GA)	0	0	0	0	0	0	0	0	0
MTR- State (GA}, adj. for fed. deductibility	3.9%	3.9%	3.9%	3.9%	3.9%	3.9%	3.9%	3.9%	3.9%
Tax Liability Offset- State (GA)	0	0	0	0	0	0	0	0	0
Net After-Tax Cash Flow	0	0	0	0	0	0	0	0	0
PV Factor: Adjusts Cash Flow to NCD	0.6436	0.6209	0.5781	0.5383	0.5011	0.4665	0.4344	0.4045	0.3765
PV Cash Flow as of NCD	0	0	0	0	0	0	0	0	0

PV Cash Flow of NCD: 0

Federal Utilized Depreciation Schedule:	60.00%	16.00%	9.60%	5.76%	5.76%	2.88%	0.00%	0.00%
State Utilized Depreciation Schedule: ·	20.00%	32.00%	19.20%	11.52%	11.52%	5.76%	0.00%	0.00%

C) Avoided Annually Recurring Costs

PCI *value* as *of* cost *estimate date= 590.800*

PCI *mid-point value:*	596.100	582.200	564.000	576.900	556.300	544.900	548.525
Period of Avoided Annual Costs; From:	01-May-2011	01-Jan-2012	01-Jan-2013	01-Jan-2014	01-Jan-2015	01-Jan-2016	01-Jan-2017
To:	31-Dec-2011	31-Dec-2012	31-Dec-2013	31-Dec-2014	31-Dec-2015	31-0ec-2016	O1-Jul-2017
Annual Costs Avoided	(100,101)	(146,052)	(141,099)	(144,327)	(139,173)	(136,694)	(68,426)
Marginal Tax Rate	38.9%	38.9%	38.9%	38.9%	38.9%	38.9%	38.9%
Net After-Tax Cash Flow	(61,162)	(89,237)	(86,212)	(88,184)	(85,035)	(83,520)	(41,808)
PV Factor: Adjusts Cash Flow to NCO	0.9764	0.9198	0.8563	0.7973	0.7424	0.6912	0.6551
PV Cash Flow as of NCO	(59,720)	(82,079)	(73,825)	(70,311)	(63,129)	(57,727)	(27,389)

NPV of Avoided Annual Costs as of NCD	($434,180)

Forensic Engineering Analysis of Fire Caused by Control Failure Due to Deviation from Patented Design

By John Certuse, PE (NAFE 708F)

Abstract

A fire in a multi-unit condominium complex occurred, causing the building to be a complete loss. The point of the fire's origin was traced to a recently drained hot tub's electric heater. Examination of an exemplar heater revealed that a key safety-related control feature was manufactured in a configuration inconsistent with its original patent drawings in a way that would have lessened its performance for what may have been cost of manufacturing considerations. This change also brought into question whether the control that was reportedly tested at Underwriters Laboratory was one designed to the patent specifications. The manufacturer has since discontinued use of the control for subsequent installations.

Keywords

Fire, hot tub fire, positive temperature coefficient heater, PTC, hot tub heater, over temperature shutoff control, NFPA 921, forensic engineering

Background

In October of 2010, a fire occurred in a condominium at a New England ski resort, resulting in a total loss of the subject and adjacent condominium units (**Figure 1**). This condominium included a four-person hot tub spa that was installed on the second-floor exterior porch of the 900-square-foot property. The hot tub spa was installed in 1997, and past service work included the installation of a new electric spa heater and circulating pump in 2003. The spa heater was again replaced in 2006.

The vacation property had not been used since the previous winter and was being prepared for the upcoming skiing season. Activities included cleaning and other property maintenance needed to make the condominium unit ready for winter renters. During nonuse periods, the hot tub spa was drained and covered with an insulated spa cover.

For what appears to be aesthetic purposes, the spa's electrical disconnect was installed 7 feet above the second-floor deck where the tub was located. This height was contrary to the National Electrical Code and the spa's manufacturer's installation instructions. Both documents require that this component of the tub's electrical system must be readily accessible; however, access to this spa's electrical disconnect required a step ladder.

Reportedly, during summertime periods of nonuse, the branch circuit breaker to the tub was shut off at the electrical panel that was not within line of site of the equipment. During the "opening" of the property for the upcoming rental season, many circuit breakers were closed to re-establish power to de-energized appliances. Possibly due to the 7-foot elevation of the tub's electrical disconnect

Figure 1
Location of fire indicated by arrow.

John Certuse, PE, 15 Extension St., Attleboro, MA 02703; (508) 226-8800; john@iseengineering.com

Figure 2
Spa as seen. Fire patterns and other fire investigation techniques identified it as the origin of the building fire.

switch, the owner did not notice the position of the disconnect due to its inaccessibility — and the switch was left in the on position from the previous season. This allowed the empty spa's heater and controls to become electrically energized when the circuit breaker was closed, even though the spa had no water in it.

A fire occurred a few days after the property was opened by the owner, resulting in extensive damage to the property that required teardown and rebuilding of the condo and adjacent units.

Origin

Fire investigators determined that the fire originated from the hot tub spa located on the porch of the second floor (**Figure 2**). All other sources of the fire were eliminated both through visual examination, arc mapping, and fire pattern analysis. Part of the investigation included identifying parties that had access to or involvement with the condominium unit and spa including distributors, the manufacturer, ongoing maintenance repair technicians, as well as spare parts providers. Aside from the focus on the manufacturing and repair of the spa (and associated parts), the investigation also included recent carpentry work, because the second-floor porch where the spa was situated had recently been rebuilt. All parties were afforded the opportunity to conduct a fire scene examination. With winter weather conditions approaching — and in the interest of preserving the evidence from the fire scene — the spa and all electrical components were retained by the condominium owner's expert for later analysis.

Area of Origin within Hot Tub Control Cabinet

The construction of this 15-year-old spa was of a fiberglass tub shell and a cedar enclosure that housed the

Figure 3
Spa and evidence in forensic laboratory.

spa's circulating pumps, controller, and electric heater. Additionally, closed cell polyethylene foam was used on the underside of the spa shell.

Once the hot tub spa became the focus of the cause, the wiring and components of the tub that had not been rendered unidentifiable by the fire were examined and analyzed. Major components of the spa were examined for evidence of heat generation, consumption, and arcing to identify any involvement in the fire (**Figure 3**).

After major components were identified within the mass of melted foam and fiberglass, X-ray and computed tomography (CT) scanning were performed to identify features not initially visible (**Figure 4**). Examination of the heater identified electrical activity consistent with a malfunction and arcing event.

Figure 4
After debris removed, spa heater located.

Heater Design

Overheating protection in hot tub spas is accomplished by a variety of control choices, including differential pressure switches that sense water flow through the heater vessel or by water-sensing probes. The basis of this control, however, was unique in that it did not verify the presence of water with a separate control BEFORE the heater electrical element was energized, instead relying upon a thermal sensing bulb and attached capillary tubing to REACT to overheating first, causing an "over-temperature shutoff switch" to open the heater circuit.

A second feature of the control — designed to prevent the sensing bulb from cooling and then allowing the over temperature shutoff switch to re-energize the circuit and start the overheating cycle again — was to use a positive temperature coefficient (PTC) heater. This heater, if configured in accordance with a patent referenced on the heater control's enclosure, was intended to be encircled by a number of turns of capillary tubing to heat the capillary tubing and its internal fluid. This appears to have been an intentional design feature to enhance heat transfer from the PTC heater to the capillary tubing and the over-temperature control switch (**Figure 5**).

Activation of the over-temperature switch removed power from the water heater and applied power to the PTC heater. This continuous heating of the PTC would keep the over-temperature shutoff switch in the activated position and prevent the water heater from being energized until power from the control circuit was removed. Overall, however, this control scheme was problematic in that it did not prevent the water heater from being energized when water was not present. Manufacturers of electric heating elements used in spas warn against dry firing elements (even instantaneously) because this causes damage to these elements. This heater control system only provided post-over temperature "lockout" protection. For convenience to the installer, the heater control was one self-contained unit.

Arcing Damage Found

Examination of the control unit identified that the heater vessel was damaged by arcing, which burned through the vessel over a length of approximately 3 inches (**Figure 6**). No other electrical activity was found on any wiring, spa control, or component. As such, the heater was identified as the point of origin of the fire within the spa. Examination of the heater identified that the heater element was melted and damaged as a result of uncontrolled electrical application. The end of the element coinciding with the arcing through the heater vessel was missing due to consumption.

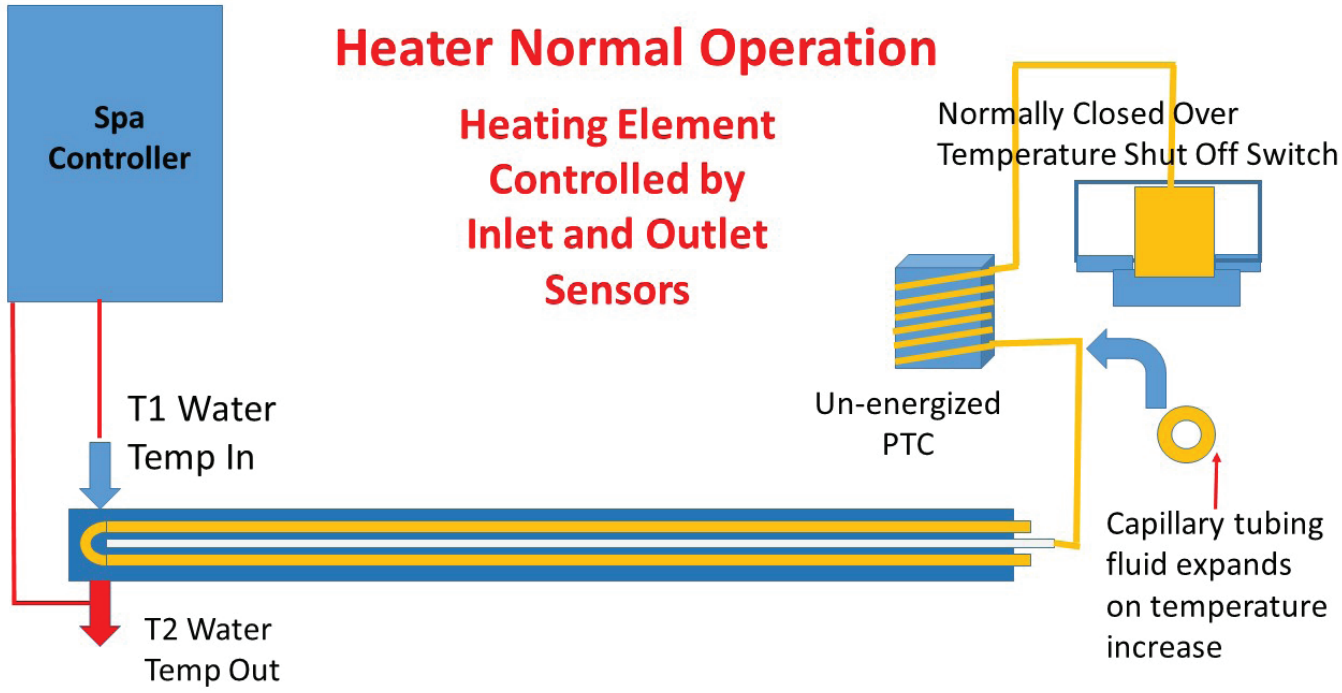

Figure 5
Drawing showing orientation of heater, sensing bulb and over-temperature shutoff switch.

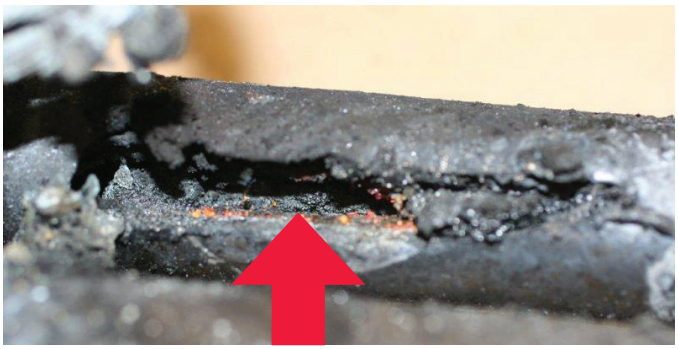

Figure 6
Arcing damage found to heater vessel.

Understanding Subject Component's Manufacturing

The first step in forensic failure analysis is understanding how a component suspected of failing normally works as well as its manufacturing features. Past experience with similar equipment can be drawn upon as well as available manufacturer's instructions and drawings. Some of this information may be unavailable or considered proprietary, causing the forensic investigator to seek other means of understanding the machine's design. However, additional information of an unfamiliar machine design can be obtained by examination, testing, and disassembly of an exemplar component as well as patent documentation.

Review of Patent

The patent (with images) for the subject heater was identified, and the features of the patented design were compared to the subject heater as well as a recently purchased exemplar heater (**Figure 7**). In comparison to the patent's Detailed Description of the Preferred Embodiment of the design, a major deviation on the subject and exemplar heaters was identified. The patent design of the overheating protection circuit and controls featured a heat generating positive temperature coefficient PTC heater that was designed to be encircled with capillary tubing, leading to the over-temperature shutoff switch.

This design would keep the over-temperature shutoff switch in the open position and prevent the heater from being energized until power was removed to prevent continuous OFF-ON cycling of the heater. Additionally, the patent design documentation was quite specific in that it directed that the PTC heater be encircled by a specific number of turns of capillary tubing, to provide a thermal coupling (as shown in **Figure 8**).

Subject Artifact Examination

In examining the artifacts that survived the fire, what became apparent was that the PTC heater, which was crucial to the over-temperature protection features of the heater's

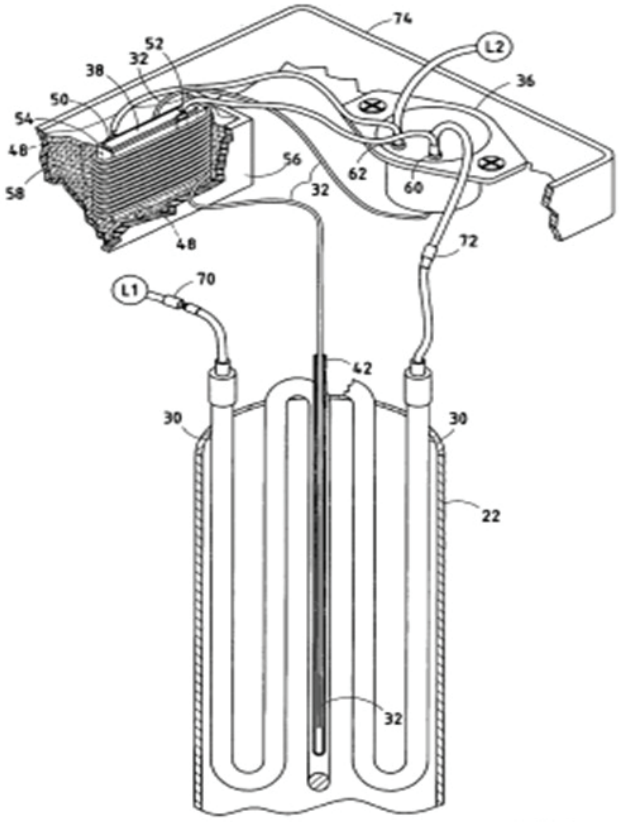

Figure 7
Drawing from heater patent filing.

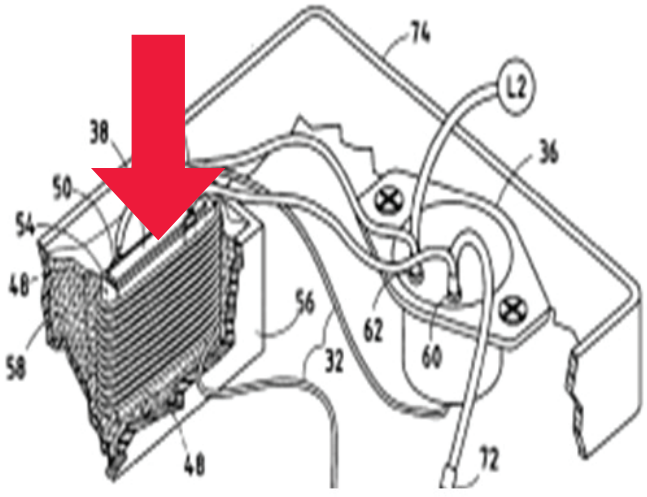

Figure 8
Number of turns as described in patent drawing. Item 38 is the PTC with capillary tubing wrapped around it (see red arrow).

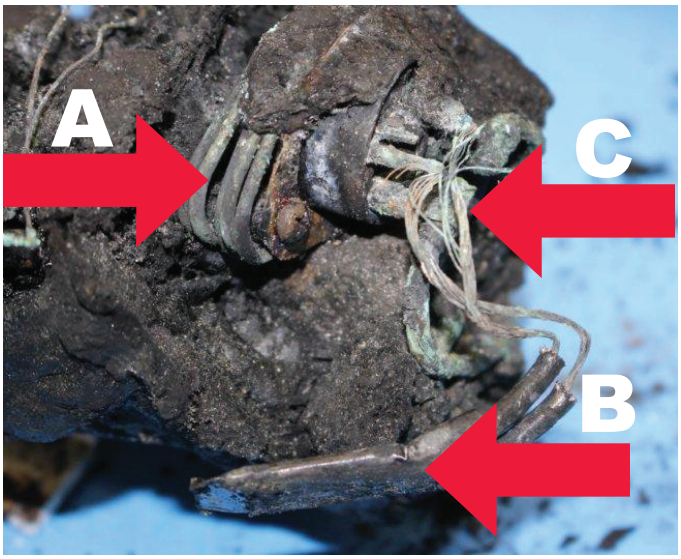

Figure 9
Over-temperature protection components of the heater as seen in fire debris: A – capillary tubing, B – PTC heater, C- Over-temperature shutoff switch.

patented design, was not encircled by capillary tubing in the manner shown in the patent documentation (**Figure 9**). Speculation was generated regarding whether this was the result of the fire. This led to further nondestructive tests, including X-ray and CT scanning examinations of the suspect components.

CT Scanning Examination

CT scanning and other means of evidence examination confirmed that the PTC heater was not encircled by the capillary tubing in the manner shown in the patent documents (**Figure 10**). Additionally, in the exemplar heater purchased, the same configuration (as the subject heater) confirmed that the capillary tubing merely passed by the PTC heater in its path between the thermal sensing bulb within the heater vessel and the over-temperature shutoff switch. The deviation from the design shown in the patent resulted in a reduction in surface area between the capillary tubing and PTC heater, which would serve to diminish heat transfer between these two components and reduce control performance and effectiveness.

Exemplar Heater Examination

In the examination of the exemplar heater, the PTC heater was a "standalone" component not encircled with capillary tubing — contrary to patent documentation (**Figure 11**).

The securing of the PTC within the control box was not affixed and was free to move within the enclosure. Furthermore, contact with the capillary tubing, if any, was minimal — with only one segment of the capillary tubing (less than an inch long) being in direct contact with the heater. This comparatively reduced surface area between the PTC heater and capillary tubing would likely cause a proportionately different change in reaction time and performance. The author opined that this deviation between the patent design and the production components may have been a cost-driven manufacturing alteration.

Underwriters Laboratory Testing

The heater received the UL symbol for approval per UL 1563[1] and 1261[2]. Recommendations were made to attorneys in the case to obtain the actual prototype heaters and UL test reports to determine if the UL test configuration was the same as the subject heater, though the case

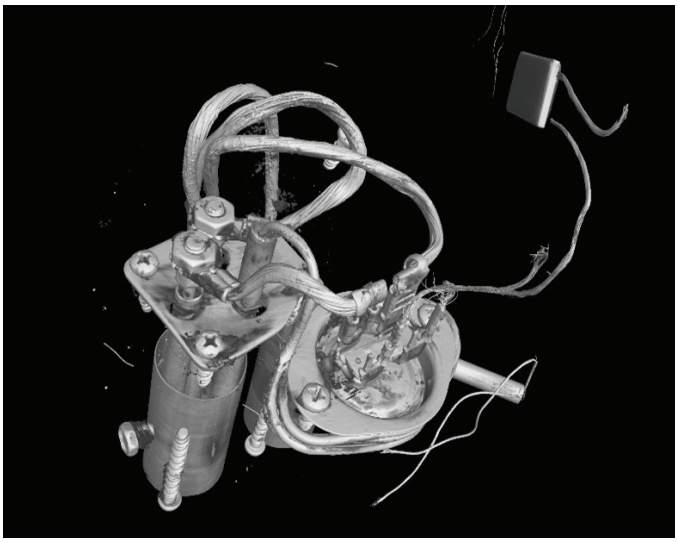

Figure 10
CT scan showing PTC heater and capillary tubing.

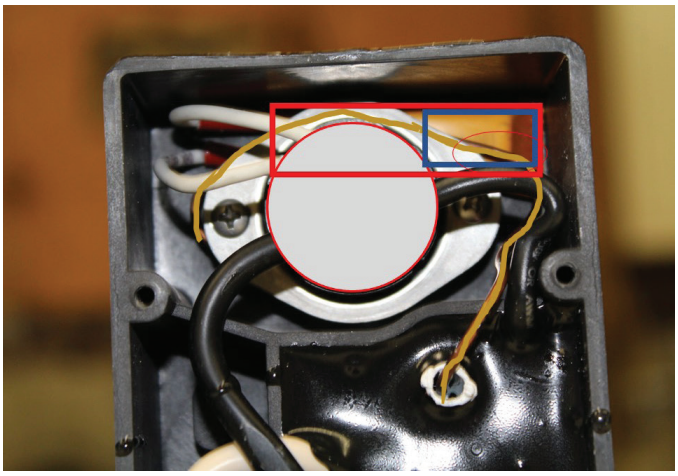

Figure 11
Examining exemplar heater to locate placement of PTC and other components. Blue rectangle shows placement of PTC behind switch. Yellow line depicts capillary tubing NOT encircled around PTC.

settled before this occurred.

Testing the Hypothesis

Exemplar testing of an identical heater was performed by applying thermocouples to the heater barrel and thermal sensing bulb in a test duplicating the conditions of the heater from the fire.

As opposed to a lockout condition of the over-temperature switch occurring as intended, cyclic heating and cooling resulted, allowing the heating element to be continuously and repeatedly exposed to heating and cooling cycles. The resulting temperatures (in the exemplar testing) were higher than what would have been experienced during normal operation (**Figure 12**). Nevertheless, this repeated short cycling of the over-temperature shutoff switch would induce accelerated operational cycles, leading to more rapid switch failure and potential overheating and arc welding of the contacts. Additionally, the continuous heating and cooling could have the effect of inducing heater element damage and thermal sensing bulb leakage, which would make this position of the heater incapable of transmitting an increased internal pressure due to increased temperature within the heater.

Failure of the sensing bulb, which is attached to the capillary tubing, would then prevent increases in capillary tubing fluid pressure from being transmitted to the

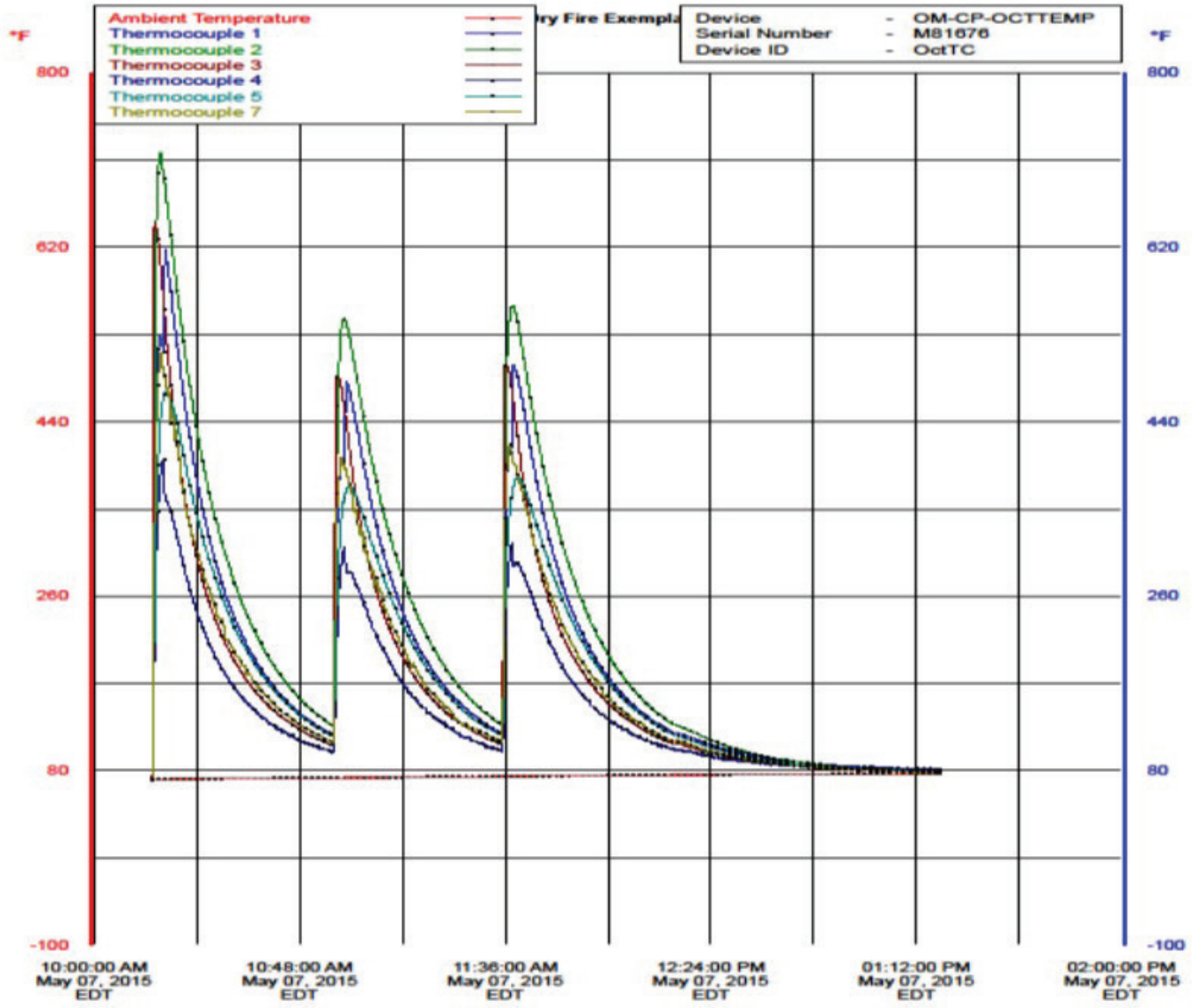

Figure 12
Temperature data logging of heater in operation.

Figure 13
Heater arcing due to overheating damage.
https://youtu.be/KJ8sIBma22o

over-temperature shutoff switch, allowing a continuously energized heater element to occur.

Exemplar testing of an unsubmerged heater element resulted in arcing, flames, and molten steel, all of which would be easily capable of igniting combustibles within the control cabinets, such as the wooden cabinetry and instruction manual typically left in this area of the spa (**Figure 13**).

Conclusion

This fire investigation exemplifies the analysis of the larger "macro" view of the fire scene in identifying the area of origin within the building to the "micro" view of the fire occurring not only within the appliance but also within the appliance's controls. The joint cooperation of the fire investigator and supporting engineer together identified the origin and cause of the fire by further refining the fire's point of origin within the appliance and then investigating component design and manufactured characteristics to determine the cause.

Despite a lack of manufacturer-provided documentation, including manufacturing drawings (which were requested but not received), the patented design of the heater was identified by using exemplar controls and components as well as the control's patent descriptions and images. This information was then compared to the actual manufacturing configuration of the recovered subject heater as well as an exemplar unit. It was also noted that the use of this heater design was discontinued by the manufacturer.

Once the patented design as well as the "as-built" design (actual conditions of how the control was manufactured) were established, testing of an exemplar heater was able to fairly and accurately represent a condition of failure consistent with the fire patterns and conditions of the heater components involved in the fire. It was also noted that this heater was listed by UL. Recommendations were given to attorneys in the case to obtain the heater's design drawings and reports from UL testing to determine the configuration of the heater that was tested. However, after depositions of experts and investigators, the case settled, and detailed testing conditions from the UL testing were not produced.

Based upon the investigation it is the author's opinion that had the heater been built consistent to the patent, with the capillary tubing "wrapped" around the PTC heater, the control would have been more responsive to low water conditions and performed more reliably. The choice of the manufacturer to deviate from the patent design defeated the intended interaction of the heat-generating PTC component and capillary thermal sensing element, which was a key element of the patent, and which led to the fire. The reason for the design change is unknown, however the simplification of the design was likely less labor-intensive to manufacture and as such likely less expensive. As such, regardless as to why the design specified in the patent differed from how the control was actually built, the final design was one conducive to heater element overheating and failure.

Acknowledgements

Victor DaCosta, Electrical Fire Investigator
Tom Zarek

Bibliography

Icove DJ, Haynes GA. Kirk's Fire Investigation. 8th Ed. London (UK): Pearson; 2018

NFPA 921-2011. Guide for Fire and Explosion Investigations. Quincy (MA); National Fire Protection Association.

NFPA 70-2011. National Electrical Code. Quincy (MA); National Fire Protection Association.

References

1. UL 1563-2009. Standard for Electric Spas, Equipment Assemblies, and Associated Equipment. Northbrook (IL); Underwriters Laboratory.

2. UL 1261-2001. Standard for Electric Water Heaters for Pools and Tubs. Northbrook (IL); Underwriters Laboratory.

Forensic Engineering Analysis of Commercial Vehicle Air Brake Systems Performance

By Jerry S. Ogden, PhD, PE (NAFE 561F) and Mathew Martonovich, PE (NAFE 968M)

Abstract

Braking systems for heavy commercial vehicles differ greatly from the design for light-duty motor vehicles. For example, 49 CFR 571.121 and 49 CFR 393.52 require loaded buses, single unit commercial vehicles, and vehicle-trailer combinations equipped with air brake systems to generate sufficient braking force to meet specific stopping distance, stopping acceleration rate, and brake force-to-weight percentage performance criteria. The combination of unique design, mechanical complexity, and maintenance issues characteristic to air brake systems also pose difficulty in the analysis of air brake system performance. Air brake system performance presents a difficult problem for the forensic engineer with limited familiarity regarding air brake system functions and the elements affecting brake performance. This paper provides insight into the evolution of air brake system standards and the applicable performance criteria for heavy commercial vehicles. The methods presented allow the forensic engineer to mathematically analyze and determine the effects of brake size, mismatched components, brake adjustment, and system air pressure on the overall braking force and stopping capabilities of air brake equipped commercial vehicles.

Keywords

Forensic engineering, air brakes, pneumatic brakes, commercial vehicles, commercial vehicle brakes, braking performance, s-cam brakes, air brake standards

Background

Analyzing single and multiple vehicle crashes involving commercial vehicles often requires the expertise of a knowledgeable forensic engineer. Commercial vehicle collisions oftentimes require investigations into potential pneumatic braking system failures. Several completed and ongoing studies attempt to quantify the frequency of braking defects present on commercial vehicles operating on public roadways. In 2001, the National Highway Traffic Safety Administration (NHTSA) and the Federal Motor Carrier Safety Administration (FMCSA) initiated the Large Truck Crash Causation Study (LTCCS). Results of the study estimate that deficient braking systems played a part in 26% of all heavy vehicle crashes[1]. The Fatal Accident Complaint Team of the Michigan State Police Motor Carrier Enforcement Division found that during inspections of 407 heavy vehicles following crashes, 32.7% of the involved heavy vehicles had one or more braking system deficiencies[2].

Pneumatic braking systems were originally developed for use by the locomotive industry. The fundamental design principles for pneumatic braking systems on most modern commercial vehicles stem from the original design principles used for locomotive brakes. George Lane was the first to develop and deploy pneumatic brakes for on-road heavy vehicles. Lane worked as a logging truck driver in the northwestern United States and observed the need for better, more reliable braking systems on the logging trucks in operation at the time. As a result, the original "Lane" braking system for commercial vehicle use was introduced in 1919. The Lane braking system consisted of an accumulator attached to the engine's combustion chamber, allowing compressed gas developed during the engine's compression stroke to pass through a one-way check valve and into a holding reservoir. The compressed gas was stored in a holding reservoir until brake application. The Lane brake was designed to function on only the rear axle of a heavy vehicle[3].

Jerry S. Ogden, PhD, PE and Mathew Martonovich, PE, P.O. Box 621519, Littleton, CO, 80162; (303) 795-1515; jogden@OEC4N6.com; mmartonovich@OEC4N6.com.

The Lane brake system had the following major design flaws, which limited universal adoption for use on heavy vehicles:

• Decrease of the engine's effective compression ratio due to the accumulator valve capturing a portion of the engine's cylinder gases during the compression stroke.

• Introduction of contaminants from the engine into the braking system.

By 1924, Westinghouse developed an engine-driven air compressor to operate a commercial vehicle's pneumatic braking system in lieu of an accumulator valve. The engine-driven compressor heralded the coming of the modern pneumatic braking system. Following the advent of the engine-driven compressor, foot-operated brake valves (treadle valves) and pressure regulators were deployed on commercial vehicles, ensuring the braking system operated within normalized pressures.

Commercial Vehicle Braking Performance Standards

Following the rapid developments of the commercial vehicle pneumatic braking system, the U.S. government initiated braking system type and performance regulations. Government-mandated stopping distance performance regulations for commercial vehicles were first issued in 1933. The regulation required a pneumatically braked commercial vehicle to stop from 20 mph within 50 feet.

The 1950s through '70s saw the introduction of numerous regulations for commercial vehicle braking systems. However, none was more widespread and influential than the major legislative effort of the Federal Motor Vehicle Safety Standard (FMVSS) 121 (49 CFR 571.121) in the 1970s. FMVSS 121 was issued in 1971, but implementation was delayed — and the regulations were amended until 1975. FMVSS 121 required newly manufactured commercial vehicles to be equipped with many of the following safety features found on modern vehicles:

• Anti-lock braking systems (ABS)

• Brakes on all axles, including front axle brakes

• Spring-actuated parking brakes

• Dual circuit braking systems

The original version of FMVSS 121 required commercial vehicles to stop from 60 mph in 217 feet (0.55 g). This stopping distance was amended first to 245 feet (0.49 g), then to 258 feet (0.47 g), and then to a 277 foot (0.43 g) stopping distance with the implementation of the law in 1975. To meet these early FMVSS 121 stopping distance criteria, commercial vehicles were designed with front brakes that generated significantly more torque than previous designs. The "overpowered" front brakes were prone to locking when the ABS system malfunctioned or failed, which occurred with regularity during the infancy of pneumatic ABS. When the front wheels stop rotating and lock, the vehicle loses directional stability and functional steering. Due to the "overpowered" front brake issue and others, the stopping distance requirement in FMVSS 121 was again amended in 1978 to 293 feet (0.41 g)[4]. In 1978, Paccar and the American Trucking Association successfully sued NHTSA to repeal the requirement for ABS brakes and the 293-foot stopping distance requirement.

The update of FMVSS 121 in 1995 re-established stopping distance requirements. The new requirement mandated that most truck tractors stop from 60 mph within 355 feet (0.34 g) while pulling an un-braked semi-trailer at its gross vehicle weight rating (GVWR). Unloaded tractors were mandated to stop within 335 feet (0.36 g)[5]. It would take until 1997 for a new legislative effort to again require ABS braking systems on pneumatically braked commercial vehicles.

In 2009, FMVSS 121 was again updated and beginning in 2011, most newly manufactured tractors were required to stop from 60 mph within 250 feet (0.48 g) while pulling an un-braked semi-trailer at GVWR. FMVSS 121 requires unloaded tractors to stop within 235 feet (0.51 g). It should be noted that even under the updated FMVSS 121, vehicles are not required to stop as quickly as mandated by the 1971 version of FMVSS 121[6]. **Figure 1** depicts the stopping distance requirements of FMVSS 121 for commercial vehicles manufactured after 2011/2013.

In-service vehicles are governed by Federal Motor Carrier Safety Regulations (FMCSR) — specifically FMCSR 393 (49 CFR 393) — with regard to the braking system. A common area of confusion in collision investigation and litigation involving commercial vehicles surrounds which braking performance regulation applies to the vehicle in question. The simple answer is FMVSS only applies to newly manufactured vehicles, not in-service vehicles. If, as manufactured, the vehicle in question

TABLE II - STOPPING DISTANCE IN FEET

Vehicle speed in miles per hour	Service brake						Emergency brake	
	PFC 0.9	PFC 0.9	PFC 0.9	PFC 0.9	PFC 0.9	PFC 0.9	PFC 0.9	PFC 0.9
	(1)	(2)	(3)	(4)	(5)	(6)	(7)	(8)
30	70	78	65	78	84	61	170	186
35	96	106	89	106	114	84	225	250
40	125	138	114	138	149	108	288	325
45	158	175	144	175	189	136	358	409
50	195	216	176	216	233	166	435	504
55	236	261	212	261	281	199	520	608
60	280	310	250	310	335	235	613	720

NOTE:

(1) Loaded and Unloaded Buses.

(2) Loaded Single-Unit Trucks.

(3) Loaded Tractors with Two Axles; or with Three Axles and a GVWR of 70,000 lbs. or less; or with Four or More Axles and a GVWR of 85,000 lbs. or less. Tested with an Unbraked Control Trailer.

(4) Loaded Tractors with Three Axles and a GVWR greater than 70,000 lbs.; or with Four or More Axles and a GVWR greater than 85,000 lbs. Tested with an Unbraked Control Trailer.

(5) Unloaded Single-Unit Trucks.

(6) Unloaded Tractors (Bobtail).

(7) All Vehicles except Tractors, Loaded and Unloaded.

Figure 1
FMVSS 121 table.

does not meet FMVSS regulations, then it would be in violation of FMVSS standards. However, if an in-service vehicle has not been properly maintained and no longer meets FMVSS standards, this is not in violation of FMVSS regulations, but rather a potential violation of the Federal Motor Carrier Safety Regulations.

FMCSR 393 mandates that tractor semi-trailers be capable of generating 43.5% peak braking force (0.435 g) as a percentage of their combination weight, decelerate with a peak rate of at least 14 feet/sec^2 (0.435 g), and stop from 20 mph within 40 feet (0.33 g). These criteria must be met by in-service vehicles in the as-loaded condition. Take note that the deceleration rate and braking force percentage of vehicle/combination weight is the peak value, not the average, whereas the stopping distance is a road test designed to account for overall braking system effectiveness. **Figure 2** depicts the braking performance mandated for in-service vehicles[7].

General Pneumatic Brake System Overview

Pneumatic braking systems have several commonalities with the hydraulic braking system employed in passenger vehicles. However, instead of using an (ideally) incompressible fluid in a hydraulic system, a pneumatic system uses a compressible fluid (air). Pneumatic braking systems, in general, are more complex when compared to hydraulic braking systems. The majority of pneumatic braking systems on heavy vehicles in the United States employ a type of brake system called S-cam drum brakes.

Pneumatic braking systems use compressed air to activate a series of mechanical linkages, which, in turn, press friction material (brake shoe/pad) into a heat sink (brake drum/rotor). Brakes, whether a passenger vehicle equipped with a hydraulic braking system or a heavy vehicle equipped with pneumatic brakes, complete the same function, converting kinetic energy into thermal energy to slow the vehicle. The thermal energy is then dissipated into the atmosphere so that the vehicle braking system's heat sinks can accept more energy.

Modern pneumatic brakes consist of two braking systems: service brakes and parking brakes. Service brakes simply provide stopping power while the vehicle is in service. The parking, or spring brakes, ensure that a vehicle does not move while parked, and will not release until the system has built enough pressure to operate the service brakes. Additionally, spring brakes activate to slow a vehicle when absent sufficient air pressure to operate

Type of motor vehicle	Service brake systems			Emergency brake systems
	Braking force as a percentage of gross vehicle or combination weight	Deceleration in feet per second per second	Application and braking distance in feet from initial speed at 20 mph	Application and braking distance in feet from initial speed of 20 mph
A. Passenger-carrying vehicles:				
(1) Vehicles with a seating capacity of 10 persons or less, including driver, and built on a passenger car chassis	65.2	21	20	54
(2) Vehicles with a seating capacity of more than 10 persons, including driver, and built on a passenger car chassis; vehicles built on a truck or bus chassis and having a manufacturer's GVWR of 10,000 pounds or less	52.8	17	25	66
(3) All other passenger-carrying vehicles	43.5	14	35	85
B. Property-carrying vehicles:				
(1) Single unit vehicles having a manufacturer's GVWR of 10,000 pounds or less	52.8	17	25	66
(2) Single unit vehicles having a manufacturer's GVWR of more than 10,000 pounds, except truck tractors. Combinations of a 2-axle towing vehicle and trailer having a GVWR of 3,000 pounds or less. All combinations of 2 or less vehicles in drive-away or tow-away operation	43.5	14	35	85
(3) All other property-carrying vehicles and combinations of property-carrying vehicles	43.5	14	40	90

Figure 2
FMCSR table.

the service brakes. Spring brakes are operated by evacuating air from the spring brake chamber, which is facilitated through a push/pull button on the dash at the driver's position in the cab.

Generally, S-cam drum brake function can be described in the following manner:

• The driver presses the treadle valve (foot brake) to apply the service brakes.

• Valves are opened, allowing compressed air to flow into the braking circuit from the supply circuit.

• Compressed air pressurizes the brake chambers at each axle, energizing the brakes.

• The brake pushrod extends from the brake chamber and applies a force to the brake slack adjustor

• In response to the force from the brake pushrod, the slack adjustor rotates and applies torque to the S-cam.

• The S-cam rotates, forcing the brake shoes to ride up the S-cam and displace outward.

• The friction lining on the brake shoes are forced against the inner surface of the brake drum, generating friction.

• The friction generated between the brake shoe lining and the brake drum surface converts the vehicle's kinetic energy into thermal energy.

• The brake drum acts as a heat sink and radiates heat to the atmospheres.

• Upon release of the treadle valve, air is evacuated from the brake chambers and the pushrods retract.

• As the pushrods retract, the brake shoes move away from the drum and cease to generate friction.

Braking System Failures

During the century following the invention of the commercial vehicle pneumatic braking system, pneumatic brakes have been refined with greater efficiency and reliability. Still, braking system deficiencies are found on a regular basis during inspections or following a collision event. Ineffective pre-trip inspections and a lack of proper maintenance lead to many braking deficiencies overlooked prior to a potentially catastrophic event.

The factors involved in partial or complete braking system failure are often not readily evident without a technical inspection of the braking system. Following are some of the most common areas where deficiencies are found within a commercial vehicle's braking system:

- Excessive pushrod stroke (out of adjustment)
- Thermal failures in the drum
- Fluid contamination between the drum and brake shoe friction material
- Air leaks or low pressure
- Non-functioning valves
- Worn drums and/or shoes
- Improperly matched brake components
- S-cam rollover (i.e., beyond operational limits)
- ABS failures

Excessive pushrod travel, or "stroke," is the most commonly cited brake system deficiency found during roadside inspection of heavy vehicles[8]. Excessive pushrod travel during brake application results in an "out-of-adjustment" brake. Pushrod travel is simply the change in distance between the fully retracted (no braking) position of the pushrod and its fully extended (full braking air pressure applied) position. The travel of the pushrod is commonly referred to as "pushrod stroke." Pushrod stroke is determined by measuring the distance of an arbitrary point on the pushrod (usually the clevis pin connection to the slack adjuster) from the brake chamber face without brake application. Following brake application with 90 to 100 psi of pressure, the distance from the brake chamber face to the same arbitrary point on the pushrod is again measured. The difference between the two measurements provides the pushrod stroke.

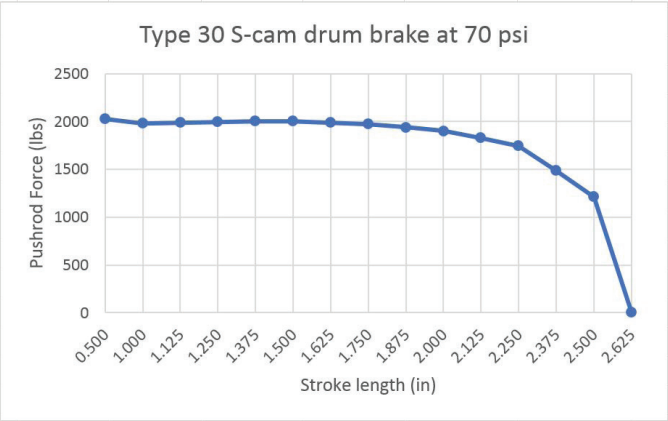

Figure 3
Type 30 S-cam at 70 psi pressure.

Excessive pushrod stroke decreases the available braking force to activate a given brake. The reason excessive pushrod stroke is detrimental to braking force generation lies in the fact that the brake chamber diaphragm can only flex so much before it starts binding on the interior of the brake chamber. Once binding occurs, the applied force decreases rapidly. At the extreme end of the excessive pushrod travel, the pushrod "strokes out" or "bottoms out," such that the diaphragm can no longer move the pushrod to apply further torque to the S-cam. When the diaphragm bottoms out, no additional braking force can be generated, regardless of applied air pressure. Plotting the force applied through the pushrod at a given brake pressure application for increasing pushrod strokes based upon published data[9] generates the graph shown in **Figure 3**. The force curve illustrates that the force generated decreases as the stroke length increases, and finally drops to zero when the brake diaphragm bottoms out.

If the brake shoe does not sufficiently engage the brake drum as a brake strokes-out, the brake will cease to develop braking force. When one brake fails to develop force, the amount of work required at the other brakes to slow the vehicle will increase. Increasing the work required of otherwise fully functioning brakes, even in non-emergency slowing situations, can lead to excessive heat build-up, which, in turn, can produce additional brake failures. Additionally, one non-functioning brake on an axle can lead to imbalance, and potentially decrease the vehicle's linear stability while braking.

To combat excessive pushrod stroke, the Federal Motor Carrier Safety Regulations (FMCSR) were modified to mandate automatic slack adjustors. Even following this 1994 mandate, excessive pushrod travel remains a common braking deficiency issue, although with less frequency.

Automatic slack adjustors are not the panacea for excessive pushrod stroke. On September 7, 2017, the Commercial Vehicle Safety Alliance conducted its annual Brake Safety Day, in which 7,698 commercial motor vehicles were inspected. As a result, 14% of the

commercial motor vehicles were deemed "Out-of-Service"[10] due to brake system deficiencies. The "Out-of-Service" designation indicates that, at a minimum, 20% of the vehicle's brakes were defective/out-of-adjustment, or the braking system had other significant safety issue(s).

Braking Performance Analysis

Several available methods provide for the analysis of pneumatic braking system performance. The methods range from simple to complex modeling. Several software suites offer brake analysis packages utilizing a variety of these methods. The methods presented in this study have their foundations in both physical constraints and empirical modeling. The selection of a brake analysis methodology depends upon the information available and the level of precision necessary to assess performance. The models presented are commonly used to determine the rate of deceleration of a heavy vehicle, and the speed of the vehicle at the beginning of observable brake application.

Commercial Vehicle Factor Method Using Skid to Stop

The Commercial Vehicle Factor (CVF) method, also known as the commercial motor vehicle factor (CMV_n)[11] or single adjusted drag factor method[12], uses an empirical percentage of the full drag factor to estimate the deceleration of a vehicle under full locked-wheel brake application. Using a CVF requires knowledge of the coefficient of tire-roadway friction for a passenger vehicle on the surface in question. Once the coefficient of tire-roadway friction for a passenger vehicle is known or determined, a CVF efficiency percentage is applied to approximate an effective drag factor for the heavy vehicle braking on the same roadway surface. The CVF is based upon empirical testing of heavy vehicles on surfaces with known passenger vehicle tire-roadway friction. The CVF is commonly ranged anywhere between 65% to 85%, depending upon the vehicle configuration, condition, tread of the tires, and other factors related to tire design. Multiplying the passenger vehicle tire-roadway coefficient of friction by the proper CVF determines the effective drag factor for a heavy vehicle. Using the adjusted drag factor, kinematic principles are applied to estimate the vehicle's speed at the beginning of observable brake application using a "skid-to-stop" formula, provided the vehicle skids to a complete stop. An example of this type of analysis is shown in **Figure 4**.

Weight Distribution Method

The weight distribution method provides the simplest analysis accounting for non-functioning brakes on a multi-axle vehicle. As with the CVF method, this method cannot account for brakes having partial functionality below wheel lockup. This method expands upon the CVF method with added considerations.

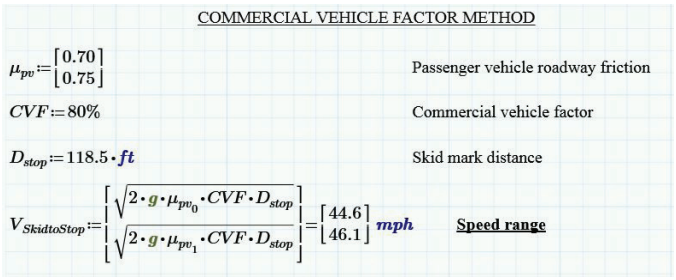

Figure 4
Commercial vehicle factor.

The weight distribution method requires knowing or estimating the weight at each axle end. This is accomplished by either measuring the weight at each wheel or set of duals, or by using general models of weight distribution based upon load and configuration. In this analysis, if a brake at any road wheel position is non-functional, the CVF for that braked wheel position (CVFn) is set to 0%, which results in no braking force at that wheel. The following equations determine the slowing acceleration rate and the vehicle's speed at the beginning of the observable brake application. An example analysis, conducted using the weight distribution method of both a fully braked vehicle and a vehicle with disabled semi-trailer brakes, are contained in **Appendix A** to this paper.

Braking force at each brake position/axle end:

$$F_n = \mu \times CVF_n \times w_n \quad (1)$$

Where,
F_n=braking force at brake n (lbs)
μ=passenger vehicle tire-roadway coefficient of friction
CVF_n=commercial vehicle factor at brake n
w_n=weight at n axle end (lbs)

Effective braking acceleration rate of heavy vehicle:

$$\mu_{cmv} = (\sum_{n}^{i=1} F_n) \div W \quad (2)$$

Where,
μ_{cmv}=drag factor of commercial vehicle
W=total weight (lbs)

Velocity at start of full brake application:

$$v=\sqrt{2\times D\times \mu_{cmv}\times g} \quad (3)$$

Where,
v=velocity at start of full brake application
D=distance of full braking marks (ft)

Heusser Method[13]

In 1991, Heusser published the first practical pneumatic braking analysis method considering the air pressure at the brake chamber and the measured brake stroke. Heusser obtained data from brake dynamometer tests performed by NHTSA, and developed his analysis method based upon applying regression analysis to the data, as well as obtaining test data from brake manufacturers.

The Heusser analysis uses a brake force design calculation modified to fit empirical data. The Heusser method calculates the force applied by the brakes at the tire-road interface for each of n brake positions using the following Equation 4.

Attempted braking force from each n brake:

$$Bforce_n=\left[\frac{2\times Pforce\times SL\times 0.35\times DRad}{CamRad\times TRad}\right]\times 0.6 \quad (4)$$

Where,
Pforce=force of pushrod (lbs)
SL=slack adjustor length (in)
DRad=brake drum radius (in)
CamRad=S-cam radius (in)
TRad=loaded radius of tire (in)

All variables, with the exception of the pushrod force, are directly measured on the vehicle. The ideal pushrod force is calculated by multiplying the air pressure at the brake chamber by the surface area in square-inches of the brake chamber diaphragm. However, direct measurement of pushrod force reveals losses in the system that cannot be accounted for by this idealized equation.

Pushrod force tables have been generated from testing by brake manufacturers and other researchers. Heusser's paper provided pushrod force tables, and some data can be found from other sources. These tables have two independent variables: air pressure and pushrod stroke. Once air pressure at the brake chamber and pushrod stroke are determined, pushrod force is extracted from the tables and entered into Equation 4 to solve for the brake force at each of n brake positions.

When using the Heusser method, it is important to ensure that the calculated attempted brake force does not exceed the maximum force to fully lock the tire(s) at the brake position. The maximum force for each brake position is calculated using Equation 1 of the weight distribution method. The smaller value between the calculated attempted brake force and calculated maximum brake force must be used in the determination of the vehicle drag factor or the analysis is invalid. This check is necessary because a brake cannot generate more force than when it is fully locked. An example using the Heusser analysis method is presented in **Appendix B** to this paper.

Bartlett/Heusser Method[14]

In 2007, the Heusser method was modified by Bartlett[14] to account for the effects of ABS braking within a pneumatic brake force analysis. Bartlett's method introduces modifications to the Heusser braking force equation when the attempted brake force (Equation 4) is greater than the force required to lock the wheel (Equation 1), and the vehicle is equipped with anti-lock brakes. The modification involves reducing the brake application pressure between 8 psi to 20 psi below the pressure required to lock the wheel(s) at the brake location and then recalculating the braking force with this lower application pressure. Here Bartlett suggests that reducing the brake application pressure by 8 psi below what is required to fully lock the wheel(s) at any braking position represents what occurs during the pressure cycling of full ABS braking on a modern pneumatic braking system. Reducing the brake application pressure by 20 psi at a brake position for the analysis is recommended to compensate for the slower cycling rate of previous generations of ABS system.

In a 2004 SAE paper[15], Bartlett rearranged and graphed Heusser's tabulated pushrod force data with brake application pressure as the independent variable on the horizontal axis and pushrod force as the dependent variable on the vertical axis for a fixed brake stroke. This rearrangement of the tabulated pushrod force data for stroke produced a mostly linear data correlation as depicted by **Figure 5**, as opposed to the traditional Heusser method depicted in **Figure 3**. **Figure 5** depicts pushrod force versus pressure for a Type 30 S-cam brake with a stroke of 1.000 inches, 2.000 inches and 2.375 inches.

Rearranging the brake force tables in this manner as put forth by Bartlett allows for a linear regression analysis to determine the slope (mL) and y-intercept (bL) of the pushrod force of a brake at varying pressures with a given stroke. Using the equation generated by the linear

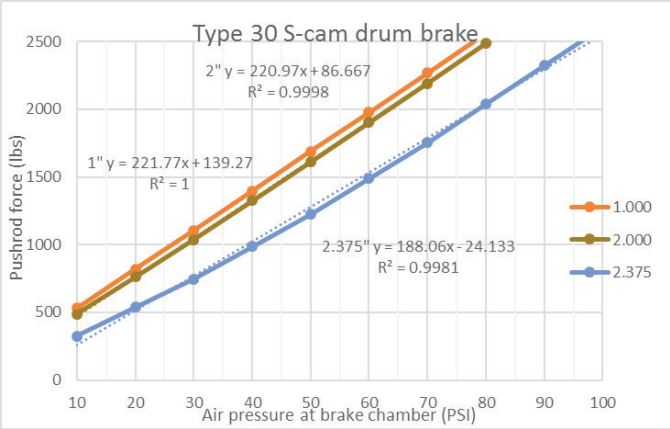

Figure 5
Type 30 S-cam drum brake.

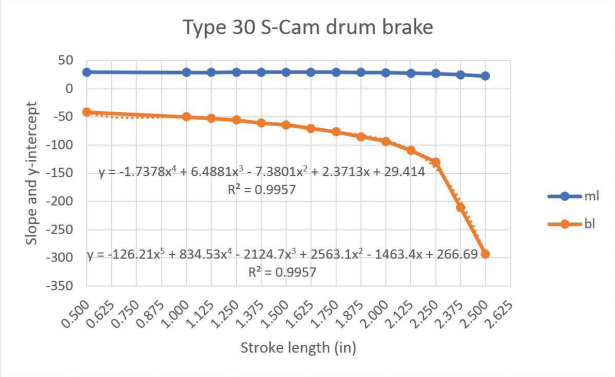

Figure 6
Type 30 S-cam regression analysis.

regression analysis eliminates the arduous task of interpolation and iteration required for the Heusser method, resulting in fewer steps where errors can be introduced when determining the brake force to lock.

Additionally, Bartlett advocates using polynomial regression analysis on both the calculated slope and y-intercepts of the linear regressions. After completing a polynomial regression analysis, the resulting equations result in pushrod force expressed as only a function of pushrod stroke and applied air pressure. This eliminates the need for interpolation for stroke lengths, as depicted in **Figure 6**.

Using the equations from the regression analysis of the brake tables, the brake force equation is rewritten to solve for brake application pressure required to lock the tire(s) at the n brake position. This is accomplished by setting the attempted brake force equal to the maximum brake force at each n brake position and incorporating the results of the regression analysis. Bartlett's brake application pressure to lock is presented as Equation 5.

Brake application pressure to lock each n brake:

$$P_L = \frac{W \times f_r \times CamRad \times TRad}{2 \times SL \times 0.6 \times 0.35 \times DRad \times m_L} - b_L \div m_L \quad (5)$$

Where,
P_L = Brake pressure to lock brake (psi)
W=weight at wheel end (lbs)
f_r=μ*CVF
CamRad=S-cam radius (in)
TRad=loaded radius of tire (in)
SL=slack adjustor length (in)
DRad=brake drum radius (in)
m_L=the slope of the linear regression (lbs/psi)
b_L=the Y-intercept of the linear regression (lbs)

If the heavy vehicle is generating more attempted brake force than the maximum available brake force (force to lock the wheel), then the brake application pressure at lockup is calculated. Then, the reduction of brake application pressure (8 psi to 20 psi depending upon ABS brake system vintage) for ABS cycling during ABS locked wheel braking is applied. Using this resultant brake application pressure and the regression analysis in **Figure 5**, the pushrod force is calculated. This pushrod force is then used to calculate the brake force during full ABS braking using Equation 4. The summation of brake force at each wheel is then used to determine the slowing acceleration rate of the commercial vehicle during full ABS locked braking by dividing the total brake force by the total weight of the commercial vehicle combination. The Bartlett method produces an accurate and reliable means to analyze the braking capabilities of a pneumatically braked vehicle equipped with anti-lock brakes while accounting for brake system deficiencies.

A complete work-through example analysis using the Bartlett method is presented in **Appendix C**. The example in **Appendix C** covers both full activation of the anti-lock braking system on a tractor and semi-trailer, and the situation where only two lightly loaded axles produce lock up, and a limiting brake application pressure for the entire braking system is determined.

Performance Analysis Steps

When dealing with commercial vehicle braking systems, the forensic engineer must determine several variables. The most accurate means to gather analysis variables results from direct inspection of the braking system

following the collision or incident event. However, oftentimes the involvement in a case occurs after the vehicle has been altered or is no longer available. When direct inspection and measurement of the braking system cannot occur, reliable sources of data and sound engineering judgement must be used to determine the variables needed for analysis.

The following items should be collected at a minimum during a direct inspection of the braking system to complete a proper braking performance analysis:

- Weight at each axle end
- Pushrod stroke at each brake
- Brake chamber size/type
- Slack adjustor length
- Brake drum diameter
- Tire rolling radius

Additional braking system information such as ABS configuration, placement of sensors and modulators, etc., may become beneficial to obtain during an inspection depending upon the scope of the analysis and particulars of the incident.

The following general analytical steps provide the braking force and deceleration rate of a pneumatically braked vehicle:

1. Determine force to lock wheel(s) at each axle end (Equation 1).

2. Obtain pushrod force from tables[9,13] or regression analysis (**Figure 4** and **Figure 6**), based upon application pressure, brake chamber type/size, and pushrod stroke.

3. Calculate attempted brake force (Equation 4).

4. Determine if attempted brake force is greater than the force required to cause the wheel(s) on the axle ends to lock (Equation 4 ≥ Equation 1).

5. If vehicle/vehicle combination is not equipped with an ABS system, or attempted brake force is less than force to lock wheel(s) at axle end (Equation 4 < Equation 1), then calculate deceleration rate using the lower of the attempted brake force versus the force to lock the wheel(s) (Equation 2).

6. If vehicle/vehicle combination is equipped with a functioning anti-lock braking system and the attempted brake force is greater than the force to lock the wheel(s) at axle end (Equation 4 ≥ Equation 1), then calculate the brake application pressure to lock the wheel(s) at each axle end (Equation 5).

6a. Alternatively, if the pushrod force tables are used instead of the regression analysis, then Equation 6 determines the pushrod force to lock the brake at an axle end.

Pushrod force to lock each n brake:

$$PR_L = \frac{W \times f_r \times CamRad \times TRad}{2 \times SL \times 0.6 \times 0.35 \times DRad} \quad (6)$$

Where,
PR_L= Pushrod force to lock wheel (lbs)
W=weight at wheel end (lbs)
f_r=μ*CVF
CamRad=S-cam radius (in)
TRad=loaded radius of tire (in)
SL=slack adjustor length (in)
DRad=brake drum radius (in)

Interpolation can then be used to determine brake application pressure, which will lock the brake at an axle end (P_L) by using Equation 7.

Brake application pressure to lock each n brake:

$$P_L = \frac{\Delta P}{PF_{L+10} - PF_{L+10}} \times (PF_L - PF_{L-10}) + PSI_{-10} \quad (7)$$

Where,
P_L =Pressure to lock by interpolation (PSI)
PSI_{-10}=Air pressure at data point in pushrod force tables below pushrod force required to lock n brake
ΔP=Difference in pressure between to two data points in table (typically 10)
PF_{L+10}=Pushrod force from tables at data point greater than calculated pushrod force to lock
PF_{L-10}=Pushrod force from tables at data point less than calculated pushrod force to lock

7. Reduce the brake application pressure by 8 psi for faster cycling modern ABS systems and up to

20 psi for slower cycling ABS systems generally seen on older vehicles — from the brake application pressure calculated in Step 6, and recalculate pushrod force from tables[9,13] or regression analysis with new, lower brake application pressure (PFABS) (Fig. 4 and 6)

7a. If using the tables instead of regression analysis, interpolate the pushrod force under full ABS braking (Equation 8).

Pushrod force during full ABS braking at each n brake:

$$PF_{ABS} = \frac{PF_{L+10} - PF_{L+10}}{\Delta P} \times (PSI_{ABS} - PSI_{-10}) + PF_{L-10} \qquad (8)$$

Where,
PF_{ABS}=Pushrod force during full ABS braking (lbs)
PSI_{ABS}=8 psi to 20 psi subtracted from pressure to lock
PSI_{-10}= Air pressure at data point in pushrod force tables below calculated pushed force
ΔP=Difference in pressure between to two data points in table (typically 10)
PF_{L+10}=Pushrod force from tables at data point greater than calculated pushrod force
PF_{L-10}=Pushrod force from tables at data point less than calculated pushrod force

8. Calculate brake force using newly calculated pushrod force (PFABS) (Equation 4).

9. Determine deceleration rate using the calculated ABS brake force (Equation 2).

Findings and Final Observations

The braking system of modern commercial vehicles is complex, presenting many different areas where defects can occur. A thorough technical understanding of pneumatic brakes is necessary for the forensic engineer to accomplish a proper inspection and analysis of the braking system. Thorough post-crash inspection of braking components often represents an important step in the scope of a forensic engineering investigation. Oftentimes, without the thorough inspection of the braking system, factors related to speed and avoidance may be mistakenly identified or missed altogether.

A proper commercial vehicle's braking system performance analysis may be crucial to determining the speed, deceleration or elements related to vehicle loss of control for a commercial vehicle leading up to a collision or incident event. The methods presented in this paper, which are generally accepted and widely used when assessing pneumatic braking system performance, produce reliable results when performed correctly.

Future work should investigate and publish data regarding the brake application pressure drop during full ABS braking. To-date, no publicly published papers measure and report more exacting data regarding the air pressure drop during ABS cycling. Such research is anticipated to provide greater understanding to the forensic engineering community with increased precision when analyzing full ABS locked wheel braking events.

References

1. Office of Research and Analysis. Large Truck Crash Causation Study FMCSA-RI-05-037. Washington D.C.: Federal Motor Carrier Safety Administration; 2006.

2. Michigan State Police Motor Carrier Enforcement Division. Fatal Accident Complaint Team Data 1996-2001. Detroit, MI: Michigan State Police; 2002.

3. Buckman L. Commercial Vehicle Braking Systems: Air Brakes, ABS and Beyond, Warrendale, PA: Society of Automotive Engineers International; 1998.

4. Paccar, Inc v. National Highway Traffic Safety, 573 F.2d 632 (9th Cir. 1978).

5. Bendix Spicer Foundation Brake LLC. The Federal Reduced Stopping Distance Mandate: Impact and Solutions Updated August 2013. Elyria, OH: Bendix Spicer Foundation Brake LLC; 2013.

6. 49 CFR 571.121 - Standard No. 121; Air brake systems

7. 49 CFR 393 subpart C – Brakes

8. State of California Department of Motor Vehicles. Commercial Driver Handbook, Section 5: Air Brakes. California Department of Motor Vehicles; 2017. [Online].

9. Grimes W, Heusser R. Updated Heavy Truck Air Chamber Force Data Charts. Accident Reconstruction Journal Volume 26, Number 6, November/December 2016.

10. Leandro N. CSVA Releases Results from Brake Safety Day, Greenbelt: Commercial Vehicle Safety Alliance, 2017.

11. Brill D. Commercial Motor Vehicle Crash Investigation, Jacksonville, FL, Institute of Police Technology and Management; 2000.

12. Fricke L. Traffic Crash Reconstruction, Evanston, IL: Northwestern University Center for Public Safety; 2010.

13. Heusser R. Heavy Truck Deceleration Rates as a Function of Brake Adjustment. SAE Technical Paper 910126. Warrendale, PA: Society of Automotive Engineers; 1991.

14. Bartlett W. Calculation of Deceleration Rates for S-Cam Air-Braked Heavy Trucks Equipped with Anti-Lock Brake Systems. SAE Technical Paper 2007-01-0714. Warrendale, PA: SAE International; 2007.

15. Bartlett W. Calculation of Heavy Truck Deceleration Based on Air Pressure Rise-Time and Brake Adjustment. SAE Technical Paper 2004-01-2632. Warrendale, PA: SAE International; 2004.

Appendix A

WEIGHT DISTRIBUTION METHOD:
WEIGHTS, LOADS:

$i := 1 .. 2$

Left side weight by axle:

$$W_L := \begin{bmatrix} 5300 \\ 3650 \\ 3500 \\ 2900 \\ 2500 \end{bmatrix} \cdot lb$$

Right side weight by axle:

$$W_R := \begin{bmatrix} 5650 \\ 3400 \\ 3200 \\ 3650 \\ 3300 \end{bmatrix} \cdot lb$$

$$Weight1 := \sum_{i=1}^{5} W_{L_i} + \sum_{i=1}^{5} W_{R_i} = 37050\ lb$$

$$\mu_{pv} := \begin{bmatrix} 0.70 \\ 0.75 \end{bmatrix}$$ Passenger vehicle roadway friction

$CVF := 80\%$ Commercial vehicle factor

Force generated by left side brakes (all brakes functioning)

$$F_{nLf} := \begin{bmatrix} \text{mean}\langle \mu_{pv} \cdot CVF \rangle \cdot W_{L_1} \\ \text{mean}\langle \mu_{pv} \cdot CVF \rangle \cdot W_{L_2} \\ \text{mean}\langle \mu_{pv} \cdot CVF \rangle \cdot W_{L_3} \\ \text{mean}\langle \mu_{pv} \cdot CVF \rangle \cdot W_{L_4} \\ \text{mean}\langle \mu_{pv} \cdot CVF \rangle \cdot W_{L_5} \end{bmatrix} = \begin{bmatrix} 3074 \\ 2117 \\ 2030 \\ 1682 \\ 1450 \end{bmatrix} lb$$

Force generated by right side brakes

$$F_{nRf} := \begin{bmatrix} \text{mean}\langle \mu_{pv} \cdot CVF \rangle \cdot W_{R_1} \\ \text{mean}\langle \mu_{pv} \cdot CVF \rangle \cdot W_{R_2} \\ \text{mean}\langle \mu_{pv} \cdot CVF \rangle \cdot W_{R_3} \\ \text{mean}\langle \mu_{pv} \cdot CVF \rangle \cdot W_{R_4} \\ \text{mean}\langle \mu_{pv} \cdot CVF \rangle \cdot W_{R_5} \end{bmatrix} = \begin{bmatrix} 3277 \\ 1972 \\ 1856 \\ 2117 \\ 1914 \end{bmatrix} lb$$

Force generated by left side brakes (trailer brakes disabled)

$$F_{nL} := \begin{bmatrix} \text{mean}\langle \mu_{pv} \cdot CVF \rangle \cdot W_{L_1} \\ \text{mean}\langle \mu_{pv} \cdot CVF \rangle \cdot W_{L_2} \\ \text{mean}\langle \mu_{pv} \cdot CVF \rangle \cdot W_{L_3} \\ \text{mean}\langle \mu_{pv} \cdot 0 \rangle \cdot W_{L_4} \\ \text{mean}\langle \mu_{pv} \cdot 0 \rangle \cdot W_{L_5} \end{bmatrix} = \begin{bmatrix} 3074 \\ 2117 \\ 2030 \\ 0 \\ 0 \end{bmatrix} lb$$

Force generated by right side brakes

$$F_{nR} := \begin{bmatrix} \text{mean}\langle \mu_{pv} \cdot CVF \rangle \cdot W_{R_1} \\ \text{mean}\langle \mu_{pv} \cdot CVF \rangle \cdot W_{R_2} \\ \text{mean}\langle \mu_{pv} \cdot CVF \rangle \cdot W_{R_3} \\ \text{mean}\langle \mu_{pv} \cdot 0 \rangle \cdot W_{R_4} \\ \text{mean}\langle \mu_{pv} \cdot 0 \rangle \cdot W_{R_5} \end{bmatrix} = \begin{bmatrix} 3277 \\ 1972 \\ 1856 \\ 0 \\ 0 \end{bmatrix} lb$$

$$\mu_{cmvf} := \frac{\left(\sum F_{nLf} + \sum F_{nRf} \right)}{Weight1} = 0.58$$

Drag factor of commercial vehicle with all brakes functioning

Appendix A

$$\mu_{cmv} := \frac{\left(\sum F_{nL} + \sum F_{nR}\right)}{Weight1} = 0.387$$

Drag factor of heavy vehicle with trailer brakes disabled

$$D_{stop} := 118.5 \cdot ft$$

Skid mark distance

$$V_{SkidtoStop} := \begin{bmatrix} \sqrt{2 \cdot g \cdot \mu_{cmv} \cdot D_{stop}} \\ \sqrt{2 \cdot g \cdot \mu_{cmvf} \cdot D_{stop}} \end{bmatrix} = \begin{bmatrix} 37.0 \\ 45.3 \end{bmatrix} mph$$

Speed range by weight distribution method

Appendix B

HEUSSER METHOD
WEIGHTS, LOADS:

$i := 1..5$

Left side weight/slack adj(in)/stroke(in) by axle:

$$W_L := \begin{bmatrix} 5300 \\ 3650 \\ 3500 \\ 2900 \\ 2500 \end{bmatrix} \cdot lb \qquad SA_L := \begin{bmatrix} 5.5 \\ 5.5 \\ 5.5 \\ 5.5 \\ 6.0 \end{bmatrix} \cdot in$$

Right side weight/slack adj(in)/stroke(in) by axle:

$$W_R := \begin{bmatrix} 5650 \\ 3400 \\ 3200 \\ 3650 \\ 3300 \end{bmatrix} \cdot lb \qquad SA_R := \begin{bmatrix} 5.5 \\ 5.5 \\ 5.5 \\ 5.5 \\ 5.5 \end{bmatrix} \cdot in$$

$$Weight1 := \sum_{i=1}^{5} W_{L_i} + \sum_{i=1}^{5} W_{R_i} = 37050\ lb$$

$$ST_L := \begin{bmatrix} 1.25 \\ 1.375 \\ 1.625 \\ 1.875 \\ 1.5 \end{bmatrix}$$

Measured brake stroke

$$ST_R := \begin{bmatrix} 1.375 \\ 1.375 \\ 1.75 \\ 1.75 \\ 1.875 \end{bmatrix}$$

Left brake lining coeff. by axle:

$$L_L := \begin{bmatrix} 0.35 \\ 0.35 \\ 0.35 \\ 0.35 \\ 0.35 \end{bmatrix}$$

(SAE 910126)

Right brake lining coeff. by axle:

$$L_R := \begin{bmatrix} 0.35 \\ 0.35 \\ 0.35 \\ 0.35 \\ 0.35 \end{bmatrix}$$

Left Drum/Tire rolling radius (in) by axle

$$D_L := \begin{bmatrix} 8.25 \\ 8.25 \\ 8.25 \\ 8.25 \\ 8.25 \end{bmatrix} \cdot in \qquad T_L := \begin{bmatrix} 20.25 \\ 21 \\ 21 \\ 21 \\ 21 \end{bmatrix} \cdot in$$

Right Drum/Tire rolling radius (in) by axle:

$$D_R := \begin{bmatrix} 8.25 \\ 8.25 \\ 8.25 \\ 8.25 \\ 8.25 \end{bmatrix} \cdot in \qquad T_R := \begin{bmatrix} 20.25 \\ 21 \\ 21 \\ 21 \\ 21 \end{bmatrix} \cdot in$$

$Rc := 0.5 \cdot in$ S-Cam Radius (SAE 910128)

$Cf := 0.6$ Chamber Factor (SAE 910128)

$\mu_{pv} := \begin{bmatrix} 0.71 \\ 0.77 \end{bmatrix}$ Passenger vehicle roadway friction

$CVF := 80\%$ Commercial vehicle factor

Appendix B

$$FL_{max} := \begin{bmatrix} \text{mean}(\mu_{pv}) \cdot CVF \cdot W_{L_1} \\ \text{mean}(\mu_{pv}) \cdot CVF \cdot W_{L_2} \\ \text{mean}(\mu_{pv}) \cdot CVF \cdot W_{L_3} \\ \text{mean}(\mu_{pv}) \cdot CVF \cdot W_{L_4} \\ \text{mean}(\mu_{pv}) \cdot CVF \cdot W_{L_5} \end{bmatrix} = \begin{bmatrix} 3138 \\ 2161 \\ 2072 \\ 1717 \\ 1480 \end{bmatrix} lb$$

Maximum braking force prior to tire(s) lockup on left side

$$FR_{max} := \begin{bmatrix} \text{mean}(\mu_{pv}) \cdot CVF \cdot W_{R_1} \\ \text{mean}(\mu_{pv}) \cdot CVF \cdot W_{R_2} \\ \text{mean}(\mu_{pv}) \cdot CVF \cdot W_{R_3} \\ \text{mean}(\mu_{pv}) \cdot CVF \cdot W_{R_4} \\ \text{mean}(\mu_{pv}) \cdot CVF \cdot W_{R_5} \end{bmatrix} = \begin{bmatrix} 3345 \\ 2013 \\ 1894 \\ 2161 \\ 1954 \end{bmatrix} lb$$

Maximum braking force prior to tire(s) lockup on right side

$$PF_{L40} := \begin{bmatrix} 818 \\ 1112 \\ 1100 \\ 1064 \\ 1110 \end{bmatrix} \cdot lb$$

Pushrod force at 40psi at measured pushrod stroke for each brake from tables

$$PF_{R40} := \begin{bmatrix} 822 \\ 1112 \\ 1088 \\ 1088 \\ 1064 \end{bmatrix} \cdot lb$$

Brake Force equation (calculated for 40 psi brake application)

$$BF_{L40} := \begin{bmatrix} \frac{2 \cdot PF_{L40_1} \cdot SA_{L_1} \cdot Cf \cdot L_{L_1} \cdot D_{L_1}}{Rc \cdot T_{L_1}} \\ \frac{2 \cdot PF_{L40_2} \cdot SA_{L_2} \cdot Cf \cdot L_{L_2} \cdot D_{L_2}}{Rc \cdot T_{L_2}} \\ \frac{2 \cdot PF_{L40_3} \cdot SA_{L_3} \cdot Cf \cdot L_{L_3} \cdot D_{L_3}}{Rc \cdot T_{L_3}} \\ \frac{2 \cdot PF_{L40_4} \cdot SA_{L_4} \cdot Cf \cdot L_{L_4} \cdot D_{L_4}}{Rc \cdot T_{L_4}} \\ \frac{2 \cdot PF_{L40_5} \cdot SA_{L_5} \cdot Cf \cdot L_{L_5} \cdot D_{L_5}}{Rc \cdot T_{L_5}} \end{bmatrix} = \begin{bmatrix} 1540 \\ 2018 \\ 1997 \\ 1931 \\ 2198 \end{bmatrix} lb$$

$$BF_{R40} := \begin{bmatrix} \frac{2 \cdot PF_{R40_1} \cdot SA_{R_1} \cdot Cf \cdot L_{R_1} \cdot D_{R_1}}{Rc \cdot T_{R_1}} \\ \frac{2 \cdot PF_{R40_2} \cdot SA_{R_2} \cdot Cf \cdot L_{R_2} \cdot D_{R_2}}{Rc \cdot T_{R_2}} \\ \frac{2 \cdot PF_{R40_3} \cdot SA_{R_3} \cdot Cf \cdot L_{R_3} \cdot D_{R_3}}{Rc \cdot T_{R_3}} \\ \frac{2 \cdot PF_{R40_4} \cdot SA_{R_4} \cdot Cf \cdot L_{R_4} \cdot D_{R_4}}{Rc \cdot T_{R_4}} \\ \frac{2 \cdot PF_{R40_5} \cdot SA_{R_5} \cdot Cf \cdot L_{R_5} \cdot D_{R_5}}{Rc \cdot T_{R_5}} \end{bmatrix} = \begin{bmatrix} 1547 \\ 2018 \\ 1975 \\ 1975 \\ 1931 \end{bmatrix} lb$$

Appendix B

Use smaller of maximum brake force and brake force at application pressure

$$BF_{L_i} := min\left(FL_{max_i}, BF_{L40_i}\right) = \begin{bmatrix} 1540 \\ 2018 \\ 1997 \\ 1717 \\ 1480 \end{bmatrix} lb \qquad BF_{R_i} := min\left(FR_{max_i}, BF_{R40_i}\right) = \begin{bmatrix} 1547 \\ 2013 \\ 1894 \\ 1975 \\ 1931 \end{bmatrix} lb$$

Calculated deceleration determination:

$$Decel_{40} := \frac{\left(\sum BF_L + \sum BF_R\right)}{\left(\sum W_L + \sum W_R\right)} = 0.49$$

$D_{stop} := 118.5 \cdot ft$ Skid mark distance

$V := \sqrt{2 \cdot g \cdot Decel_{40} \cdot D_{stop}} = 41.6\ mph$ **Speed at beginning of skid mark with 40psi brake application**

Appendix C

$i := 1 .. 5$

BARTLETT/HEUSSER METHOD
WEIGHTS, LOADS:

Left side weight/slack adj(in)/stroke(in) by axle:

$$W_L := \begin{bmatrix} 5300 \\ 3650 \\ 3500 \\ 2900 \\ 2500 \end{bmatrix} \cdot lb \qquad SA_L := \begin{bmatrix} 5.5 \\ 5.5 \\ 5.5 \\ 5.5 \\ 6.0 \end{bmatrix} \cdot in$$

Right side weight/slack adj(in)/stroke(in) by axle:

$$W_R := \begin{bmatrix} 5650 \\ 3400 \\ 3200 \\ 3650 \\ 3300 \end{bmatrix} \cdot lb \qquad SA_R := \begin{bmatrix} 5.5 \\ 5.5 \\ 5.5 \\ 5.5 \\ 5.5 \end{bmatrix} \cdot in$$

$$Weight1 := \sum_{i=1}^{5} W_{L_i} + \sum_{i=1}^{5} W_{R_i} = 37050\ lb$$

$$ST_L := \begin{bmatrix} 1.25 \\ 1.375 \\ 1.625 \\ 1.875 \\ 1.5 \end{bmatrix}$$

Measured brake stroke

$$ST_R := \begin{bmatrix} 1.375 \\ 1.375 \\ 1.75 \\ 1.75 \\ 1.875 \end{bmatrix}$$

Left brake lining coeff. by axle:

$$L_L := \begin{bmatrix} 0.35 \\ 0.35 \\ 0.35 \\ 0.35 \\ 0.35 \end{bmatrix}$$

(SAE 910126)

Right brake lining coeff. by axle:

$$L_R := \begin{bmatrix} 0.35 \\ 0.35 \\ 0.35 \\ 0.35 \\ 0.35 \end{bmatrix}$$

Left Drum/Tire rolling radius (in) by axle

$$D_L := \begin{bmatrix} 8.25 \\ 8.25 \\ 8.25 \\ 8.25 \\ 8.25 \end{bmatrix} \cdot in \qquad T_L := \begin{bmatrix} 20.25 \\ 21 \\ 21 \\ 21 \\ 21 \end{bmatrix} \cdot in$$

Right Drum/Tire rolling radius (in) by axle:

$$D_R := \begin{bmatrix} 8.25 \\ 8.25 \\ 8.25 \\ 8.25 \\ 8.25 \end{bmatrix} \cdot in \qquad T_R := \begin{bmatrix} 20.25 \\ 21 \\ 21 \\ 21 \\ 21 \end{bmatrix} \cdot in$$

$Rc := 0.5 \cdot in$ S-Cam Radius (SAE 910128)

$Cf := 0.6$ Chamber Factor (SAE 910128)

$\mu_{pv} := \begin{bmatrix} 0.71 \\ 0.77 \end{bmatrix}$ Passenger vehicle roadway friction

$CVF := 80\%$ Commercial vehicle factor

Appendix C

Maximum braking force prior to tire(s) lockup

$$FL_{max} := \begin{bmatrix} \text{mean}(\mu_{pv}) \cdot CVF \cdot W_{L_1} \\ \text{mean}(\mu_{pv}) \cdot CVF \cdot W_{L_2} \\ \text{mean}(\mu_{pv}) \cdot CVF \cdot W_{L_3} \\ \text{mean}(\mu_{pv}) \cdot CVF \cdot W_{L_4} \\ \text{mean}(\mu_{pv}) \cdot CVF \cdot W_{L_5} \end{bmatrix} = \begin{bmatrix} 3138 \\ 2161 \\ 2072 \\ 1717 \\ 1480 \end{bmatrix} lb \quad FR_{max} := \begin{bmatrix} \text{mean}(\mu_{pv}) \cdot CVF \cdot W_{R_1} \\ \text{mean}(\mu_{pv}) \cdot CVF \cdot W_{R_2} \\ \text{mean}(\mu_{pv}) \cdot CVF \cdot W_{R_3} \\ \text{mean}(\mu_{pv}) \cdot CVF \cdot W_{R_4} \\ \text{mean}(\mu_{pv}) \cdot CVF \cdot W_{R_5} \end{bmatrix} = \begin{bmatrix} 3345 \\ 2013 \\ 1894 \\ 2161 \\ 1954 \end{bmatrix} lb$$

$$F_{limit} := \begin{bmatrix} FL_{max_5} \\ FR_{max_3} \end{bmatrix} = \begin{bmatrix} 1480 \\ 1894 \end{bmatrix} lb$$

Limiting force before other tractor tires lock and leave skid marks (5L and 3R)

BRAKING ANALYSIS USING:
Results of Regression Analysis

$$\begin{bmatrix} M_{L20L} \\ M_{L30L} \end{bmatrix} := \begin{bmatrix} 0.2645 \cdot ST_L^4 - 5.2403 \cdot ST_L^3 + 16.578 \cdot ST_L^2 - 16.864 \cdot ST_L + 24.211 \\ -1.7378 \cdot ST_L^4 + 6.4881 \cdot ST_L^3 - 7.3801 \cdot ST_L^2 + 2.3713 \cdot ST_L + 29.414 \end{bmatrix} \cdot \frac{lb}{psi}$$

$$\begin{bmatrix} B_{L20L} \\ B_{L30L} \end{bmatrix} := \begin{bmatrix} 19.206 \cdot ST_L^4 - 100.91 \cdot ST_L^3 + 158.54 \cdot ST_L^2 - 106.73 \cdot ST_L - 54.181 \\ -126.21 \cdot ST_L^5 + 834.53 \cdot ST_L^4 - 2124.7 \cdot ST_L^3 + 2563.1 \cdot ST_L^2 - 1463.4 \cdot ST_L + 266.69 \end{bmatrix} \cdot lb$$

$$\begin{bmatrix} M_{L20R} \\ M_{L30R} \end{bmatrix} := \begin{bmatrix} 0.2645 \cdot ST_R^4 - 5.2403 \cdot ST_R^3 + 16.578 \cdot ST_R^2 - 16.864 \cdot ST_R + 24.211 \\ -1.7378 \cdot ST_R^4 + 6.4881 \cdot ST_R^3 - 7.3801 \cdot ST_R^2 + 2.3713 \cdot ST_R + 29.414 \end{bmatrix} \cdot \frac{lb}{psi}$$

$$\begin{bmatrix} B_{L20R} \\ B_{L30R} \end{bmatrix} := \begin{bmatrix} 19.206 \cdot ST_R^4 - 100.91 \cdot ST_R^3 + 158.54 \cdot ST_R^2 - 106.73 \cdot ST_R - 54.181 \\ -126.21 \cdot ST_R^5 + 834.53 \cdot ST_R^4 - 2124.7 \cdot ST_R^3 + 2563.1 \cdot ST_R^2 - 1463.4 \cdot ST_R + 266.69 \end{bmatrix} \cdot lb$$

Appendix C

$$PL_L := \begin{bmatrix} \frac{FL_{max_1} \cdot Rc \cdot T_{L_1}}{2 \cdot SA_{L_1} \cdot Cf \cdot L_{L_1} \cdot D_{L_1}} - \frac{B_{L20L_1}}{M_{L20L_1}} \\ \frac{FL_{max_2} \cdot Rc \cdot T_{L_2}}{2 \cdot SA_{L_2} \cdot Cf \cdot L_{L_2} \cdot D_{L_2}} - \frac{B_{L30L_2}}{M_{L30L_2}} \\ \frac{FL_{max_3} \cdot Rc \cdot T_{L_3}}{2 \cdot SA_{L_3} \cdot Cf \cdot L_{L_3} \cdot D_{L_3}} - \frac{B_{L30L_3}}{M_{L30L_3}} \\ \frac{FL_{max_4} \cdot Rc \cdot T_{L_4}}{2 \cdot SA_{L_4} \cdot Cf \cdot L_{L_4} \cdot D_{L_4}} - \frac{B_{L30L_4}}{M_{L30L_4}} \\ \frac{FL_{max_5} \cdot Rc \cdot T_{L_5}}{2 \cdot SA_{L_5} \cdot Cf \cdot L_{L_5} \cdot D_{L_5}} - \frac{B_{L30L_5}}{M_{L30L_5}} \end{bmatrix} = \begin{bmatrix} 90 \\ 43 \\ 41 \\ 35 \\ 28 \end{bmatrix} psi$$

Brake application pressure to lock for left side

$$PL_R := \begin{bmatrix} \frac{FR_{max_1} \cdot Rc \cdot T_{R_1}}{2 \cdot SA_{R_1} \cdot Cf \cdot L_{R_1} \cdot D_{R_1}} - \frac{B_{L20R_1}}{M_{L20R_1}} \\ \frac{FR_{max_2} \cdot Rc \cdot T_{R_2}}{2 \cdot SA_{R_2} \cdot Cf \cdot L_{R_2} \cdot D_{R_2}} - \frac{B_{L30R_2}}{M_{L30R_2}} \\ \frac{FR_{max_3} \cdot Rc \cdot T_{R_3}}{2 \cdot SA_{R_3} \cdot Cf \cdot L_{R_3} \cdot D_{R_3}} - \frac{B_{L30R_3}}{M_{L30R_3}} \\ \frac{FR_{max_4} \cdot Rc \cdot T_{R_4}}{2 \cdot SA_{R_4} \cdot Cf \cdot L_{R_4} \cdot D_{R_4}} - \frac{B_{L30R_4}}{M_{L30R_4}} \\ \frac{FR_{max_5} \cdot Rc \cdot T_{R_5}}{2 \cdot SA_{R_5} \cdot Cf \cdot L_{R_5} \cdot D_{R_5}} - \frac{B_{L30R_5}}{M_{L30R_5}} \end{bmatrix} = \begin{bmatrix} 95 \\ 40 \\ 38 \\ 43 \\ 40 \end{bmatrix} psi$$

Brake application pressure to lock for right side

$$P_{ABS} := \begin{bmatrix} 8 \\ 20 \end{bmatrix} \cdot psi$$

Brake application pressure reduction for ABS cycling during full ABS brake application

$$P_{Labs} := PL_L - P_{ABS_1} = \begin{bmatrix} 82 \\ 35 \\ 33 \\ 27 \\ 20 \end{bmatrix} psi$$

Adjusted brake application pressure

$$P_{Rabs} := PL_R - P_{ABS_1} = \begin{bmatrix} 87 \\ 32 \\ 30 \\ 35 \\ 32 \end{bmatrix} psi$$

Appendix C

Pushrod Force to Lock

$$PF_L := \begin{bmatrix} M_{L20L_1} \cdot PL_{L_1} + B_{L20L_1} \\ M_{L30L_2} \cdot PL_{L_2} + B_{L30L_2} \\ M_{L30L_3} \cdot PL_{L_3} + B_{L30L_3} \\ M_{L30L_4} \cdot PL_{L_4} + B_{L30L_4} \\ M_{L30L_5} \cdot PL_{L_5} + B_{L30L_5} \end{bmatrix} = \begin{bmatrix} 1667 \\ 1191 \\ 1142 \\ 946 \\ 747 \end{bmatrix} lb \qquad PF_R := \begin{bmatrix} M_{L20R_1} \cdot PL_{R_1} + B_{L20R_1} \\ M_{L30R_2} \cdot PL_{R_2} + B_{L30R_2} \\ M_{L30R_3} \cdot PL_{R_3} + B_{L30R_3} \\ M_{L30R_4} \cdot PL_{R_4} + B_{L30R_4} \\ M_{L30R_5} \cdot PL_{R_5} + B_{L30R_5} \end{bmatrix} = \begin{bmatrix} 1777 \\ 1109 \\ 1044 \\ 1191 \\ 1076 \end{bmatrix} lb$$

Pushrod force for full ABS braking

$$PF_{Labs} := \begin{bmatrix} M_{L20L_1} \cdot P_{Labs_1} + B_{L20L_1} \\ M_{L30L_2} \cdot P_{Labs_2} + B_{L30L_2} \\ M_{L30L_3} \cdot P_{Labs_3} + B_{L30L_3} \\ M_{L30L_4} \cdot P_{Labs_4} + B_{L30L_4} \\ M_{L30L_5} \cdot P_{Labs_5} + B_{L30L_5} \end{bmatrix} = \begin{bmatrix} 1511 \\ 956 \\ 906 \\ 712 \\ 512 \end{bmatrix} lb \quad PF_{Rabs} := \begin{bmatrix} M_{L20R_1} \cdot P_{Rabs_1} + B_{L20R_1} \\ M_{L30R_2} \cdot P_{Rabs_2} + B_{L30R_2} \\ M_{L30R_3} \cdot P_{Rabs_3} + B_{L30R_3} \\ M_{L30R_4} \cdot P_{Rabs_4} + B_{L30R_4} \\ M_{L30R_5} \cdot P_{Rabs_5} + B_{L30R_5} \end{bmatrix} = \begin{bmatrix} 1620 \\ 874 \\ 808 \\ 955 \\ 843 \end{bmatrix} lb$$

Braking force during full ABS braking

$$BF_{Labs} := \begin{bmatrix} \frac{2 \cdot PF_{Labs_1} \cdot SA_{L_1} \cdot Cf \cdot L_{L_1} \cdot D_{L_1}}{Rc \cdot T_{L_1}} \\ \frac{2 \cdot PF_{Labs_2} \cdot SA_{L_2} \cdot Cf \cdot L_{L_2} \cdot D_{L_2}}{Rc \cdot T_{L_2}} \\ \frac{2 \cdot PF_{Labs_3} \cdot SA_{L_3} \cdot Cf \cdot L_{L_3} \cdot D_{L_3}}{Rc \cdot T_{L_3}} \\ \frac{2 \cdot PF_{Labs_4} \cdot SA_{L_4} \cdot Cf \cdot L_{L_4} \cdot D_{L_4}}{Rc \cdot T_{L_4}} \\ \frac{2 \cdot PF_{Labs_5} \cdot SA_{L_5} \cdot Cf \cdot L_{L_5} \cdot D_{L_5}}{Rc \cdot T_{L_5}} \end{bmatrix} = \begin{bmatrix} 2845 \\ 1734 \\ 1644 \\ 1293 \\ 1013 \end{bmatrix} lb \quad BF_{Rabs} := \begin{bmatrix} \frac{2 \cdot PF_{Rabs_1} \cdot SA_{R_1} \cdot Cf \cdot L_{R_1} \cdot D_{R_1}}{Rc \cdot T_{R_1}} \\ \frac{2 \cdot PF_{Rabs_2} \cdot SA_{R_2} \cdot Cf \cdot L_{R_2} \cdot D_{R_2}}{Rc \cdot T_{R_2}} \\ \frac{2 \cdot PF_{Rabs_3} \cdot SA_{R_3} \cdot Cf \cdot L_{R_3} \cdot D_{R_3}}{Rc \cdot T_{R_3}} \\ \frac{2 \cdot PF_{Rabs_4} \cdot SA_{R_4} \cdot Cf \cdot L_{R_4} \cdot D_{R_4}}{Rc \cdot T_{R_4}} \\ \frac{2 \cdot PF_{Rabs_5} \cdot SA_{R_5} \cdot Cf \cdot L_{R_5} \cdot D_{R_5}}{Rc \cdot T_{R_5}} \end{bmatrix} = \begin{bmatrix} 3048 \\ 1586 \\ 1467 \\ 1733 \\ 1530 \end{bmatrix} lb$$

Calculated ABS stop-deceleration rate determination using regression analysis:

$$Decel_{absr} := \frac{\left(\sum_{i=1}^{5} \left(BF_{Labs_i} \right) + \sum_{i=1}^{5} \left(BF_{Rabs_i} \right) \right)}{\left(\sum W_L + \sum W_R \right)} = 0.483$$

Appendix C

BRAKING ANALYSIS USING:

Interpolation

Pushrod Force to Lock

$$PFL_L := \begin{bmatrix} \frac{FL_{max_1} \cdot Rc \cdot T_{L_1}}{2 \cdot SA_{L_1} \cdot Cf \cdot L_{L_1} \cdot D_{L_1}} \\ \frac{FL_{max_2} \cdot Rc \cdot T_{L_2}}{2 \cdot SA_{L_2} \cdot Cf \cdot L_{L_2} \cdot D_{L_2}} \\ \frac{FL_{max_3} \cdot Rc \cdot T_{L_3}}{2 \cdot SA_{L_3} \cdot Cf \cdot L_{L_3} \cdot D_{L_3}} \\ \frac{FL_{max_4} \cdot Rc \cdot T_{L_4}}{2 \cdot SA_{L_4} \cdot Cf \cdot L_{L_4} \cdot D_{L_4}} \\ \frac{FL_{max_5} \cdot Rc \cdot T_{L_5}}{2 \cdot SA_{L_5} \cdot Cf \cdot L_{L_5} \cdot D_{L_5}} \end{bmatrix} = \begin{bmatrix} 1667 \\ 1191 \\ 1142 \\ 946 \\ 747 \end{bmatrix} lb$$

$$PFL_R := \begin{bmatrix} \frac{FR_{max_1} \cdot Rc \cdot T_{R_1}}{2 \cdot SA_{R_1} \cdot Cf \cdot L_{R_1} \cdot D_{R_1}} \\ \frac{FR_{max_2} \cdot Rc \cdot T_{R_2}}{2 \cdot SA_{R_2} \cdot Cf \cdot L_{R_2} \cdot D_{R_2}} \\ \frac{FR_{max_3} \cdot Rc \cdot T_{R_3}}{2 \cdot SA_{R_3} \cdot Cf \cdot L_{R_3} \cdot D_{R_3}} \\ \frac{FR_{max_4} \cdot Rc \cdot T_{R_4}}{2 \cdot SA_{R_4} \cdot Cf \cdot L_{R_4} \cdot D_{R_4}} \\ \frac{FR_{max_5} \cdot Rc \cdot T_{R_5}}{2 \cdot SA_{R_5} \cdot Cf \cdot L_{R_5} \cdot D_{R_5}} \end{bmatrix} = \begin{bmatrix} 1777 \\ 1109 \\ 1044 \\ 1191 \\ 1076 \end{bmatrix} lb$$

INTERPOLATION FOR BRAKE APPLICATION PRESSURE ANALYSIS:

$$PL_{limit} := \begin{bmatrix} PFL_{L_5} \\ PFL_{R_3} \end{bmatrix} = \begin{bmatrix} 747 \\ 1044 \end{bmatrix} lb$$

Limiting non-ABS Pushrod Force

$$PFL_{20} := \begin{bmatrix} 363 \\ 533 \\ 525 \\ 504 \\ 532 \end{bmatrix} \cdot lb$$

Pushrod force at 20psi at measured pushrod stroke for each brake from 2008 Rec-Tec tables

$$PFR_{20} := \begin{bmatrix} 364 \\ 533 \\ 516 \\ 516 \\ 504 \end{bmatrix} \cdot lb$$

$$PFL_{30} := \begin{bmatrix} 591 \\ 823 \\ 813 \\ 784 \\ 821 \end{bmatrix} \cdot lb$$

Pushrod force at 30psi at measured pushrod stroke for each brake from 2008 Rec-Tec tables

$$PFR_{30} := \begin{bmatrix} 593 \\ 823 \\ 802 \\ 802 \\ 784 \end{bmatrix} \cdot lb$$

$$PFL_{40} := \begin{bmatrix} 818 \\ 1112 \\ 1100 \\ 1064 \\ 1110 \end{bmatrix} \cdot lb$$

Pushrod force at 40psi at measured pushrod stroke for each brake from 2008 Rec-Tec tables

$$PFR_{40} := \begin{bmatrix} 822 \\ 1112 \\ 1088 \\ 1088 \\ 1064 \end{bmatrix} \cdot lb$$

$$PFL_{50} := \begin{bmatrix} 883 \\ 1409 \\ 1396 \\ 1355 \\ 1407 \end{bmatrix} \cdot lb$$

Pushrod force at 50psi at measured pushrod stroke for each brake from 2008 Rec-Tec tables

$$PFR_{50} := \begin{bmatrix} 891 \\ 1409 \\ 1382 \\ 1382 \\ 1355 \end{bmatrix} \cdot lb$$

Appendix C

$PF_{L80} := 1461 \cdot lb$ Pushrod force at 80psi at measured pushrod stroke for front axle brake from 2008 Rec-Tec tables $PF_{R80} := 1477 \cdot lb$

$PF_{L90100} := \begin{bmatrix} 1659 \\ 1857 \end{bmatrix} \cdot lb$ Pushrod force at 90psi and 100psi at measured pushrod stroke for front axle brake from 2008 Rec-Tec tables $PF_{R90100} := \begin{bmatrix} 1677 \\ 1877 \end{bmatrix} \cdot lb$

$PF_{L10} := 243 \cdot lb$ Pushrod force at 10psi at measured pushrod stroke for left axle 5 brake from 2008 Rec-Tec tables

$P_{10} := 10 \cdot psi \quad P_{20} := 20 \cdot psi \quad P_{30} := 30 \cdot psi \quad P_{40} := 40 \cdot psi \quad P_{50} := 50 \cdot psi \quad P_{80} := 80 \cdot psi$

$P_{90} := 90 \cdot psi \quad P_{100} := 100 \cdot psi \quad P_{ABS} := 8 \cdot psi$ Brake application pressure reduction for ABS activation

$$PSI_1 := \frac{\langle P_{30} - P_{20} \rangle}{\left(PFL_{30_5} - PFL_{20_5} \right)} \cdot \left(PL_{limit_1} - PFL_{20_5} \right) + P_{20} = 27.5 \ psi$$

Brake pressure to lock limiting brakes non-ABS

$$PSI_2 := \frac{\langle P_{40} - P_{30} \rangle}{\left(PFR_{40_3} - PFR_{30_3} \right)} \cdot \left(PL_{limit_2} - PFR_{30_3} \right) + P_{30} = 38.5 \ psi$$

Brake application pressure to lock limiting axles with full ABS lockup

$$PSI_{ABSL} := \begin{bmatrix} \frac{\langle P_{100} - P_{90} \rangle}{\left(PF_{L90100_2} - PF_{L90100_1} \right)} \cdot \left(PFL_{L_1} - PF_{L90100_1} \right) + P_{90} - P_{ABS} \\ \frac{\langle P_{50} - P_{40} \rangle}{\left(PFL_{50_2} - PFL_{40_2} \right)} \cdot \left(PFL_{L_2} - PFL_{40_2} \right) + P_{40} - P_{ABS} \\ \frac{\langle P_{50} - P_{40} \rangle}{\left(PFL_{50_3} - PFL_{40_3} \right)} \cdot \left(PFL_{L_3} - PFL_{40_3} \right) + P_{40} - P_{ABS} \\ \frac{\langle P_{40} - P_{30} \rangle}{\left(PFL_{40_4} - PFL_{30_4} \right)} \cdot \left(PFL_{L_4} - PFL_{30_4} \right) + P_{30} - P_{ABS} \\ \frac{\langle P_{30} - P_{20} \rangle}{\left(PFL_{30_5} - PFL_{20_5} \right)} \cdot \left(PFL_{L_5} - PFL_{20_5} \right) + P_{20} - P_{ABS} \end{bmatrix} = \begin{bmatrix} 82 \\ 35 \\ 33 \\ 28 \\ 19 \end{bmatrix} psi$$

Appendix C

$$PSI_{ABSR} := \begin{bmatrix} \frac{\langle P_{100} - P_{90} \rangle}{\left(PF_{R90100_2} - PF_{R90100_1} \right)} \cdot \left(PFL_{R_1} - PF_{R90100_1} \right) + P_{90} - P_{ABS} \\ \frac{\langle P_{40} - P_{30} \rangle}{\left(PFR_{40_2} - PFR_{30_2} \right)} \cdot \left(PFL_{R_2} - PFR_{30_2} \right) + P_{30} - P_{ABS} \\ \frac{\langle P_{40} - P_{30} \rangle}{\left(PFR_{40_3} - PFR_{30_3} \right)} \cdot \left(PFL_{R_3} - PFR_{30_3} \right) + P_{30} - P_{ABS} \\ \frac{\langle P_{50} - P_{40} \rangle}{\left(PFR_{50_4} - PFR_{40_4} \right)} \cdot \left(PFL_{R_4} - PFR_{40_4} \right) + P_{40} - P_{ABS} \\ \frac{\langle P_{50} - P_{40} \rangle}{\left(PFR_{50_5} - PFR_{40_5} \right)} \cdot \left(PFL_{R_5} - PFR_{40_5} \right) + P_{40} - P_{ABS} \end{bmatrix} = \begin{bmatrix} 87 \\ 32 \\ 30 \\ 35 \\ 32 \end{bmatrix} psi$$

Analysis of brake application pressure only reaches level to lock certain brakes Interpolated Min/Max Pushrod Force (non-ABS)

$$PF_{Lmin} := \begin{bmatrix} \frac{\left(PFL_{30_1} - PFL_{20_1} \right)}{\langle P_{30} - P_{20} \rangle} \cdot \left(PSI_1 - P_{20} \right) + PFL_{20_1} \\ \frac{\left(PFL_{30_2} - PFL_{20_2} \right)}{\langle P_{30} - P_{20} \rangle} \cdot \left(PSI_2 - P_{20} \right) + PFL_{20_2} \\ \frac{\left(PFL_{30_3} - PFL_{20_3} \right)}{\langle P_{30} - P_{20} \rangle} \cdot \left(PSI_1 - P_{20} \right) + PFL_{20_3} \\ \frac{\left(PFL_{30_4} - PFL_{20_4} \right)}{\langle P_{30} - P_{20} \rangle} \cdot \left(PSI_1 - P_{20} \right) + PFL_{20_4} \\ \frac{\left(PFL_{30_5} - PFL_{20_5} \right)}{\langle P_{30} - P_{20} \rangle} \cdot \left(PSI_1 - P_{20} \right) + PFL_{20_5} \end{bmatrix} = \begin{bmatrix} 533 \\ 1068 \\ 740 \\ 713 \\ 747 \end{bmatrix} lb$$

Appendix C

$$PF_{Rmin} := \begin{bmatrix} \frac{(PFR_{30_1} - PFR_{20_1})}{\langle P_{30} - P_{20} \rangle} \cdot (PSI_1 - P_{20}) + PFR_{20_1} \\ \frac{(PFR_{30_2} - PFR_{20_2})}{\langle P_{30} - P_{20} \rangle} \cdot (PSI_1 - P_{20}) + PFR_{20_2} \\ \frac{(PFR_{30_3} - PFR_{20_3})}{\langle P_{30} - P_{20} \rangle} \cdot (PSI_1 - P_{20}) + PFR_{20_3} \\ \frac{(PFR_{30_4} - PFR_{20_4})}{\langle P_{30} - P_{20} \rangle} \cdot (PSI_1 - P_{20}) + PFR_{20_4} \\ \frac{(PFR_{30_5} - PFR_{20_5})}{\langle P_{30} - P_{20} \rangle} \cdot (PSI_1 - P_{20}) + PFR_{20_5} \end{bmatrix} = \begin{bmatrix} 535 \\ 749 \\ 729 \\ 729 \\ 713 \end{bmatrix} lb$$

$$PF_{Lmax} := \begin{bmatrix} \frac{(PFL_{40_1} - PFL_{30_1})}{\langle P_{40} - P_{30} \rangle} \cdot (PSI_2 - P_{30}) + PFL_{30_1} \\ \frac{(PFL_{40_2} - PFL_{30_2})}{\langle P_{40} - P_{30} \rangle} \cdot (PSI_2 - P_{30}) + PFL_{30_2} \\ \frac{(PFL_{40_3} - PFL_{30_3})}{\langle P_{40} - P_{30} \rangle} \cdot (PSI_2 - P_{30}) + PFL_{30_3} \\ \frac{(PFL_{40_4} - PFL_{30_4})}{\langle P_{40} - P_{30} \rangle} \cdot (PSI_2 - P_{30}) + PFL_{30_4} \\ \frac{(PFL_{40_5} - PFL_{30_5})}{\langle P_{40} - P_{30} \rangle} \cdot (PSI_2 - P_{30}) + PFL_{30_5} \end{bmatrix} = \begin{bmatrix} 783 \\ 1067 \\ 1056 \\ 1021 \\ 1065 \end{bmatrix} lb$$

$$PF_{Rmax} := \begin{bmatrix} \frac{(PFR_{40_1} - PFR_{30_1})}{\langle P_{40} - P_{30} \rangle} \cdot (PSI_2 - P_{30}) + PFR_{30_1} \\ \frac{(PFR_{40_2} - PFR_{30_2})}{\langle P_{40} - P_{30} \rangle} \cdot (PSI_2 - P_{30}) + PFR_{30_2} \\ \frac{(PFR_{40_3} - PFR_{30_3})}{\langle P_{40} - P_{30} \rangle} \cdot (PSI_2 - P_{30}) + PFR_{30_3} \\ \frac{(PFR_{40_4} - PFR_{30_4})}{\langle P_{40} - P_{30} \rangle} \cdot (PSI_2 - P_{30}) + PFR_{30_4} \\ \frac{(PFR_{40_5} - PFR_{30_5})}{\langle P_{40} - P_{30} \rangle} \cdot (PSI_2 - P_{30}) + PFR_{30_5} \end{bmatrix} = \begin{bmatrix} 787 \\ 1067 \\ 1044 \\ 1044 \\ 1021 \end{bmatrix} lb$$

Appendix C

Interpolated Min/Max Pushrod Force (**ABS**)

$$PF_{ABSL} := \begin{bmatrix} \frac{\left(PF_{L90100_1} - PF_{L80}\right)}{\left\langle P_{90} - P_{80}\right\rangle} \cdot \left(PSI_{ABSL_1} - P_{80}\right) + PF_{L80} \\ \frac{\left(PFL_{40_2} - PFL_{30_2}\right)}{\left\langle P_{40} - P_{30}\right\rangle} \cdot \left(PSI_{ABSL_2} - P_{30}\right) + PFL_{30_2} \\ \frac{\left(PFL_{40_3} - PFL_{30_3}\right)}{\left\langle P_{40} - P_{30}\right\rangle} \cdot \left(PSI_{ABSL_3} - P_{30}\right) + PFL_{30_3} \\ \frac{\left(PFL_{30_4} - PFL_{20_4}\right)}{\left\langle P_{30} - P_{20}\right\rangle} \cdot \left(PSI_{ABSL_4} - P_{20}\right) + PFL_{20_4} \\ \frac{\left(PFL_{20_5} - PF_{L10}\right)}{\left\langle P_{20} - P_{10}\right\rangle} \cdot \left(PSI_{ABSL_5} - P_{10}\right) + PF_{L10} \end{bmatrix} = \begin{bmatrix} 1509 \\ 957 \\ 911 \\ 722 \\ 516 \end{bmatrix} lb$$

$$PF_{ABSR} := \begin{bmatrix} \frac{\left(PF_{R90100_1} - PF_{R80}\right)}{\left\langle P_{90} - P_{80}\right\rangle} \cdot \left(PSI_{ABSR_1} - P_{80}\right) + PF_{R80} \\ \frac{\left(PFR_{40_2} - PFR_{30_2}\right)}{\left\langle P_{40} - P_{30}\right\rangle} \cdot \left(PSI_{ABSR_2} - P_{30}\right) + PFR_{30_2} \\ \frac{\left(PFR_{40_3} - PFR_{30_3}\right)}{\left\langle P_{40} - P_{30}\right\rangle} \cdot \left(PSI_{ABSR_3} - P_{30}\right) + PFR_{30_3} \\ \frac{\left(PFR_{40_4} - PFR_{30_4}\right)}{\left\langle P_{40} - P_{30}\right\rangle} \cdot \left(PSI_{ABSR_4} - P_{30}\right) + PFR_{30_4} \\ \frac{\left(PFR_{40_5} - PFR_{30_5}\right)}{\left\langle P_{40} - P_{30}\right\rangle} \cdot \left(PSI_{ABSR_5} - P_{30}\right) + PFR_{30_5} \end{bmatrix} = \begin{bmatrix} 1617 \\ 878 \\ 815 \\ 959 \\ 852 \end{bmatrix} lb$$

Appendix C

Brake Force (**non-ABS**)

$$BF_{Lmin} := \begin{bmatrix} \frac{2 \cdot PF_{Lmin_1} \cdot SA_{L_1} \cdot Cf \cdot L_{L_1} \cdot D_{L_1}}{Rc \cdot T_{L_1}} \\ \frac{2 \cdot PF_{Lmin_2} \cdot SA_{L_2} \cdot Cf \cdot L_{L_2} \cdot D_{L_2}}{Rc \cdot T_{L_2}} \\ \frac{2 \cdot PF_{Lmin_3} \cdot SA_{L_3} \cdot Cf \cdot L_{L_3} \cdot D_{L_3}}{Rc \cdot T_{L_3}} \\ \frac{2 \cdot PF_{Lmin_4} \cdot SA_{L_4} \cdot Cf \cdot L_{L_4} \cdot D_{L_4}}{Rc \cdot T_{L_4}} \\ \frac{2 \cdot PF_{Lmin_5} \cdot SA_{L_5} \cdot Cf \cdot L_{L_5} \cdot D_{L_5}}{Rc \cdot T_{L_5}} \end{bmatrix} = \begin{bmatrix} 1003 \\ 1939 \\ 1343 \\ 1294 \\ 1480 \end{bmatrix} lb$$

$$BF_{Rmin} := \begin{bmatrix} \frac{2 \cdot PF_{Rmin_1} \cdot SA_{R_1} \cdot Cf \cdot L_{R_1} \cdot D_{R_1}}{Rc \cdot T_{R_1}} \\ \frac{2 \cdot PF_{Rmin_2} \cdot SA_{R_2} \cdot Cf \cdot L_{R_2} \cdot D_{R_2}}{Rc \cdot T_{R_2}} \\ \frac{2 \cdot PF_{Rmin_3} \cdot SA_{R_3} \cdot Cf \cdot L_{R_3} \cdot D_{R_3}}{Rc \cdot T_{R_3}} \\ \frac{2 \cdot PF_{Rmin_4} \cdot SA_{R_4} \cdot Cf \cdot L_{R_4} \cdot D_{R_4}}{Rc \cdot T_{R_4}} \\ \frac{2 \cdot PF_{Rmin_5} \cdot SA_{R_5} \cdot Cf \cdot L_{R_5} \cdot D_{R_5}}{Rc \cdot T_{R_5}} \end{bmatrix} = \begin{bmatrix} 1006 \\ 1360 \\ 1324 \\ 1324 \\ 1294 \end{bmatrix} lb$$

$$BF_{Lmax} := \begin{bmatrix} \frac{2 \cdot PF_{Lmax_1} \cdot SA_{L_1} \cdot Cf \cdot L_{L_1} \cdot D_{L_1}}{Rc \cdot T_{L_1}} \\ \frac{2 \cdot PF_{Lmax_2} \cdot SA_{L_2} \cdot Cf \cdot L_{L_2} \cdot D_{L_2}}{Rc \cdot T_{L_2}} \\ \frac{2 \cdot PF_{Lmax_3} \cdot SA_{L_3} \cdot Cf \cdot L_{L_3} \cdot D_{L_3}}{Rc \cdot T_{L_3}} \\ \frac{2 \cdot PF_{Lmax_4} \cdot SA_{L_4} \cdot Cf \cdot L_{L_4} \cdot D_{L_4}}{Rc \cdot T_{L_4}} \\ \frac{2 \cdot PF_{Lmax_5} \cdot SA_{L_5} \cdot Cf \cdot L_{L_5} \cdot D_{L_5}}{Rc \cdot T_{L_5}} \end{bmatrix} = \begin{bmatrix} 1474 \\ 1937 \\ 1916 \\ 1853 \\ 2109 \end{bmatrix} lb$$

$$BF_{Rmax} := \begin{bmatrix} \frac{2 \cdot PF_{Rmax_1} \cdot SA_{R_1} \cdot Cf \cdot L_{R_1} \cdot D_{R_1}}{Rc \cdot T_{R_1}} \\ \frac{2 \cdot PF_{Rmax_2} \cdot SA_{R_2} \cdot Cf \cdot L_{R_2} \cdot D_{R_2}}{Rc \cdot T_{R_2}} \\ \frac{2 \cdot PF_{Rmax_3} \cdot SA_{R_3} \cdot Cf \cdot L_{R_3} \cdot D_{R_3}}{Rc \cdot T_{R_3}} \\ \frac{2 \cdot PF_{Rmax_4} \cdot SA_{R_4} \cdot Cf \cdot L_{R_4} \cdot D_{R_4}}{Rc \cdot T_{R_4}} \\ \frac{2 \cdot PF_{Rmax_5} \cdot SA_{R_5} \cdot Cf \cdot L_{R_5} \cdot D_{R_5}}{Rc \cdot T_{R_5}} \end{bmatrix} = \begin{bmatrix} 1480 \\ 1937 \\ 1894 \\ 1894 \\ 1853 \end{bmatrix} lb$$

Appendix C

Brake Force (**ABS**)

$$BF_{ABSL} := \begin{bmatrix} \frac{2 \cdot PF_{ABSL_1} \cdot SA_{L_1} \cdot Cf \cdot L_{L_1} \cdot D_{L_1}}{Rc \cdot T_{L_1}} \\ \frac{2 \cdot PF_{ABSL_2} \cdot SA_{L_2} \cdot Cf \cdot L_{L_2} \cdot D_{L_2}}{Rc \cdot T_{L_2}} \\ \frac{2 \cdot PF_{ABSL_3} \cdot SA_{L_3} \cdot Cf \cdot L_{L_3} \cdot D_{L_3}}{Rc \cdot T_{L_3}} \\ \frac{2 \cdot PF_{ABSL_4} \cdot SA_{L_4} \cdot Cf \cdot L_{L_4} \cdot D_{L_4}}{Rc \cdot T_{L_4}} \\ \frac{2 \cdot PF_{ABSL_5} \cdot SA_{L_5} \cdot Cf \cdot L_{L_5} \cdot D_{L_5}}{Rc \cdot T_{L_5}} \end{bmatrix} = \begin{bmatrix} 2839 \\ 1737 \\ 1653 \\ 1310 \\ 1022 \end{bmatrix} lb$$

$$BF_{ABSR} := \begin{bmatrix} \frac{2 \cdot PF_{ABSR_1} \cdot SA_{R_1} \cdot Cf \cdot L_{R_1} \cdot D_{R_1}}{Rc \cdot T_{R_1}} \\ \frac{2 \cdot PF_{ABSR_2} \cdot SA_{R_2} \cdot Cf \cdot L_{R_2} \cdot D_{R_2}}{Rc \cdot T_{R_2}} \\ \frac{2 \cdot PF_{ABSR_3} \cdot SA_{R_3} \cdot Cf \cdot L_{R_3} \cdot D_{R_3}}{Rc \cdot T_{R_3}} \\ \frac{2 \cdot PF_{ABSR_4} \cdot SA_{R_4} \cdot Cf \cdot L_{R_4} \cdot D_{R_4}}{Rc \cdot T_{R_4}} \\ \frac{2 \cdot PF_{ABSR_5} \cdot SA_{R_5} \cdot Cf \cdot L_{R_5} \cdot D_{R_5}}{Rc \cdot T_{R_5}} \end{bmatrix} = \begin{bmatrix} 3044 \\ 1593 \\ 1479 \\ 1740 \\ 1546 \end{bmatrix} lb$$

Use smaller of maximum brake force and brake force at application pressure

$$BFL_{min_i} := min\left(BF_{Lmin_i}, FL_{max_i}\right) = \begin{bmatrix} 1003 \\ 1939 \\ 1343 \\ 1294 \\ 1480 \end{bmatrix} lb \quad BFR_{min_i} := min\left(BF_{Rmin_i}, FR_{max_i}\right) = \begin{bmatrix} 1006 \\ 1360 \\ 1324 \\ 1324 \\ 1294 \end{bmatrix} lb$$

$$BFL_{max_i} := min\left(BF_{Lmax_i}, FL_{max_i}\right) = \begin{bmatrix} 1474 \\ 1937 \\ 1916 \\ 1717 \\ 1480 \end{bmatrix} lb \quad BFR_{max_i} := min\left(BF_{Rmax_i}, FR_{max_i}\right) = \begin{bmatrix} 1480 \\ 1937 \\ 1894 \\ 1894 \\ 1853 \end{bmatrix} lb$$

Calculated Non-ABS deceleration rate min/max determination:

$$Decel_{min} := \frac{\left(\sum BF_{Lmin} + \sum BF_{Rmin}\right)}{\left(\sum W_L + \sum W_R\right)} = 0.361$$

Appendix C

$$Decel_{max} := \frac{\left(\sum BF_{Lmax} + \sum BF_{Rmax}\right)}{\left(\sum W_L + \sum W_R\right)} = 0.495$$

Calculated ABS deceleration rate min/max determination:

$$Decel_{ABS} := \frac{\left(\sum BF_{ABSL} + \sum BF_{ABSR}\right)}{\left(\sum W_L + \sum W_R\right)} = 0.485$$

$D_{stop} := 118.5 \cdot ft$ Skid mark distance

$$V_{nonABS} := \begin{bmatrix} \sqrt{2 \cdot g \cdot Decel_{min} \cdot D_{stop}} \\ \sqrt{2 \cdot g \cdot Decel_{max} \cdot D_{stop}} \end{bmatrix} = \begin{bmatrix} 35.8 \\ 41.9 \end{bmatrix} mph$$

Non-ABS speed range at start of skid mark

$V_{ABS} := \sqrt{2 \cdot g \cdot Decel_{ABS} \cdot D_{stop}} = 41.5\ mph$

ABS speed range at start of skid mark

VELOCITY OF HEAVY VEHICLE

$$V1 := \begin{bmatrix} V_{nonABS_1} \\ V_{ABS} \\ V_{nonABS_2} \end{bmatrix} = \begin{bmatrix} 35.8 \\ 41.5 \\ 41.9 \end{bmatrix} mph$$

$\text{mean}(V1) = 39.7\ mph$

$\text{median}(V1) = 41.5\ mph$

$\text{stdev}(V1) = 2.8\ mph$

$$RangeΔS1 := \begin{bmatrix} \text{mean}(V1) - \text{stdev}(V1) \\ \text{mean}(V1) + \text{stdev}(V1) \end{bmatrix} = \begin{bmatrix} 36.9 \\ 42.5 \end{bmatrix} mph$$

$$Decel_{stop} := \begin{bmatrix} Decel_{min} \\ Decel_{ABS} \\ Decel_{max} \end{bmatrix} = \begin{bmatrix} 0.361 \\ 0.485 \\ 0.495 \end{bmatrix}$$

$\text{mean}(\langle Decel_{stop} \rangle) = 0.45$

$\text{median}(\langle Decel_{stop} \rangle) = 0.48$

$\text{stdev}(\langle Decel_{stop} \rangle) = 0.06$

$$\mu_{Decel} := \begin{bmatrix} \text{mean}(\langle Decel_{stop} \rangle) - \text{stdev}(\langle Decel_{stop} \rangle) \\ \text{mean}(\langle Decel_{stop} \rangle) + \text{stdev}(\langle Decel_{stop} \rangle) \end{bmatrix} = \begin{bmatrix} 0.39 \\ 0.51 \end{bmatrix}$$

Forensic Engineering Analysis of an Explosion Allegedly Caused by an Overfilled Propane Cylinder

By Jerry R. Tindal, PE (NAFE 642S)

Abstract

Analyzing the origin and cause of fires or explosions for the purposes of legal proceedings requires the smooth integration of a reliable fire investigative methodology with sound engineering principles and practices. The origin of a building fire was first determined based on the methodology of NFPA 921 Guide for Fire and Explosion Investigations*. Engineering analysis was applied to witness observations, arc mapping, fire dynamics, and the evaluation of fire patterns. The fire cause was then evaluated considering NFPA 921 and integrated applied engineering analysis and calculations. The allegations of an overfilled propane cylinder as the cause of the fire were considered. Spoliation issues, poor investigation methodology, and the lack of sound engineering principles (resulting in unreliable opinions) are also contrasted and discussed.*

Keywords

NFPA 921, fire investigation, origin, pattern, arc mapping, cause, propane cylinder, overfilled, overpressure, regulator, relief valve, leak, heat transfer, fluid dynamics, propane, gas migration, dissipation, diffusion, spoliation, forensic engineering

Background

The property owner and eventual plaintiff, an elderly gentleman, was working inside his small detached office building adjacent to his residence when suddenly an explosion and fire occurred. Sometime during the incident, he sustained serious burn injuries that required hospitalization, substantial treatment, and rehabilitation. At some point after being discharged from the hospital, he collected and retained a 100-lb propane cylinder, a 12-foot section of copper tubing, and a wall-mounted space heater from the incident scene. An unburned 20-lb propane cylinder was also later collected and preserved by the owner. The owner concluded that the 100-lb propane cylinder must have been overfilled, leaked propane gas, and caused the explosion/fire incident. He then hired a plaintiff attorney to represent him.

Approximately one month after the incident, the plaintiff attorney hired an engineering firm to retain and evaluate the artifacts collected by the owner for causation purposes. At that point, the incident scene still existed; however, the engineering firm made no request nor any effort to examine, document, or process the scene. The engineering firm simply procured the artifacts from the owner, examined them, and then secured them at their facility.

Google Earth imagery indicated that the fire-damaged structure was still standing approximately eight months after the incident. Approximately 12 months after the incident, the propane company that allegedly filled the 100-lb cylinder was first placed on notice of the incident via a lawsuit filed against it. They had no prior notification of the incident. In addition, prior to the lawsuit filing, the fire scene and structure were substantially demolished and disposed of without any form of proper examination, documentation, or scene processing by a qualified party. The insurance company for the propane company retained a defense attorney, who subsequently retained this author to investigate the origin and cause of the explosion/fire.

Description of the Office

Figure 1 depicts a general plan view layout of the detached office building, which was derived from the remains of the foundation, flooring, fragments remaining at the scene, and a verbal description provided by the owner.

Jerry Tindal, PE, 922 Jeff Sharpe Road, Pelion, SC 29123; 803-394-5671; jtindal@safe-labs.com

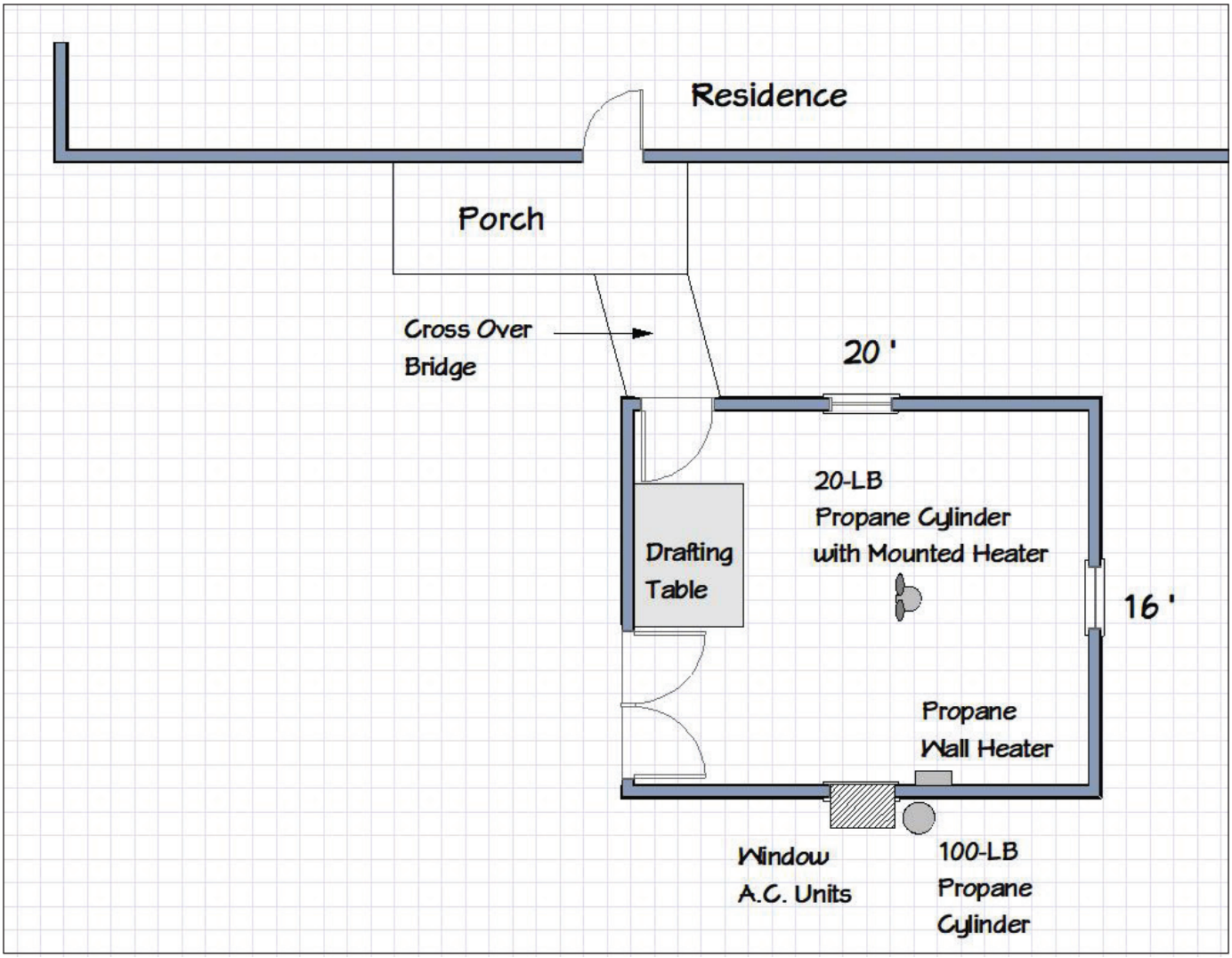

Figure 1
Office plan view layout with the approximate location of a 20-lb propane cylinder with top-mounted heater.

The incident building had been constructed by the owner approximately 16 years before the explosion/fire. The building had been a wood-framed structure, consisting of one open room that measured approximately 16 feet by 20 feet. The office had a plywood floor and was elevated above grade on concrete piers with an open crawl space and no skirting. The office was located approximately 12 feet from the owner's residence with an elevated plank walkway (cross-over bridge) connecting the covered porch of the residence to the entry door of the office building.

At the time of building construction, the owner purchased and installed an interior wall-mounted, unvented propane gas-fired heater, a 12-foot copper tubing gas supply line, and an exterior set 100-lb propane cylinder and regulator. The wall-mounted heater was installed on the interior south wall of the building. The 100-lb propane cylinder was set on patio bricks on the exterior of the south wall near two window air-conditioning units. One of the window air-conditioning units was installed in the window of the south wall. A second unit was installed through a cut-out opening in the south wall immediately below the window. According to the owner, the gaps in the wall openings around both air-conditioning units were sealed to prevent air exfiltration and infiltration.

The entry door of the office was in the north wall, which also contained a window. The west wall contained a pair of 3-foot doors located near the southwest corner, which were always closed and blocked closed by file cabinets. The east wall contained a window. The walls were insulated and sheathed with exterior wood panel T1-11 siding. The interior portions of the walls were sheathed with Oriented Strand Board (OSB). The ceiling was also

sheathed with OSB and insulated above. The roof was wood-framed and covered with metal.

Figures 2 and **3** depict the remains of the scene over a year after the incident. **Figures 4** and **5** depict the artifacts collected by the owner after he was discharged from the hospital.

Owner's Description of the Incident

Around 3:30 p.m. on the day before the incident, the owner disconnected the copper gas supply line and regulator from his 100-lb propane cylinder. Then, with

Figure 2
View from the south side of the office adjacent to the residence looking north.

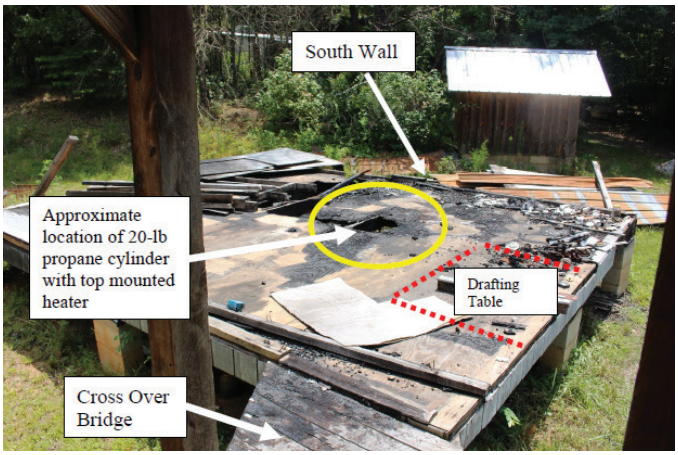

Figure 3
View from the northwest corner of the office looking from the residence porch, southeast over the elevated cross-over bridge.

Figure 4
View of the artifacts collected by the owner.

Figure 5
View of the 100-lb propane cylinder collected by the owner.

assistance from a friend, he reportedly took the cylinder to a propane refilling store and had it filled. He brought the cylinder home and reconnected the gas supply line and regulator around 4 p.m. After turning the gas on at the cylinder service valve, he indicated that he performed a soap bubble test to verify there were no leaks at the made connection points. He went inside the office, turned the gas "on" at the heater, and lit the pilot, after which time he retired for the evening to his residence. Reportedly, he never operated the heater, but only lit the pilot — and left the gas control in the pilot position the day before the explosion.

At approximately 2:30 p.m. the next day, he was in his office working at a drafting table and indicated that all of a sudden there was an explosion. He looked to his left, and realized "the whole (south) wall was burning." He went outside to turn off the gas and observed flames around the top of the 100-pound propane cylinder. The flames prevented him from turning the cylinder service valve off. He then went to retrieve a water hose and heard a second loud explosion. Upon returning with the water hose, he began trying to extinguish the fire when there was a third explosion that "tossed" him "20 feet." The fire department arrived, aided him, and extinguished the fire.

Plaintiff's Proffered Expert Opinions

The plaintiff's engineering expert did not prepare a written report, and his expert disclosures were without explanatory details or basis for his opinions. The plaintiff's engineering expert file was large, with seemingly scattered data, research, and various calculations. Part of the assignment of the author of this paper was to prepare engineering deposition questions for examination of the plaintiff's engineering expert to fully understand the opinions and the basis of the opinions intended to be offered at trial. To that end, extensive questions were prepared and implemented in the deposition. In summary, the plaintiff's engineering expert offered the following primary opinions:

1. The 100-lb propane cylinder was overfilled by the propane store.

2. At the time the cylinder was exposed to heat from the fire, it was near 96% liquid full.

3. The overfilled condition was conclusively determined based on the "vapor bubble" fire pattern remaining on the cylinder after the fire.

4. The temperature of the propane and cylinder at any given time is essentially the instantaneous ambient air temperature plus approximately 18°F for solar loading (radiant heat effect from the sun shining on the cylinder).

5. The gas leaking out of the regulator relief valve pre-incident wasn't caused by a failed regulator diaphragm.

6. Before the initial explosion and fire — and as a result of the overfilled condition — liquid propane had entered the regulator, rapidly expanded into a gas, and created a pressure of approximately 4,000 psi that destroyed the regulator diaphragm and leaked propane gas out.

7. The propane gas that leaked out of the regulator relief valve accumulated (outside and several feet above the ground) and then migrated through the wall, through the air-conditioners, into the office. It also migrated 7 to 8 feet up the exterior wall surface due to convection currents and then through the soffit into the concealed space above the ceiling.

8. The explosion ignited the accumulated propane gas that flashed back through the wall and the air conditioners to the leaking gas at the propane cylinder, igniting it and causing a continuous jet fire.

9. The propane cylinder became hot, and the relief valve on the cylinder service valve opened, discharging more gas into the fire.

10. One of the relief valve discharges and subsequent burning propane gases impacted and injured the plaintiff who had come outside to extinguish the fire with a water hose.

11. The propane cylinder, while remaining 96% full and connected to the copper tubing and regulator, was knocked over by one of the relief valve discharges and rolled away from the building. The cylinder came to rest on a slope with its foot elevated above its top. At that point, the 96% full cylinder was subjected to radiant heat impingement from the burning building that resulted in the "vapor bubble" fire pattern forming on the cylinder.

12. An investigation of the origin of the fire was not in the scope of the plaintiff expert's assignment. Note that there were no other investigators hired by the plaintiff's attorney.

13. The origin of the fire, however, became "self-revealing" and "self-apparent" after he concluded that the cause was an overfilled cylinder.

Fire Investigation Methodology

National Fire Protection Association (NFPA) 921 *Guide for Fire and Explosion Investigations* is well recognized in court systems as a peer-reviewed acceptable methodology for the investigation of fires and explosions. It provides comprehensive reliable scientific techniques in the fire investigative profession for analyzing the origin and cause of fires and explosions, including proper scene documentation, scene processing, scene data collection, evidence identification, collection and preservation, and analysis methods. Engineers performing fire investigative work must be familiar with and proficient in the application of NFPA 921; otherwise, they can expect serious court challenges to their opinions.

The subject case involved a multitude of blatant failures on the part of the plaintiff's attorney and his expert in properly investigating the incident. The extensive nature of the failures prohibits a detailed listing and discussion in the limited space available. However, some of the failures will be discussed in this paper to illustrate their significance.

In the 2014 edition[1] of NFPA 921, Chapter 4 *Basic Methodology* incorporates some of the following excerpted relevant provisions [emphasis added]:

4.1* *... The use of a systematic approach often will uncover new factual data for analysis, which may require previous conclusions to be reevaluated. With few exceptions, the proper methodology for a fire or explosion investigation is to first determine and establish the origin(s), then investigate the cause… .*

4.3 Relating Fire Investigation to the Scientific Method

4.3.3 Collect Data. *…The data collected is called empirical data because it is based on observation or experience and is capable of being verified or known to be true.*

4.4.3.3 *In any incident scene investigation,* ***it is necessary for at least one individual/organization to conduct an examination of the incident scene for the purpose of data collection and documentation****… . The use of previously collected data from a* ***properly documented scene*** *can be used successfully in an analysis of the incident to reach valid conclusions through the appropriate use of the scientific method… .*

4.4.3 Conducting the Investigation

4.4.3.1 *…The fundamental purpose of conducting an examination of any incident scene is to collect* ***all*** *of the available data and document the incident scene. … .*

4.4.3.4 … Improper scene documentation can impair the opportunity of other interested parties to obtain the same evidentiary value from the data. This potential impairment underscores the importance of performing comprehensive scene documentation and data collection.

4.6.3.1 *The methodologies used and the fire science relied on by an investigator are subject to peer review. For example,* ***NFPA 921 is a peer-reviewed document describing the methodologies and science associated with proper fire and explosion investigation*****s**.

Other relevant chapters of NFPA 921 (with provisions that were extensively referenced as part of the author's investigation into the incident and engineering report) included: 16 *Documentation of the Investigation*; 17 *Physical Evidence*; 18 *Origin Determination*; and 19 *Fire Cause Determination*.

Plaintiff's Expert Origin Analysis

The proper fire investigation sequence most commonly involves first determining the origin of the fire and then the cause of the fire. The plaintiff's expert testified in his deposition that he was not hired to perform an origin investigation or origin analysis, was not going to give an opinion as to the origin of the fire at trial, and therefore no scene examination, processing, or documentation was necessary for origin determination. Furthermore, no additional scene data or evidence was necessary to evaluate his opinions or test his hypothesis. In his opinion, the fire origin became "self-revealing" and "self-apparent" after he first determined the cause to be an overfilled cylinder. He began with a cause and then inferred an origin. He concluded the origin was at the side of the building where the 100-lb propane cylinder was located. The owner — the only witness interviewed by the plaintiff's

expert — initially reported an overfilled cylinder as the cause, and the expert never bothered to examine the scene or interview other witnesses. As such, expectation bias is strongly implicated. NFPA 921, Chapter 4 *Basic Methodology* warns against such bias in Section 4.3.8 partially excerpted below:

4.3.8 Expectation Bias. *Expectation bias is a well-established phenomenon that occurs in scientific analysis when investigator(s) reach a premature conclusion without having examined or considered all of the relevant data. Instead of collecting and examining all of the data in a logical and unbiased manner to reach a scientifically reliable conclusion, the investigator(s) uses the premature determination to dictate investigative processes, analyses, and, ultimately conclusions, in a way that is not scientifically valid.* **….**

Origin Analysis Methodology

In origin area analysis, NFPA 921 incorporates information derived from one or more of the following: witness information, fire patterns, arc mapping, and fire dynamics. Fire dynamics, in part, involve analyzing the initiation, development, and spread of a fire in the context of, and consistent with, the data obtained from the first three elements — namely witnesses observations, fire patterns, and arc-mapping. Therefore, fire dynamics is properly integrated into and considered in the analysis and discussion of those three elements.

The plaintiff's engineering expert failed to interview any witnesses as part of his investigation other than the owner. He also failed to obtain a copy of the fire department incident report, which provided the response information and the conclusions of the municipal investigation. As part of an attempt to settle the case, the author did (with the permission of defense counsel) forward a copy of the procured incident report and provided a summary of the information received during interviews of fire department personnel to the plaintiff's engineering expert during the course of the litigation.

The first responding firefighter happened to be the owner's next-door neighbor and the assistant fire chief of the responding fire department — who ultimately completed the municipal investigation and the incident report. The assistant fire chief was at his home when he heard the initial explosion, observed smoke coming from the plaintiff's property, and immediately responded. Upon arrival, he observed the owner coming out of the office with burn injuries and inquired as to what happened. The assistant chief testified, consistent with his incident report and interview, that the owner told him he was attempting to light a propane heater installed on the top of a propane cylinder inside the office when the explosion and fire occurred.

As part of his investigation after the fire, the assistant chief observed a 20-lb propane cylinder with a portable heater mounted to the top, located in the approximate center of the office. He also observed that the windows of the office building had been blown out from an explosion occurring inside the structure. Some of the window glass was lodged into the side of the adjacent residence. In addition to the observations of the assistant chief, the first firefighter that made entry into the office to extinguish the fire also observed the 20-lb propane cylinder with heater mounted to the top of it in the approximate center of the room. In his deposition, the owner denied the presence of this propane cylinder and denied the account of the assistant fire chief as to the cause of the fire.

At the time of the incident, the assistant chief concluded that based on his observations and on what the owner reported to him, the explosion/fire originated when the owner attempted to light the space heater mounted to the top of the 20-lb propane cylinder in the room. He concluded that there was most likely an accidental release or leak of gas into the room at the cylinder or at the heater mounted on top of the cylinder. Upon the owner's attempt to ignite the heater, the accumulated gas exploded. Since the assistant chief determined the incident was accidental, there was no municipal documentation or processing of the scene.

Failing to interview all relevant witnesses is a significant error that is substantially compounded when there are very different accounts, and a proper fire scene examination is not performed. NFPA 921, for example, notes:

18.3.3.15 Witness Observations*. …Witness statements regarding the location of the origin create a need for the fire investigator to conduct as thorough an investigation as possible to collect data that can support or refute the witness statements.…*

Figure 1 depicts the plan view of the office with the location of a 20-lb propane cylinder with top-mounted heater as observed by both the assistant fire chief and the first-in firefighter. **Figure 3** is annotated to indicate the general location of where the 20-lb cylinder with top-mounted heater was located. **Figure 6** depicts an "exemplar" 20-lb propane cylinder with top-mounted heater of a similar configuration

Figure 6
"Exemplar" 20-lb propane cylinder with top-mounted heater of the general type observed by the assistant fire chief and first-in firefighter.

as observed by the assistant fire chief and first-in firefighter. Since neither the cylinder nor the top mounted heater were recovered, the manufacturers are unknown — yet the configuration and style were similar, according to the witnesses.

As previously noted, fire patterns are recognized as a primary tool in the investigation of a fire or explosion. The contents of the office building were removed and disposed of without systematic examination and documentation. The walls, ceiling, roof, windows, and doors of the building were similarly demolished. The gas system components were removed and not systematically excavated, reconstructed, or documented in any fashion relative to the fire scene or contents of the scene. There was no reconstruction of contents and building structure elements and therefore no means to evaluate any fire patterns in relation to available fuel loads and configurations. In fact, there were no documented fire patterns of the scene to evaluate particularly relative to the context of the site. The isolated and alleged "vapor bubble" fire pattern used by the plaintiff's expert to conclude the cause of the fire will be discussed later. All the fire patterns should have been comprehensively examined, documented, and analyzed during a proper joint scene examination, excavation, reconstruction, and processing. The plaintiff's attorney and expert failed to perform or allow such work to be performed.

As previously noted, arc mapping is recognized as a primary tool in the investigation of a fire or explosion and is potentially useful in aiding in the establishment of the origin of the fire, in evaluating the spread of the fire and potentially in evaluating the fire cause. The electrical system of the building was demolished and discarded; therefore, there was no opportunity to properly excavate, examine, and document the electrical system. Furthermore, the window air-conditioning units and all other electrical devices within the office building were discarded, and no opportunity to properly excavate, examine, and document these components was provided. Arc mapping should have been comprehensively performed, documented, and analyzed during a proper joint scene examination and processing. The plaintiff's attorney and expert failed to perform or allow such work to be performed.

Spoliation

Spoliation was a key issue in the subject case. There were no factors or conditions that prevented the plaintiff from following proper methodologies in this investigation. Included in the author's engineering report was a time line description of events related to the investigation and the known conditions of the scene based on discovery documents and research. The plaintiff and the plaintiff's expert became involved a few weeks after the incident when the scene was still intact. Google Earth imagery, depicted in **Figure 7** and dated eight months after the incident, indicated the burned structure was still standing. There was simply no reason that the defendants could not have been notified in a timely manner of the event by the plaintiff and given an opportunity to properly jointly investigate the scene.

NFPA 921 addresses numerous issues related to spoliation, and the reader is encouraged to review those provisions. Some of these were previously mentioned in the citations of Chapter 4 as they relate to the impairment of the opportunity of other interested parties to obtain

Figure 7
Google Earth image of incident site approximately eight months after the event.
Note: The south wall of the building is completely shaded beneath the trees.

evidentiary value from the scene and the need for performing comprehensive scene documentation and data collection. The definition of spoliation is found in NFPA 921 section 3.3.167. Other sections of interest include: 12.3.5.5 *Documentation Prior to Alteration*, 18.3.2.5 *Avoiding Spoliation*, and 29.3.1 *Notice to Interested Parties*.

In addition to citing specific proper investigative methodology infractions, it is often useful to provide a list of evidence items that may have been of interest. **Figure 8** is an example of such a list that was provided in the author's report in the subject case.

Alleged "Vapor Bubble" Fire Pattern

The plaintiff's expert determined the cause of the fire based on his interpretation of a single, isolated, alleged "vapor bubble" fire pattern on the surface of the 100-lb propane cylinder. The "vapor bubble" fire pattern is depicted in **Figure 9**. He opined that the fire pattern conclusively indicated the cylinder was overfilled. According to the plaintiff's expert, the propane cylinder at some point during the event was knocked over by one of the cylinder service valve pressure relief valve (PRV) discharges. The cylinder then rolled away from the building on the slightly sloped ground surface below the building and ended up with the foot being elevated above the top of the cylinder. In addition, he opined that the copper pipe and regulator remained attached to the cylinder and uncompromised at the point it came to rest. Radiant heat from the elevated burning office building then impinged on the cylinder lying on the ground below. Differential heat transfer in the liquid and vapor regions of the cylinder produced the demarcation lines ("vapor bubble" fire pattern) on the cylinder. After measuring the dimensions of the "vapor bubble" fire pattern (excluding the portion of the pattern extending across the open foot ring), the plaintiff's expert then back-calculated the amount of liquid propane that was in the cylinder. He concluded the cylinder had 96% liquid propane in it at the time it was lying on the ground and exposed to radiant heat from the fire (even after three relief valve discharges during the fire event). Over the course of falling to the ground and during the radiant heat exposure, the regulator housing, regulator diaphragm, and copper tubing remained intact and uncompromised, according to his interpretation.

1	20-lb propane cylinder observed inside the office building
2	Portable space heater mounted to the top of the 20-lb propane cylinder observed in the building
3	Remains of the regulator reportedly attached to the 100-lb propane cylinder
4	Any securing brackets or bracing potentially associated with the soft copper tubing routed between the 100-lb cylinder and the interior wall-mounted space heater inside the office building
5	Both window air-conditioning units installed in the south wall of the office and any components associate with them
6	Electrical wiring system for the structure including but not necessarily limited to the structural wiring, electrical outlets, switches, etc.
7	Electrical appliances including but not necessarily limited to, lights, lamps and electrical equipment inside the office
8	Fire pattern documentation of the structure, interior and exterior and potential artifacts of interest in-situ (prior to disturbing the scene or any artifacts) - photography and measurements
9	Documentation of a systematic progressive excavation and reconstruction of the fire scene; including exposed fire patterns related to the structure, contents and recovered artifacts-photography and measurements
10	Construction details, documentation and measurements related to the walls, ceiling, insulation, barriers, roof, windows and doors
11	Reconstruction and documentation of the gas system and gas system components; including but not necessarily limited to the location and positioning of all propane cylinders, piping and heaters and subsequent documentation of the same relative to any fire patterns
12	Reconstruction of the 100-lb propane cylinder, copper tubing, window AC units and roof, etc. with photographic and dimensional documentation of same
*** It is not possible to state all the relevant or potentially relevant evidence items or data that may have been recovered, simply because there is no way to know what may have been discovered during a properly conducted joint scene examination, scene processing and documentation when the scene and evidence were destroyed.	

Figure 8
Examples of evidence items of potential interest***.

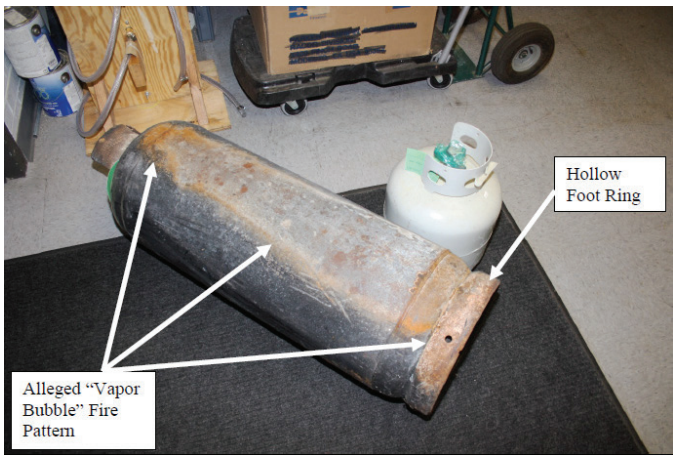

Figure 9
A view of the 100-lb propane cylinder and the alleged "vapor bubble" fire pattern. Note that the alleged fire pattern extends beyond the cylinder wall in contact with propane across and to the end of the hollow foot ring. Allegedly, the cylinder was lying on its side with the foot higher than the top, still connected to the regulator and line, 96% full, and the liquid/vapor bubble interface created the depicted pattern during radiant heat exposure from the burning building.

The interpretation of a single, isolated, alleged fire pattern, in particular relative to an undocumented and destroyed fire scene, does not constitute a proper and complete analysis of all or even most of the fire patterns of a fire scene and is not consistent with the requirements of NFPA 921. Such an evaluation is arbitrary and is similar to having a single piece of a puzzle without any other pieces to the puzzle, or even a photograph of what the completed puzzle looks like. As such, one can create any picture they want from that single puzzle piece. NFPA 921 contains a number of relevant provisions that should be reviewed related to proper scene excavation and reconstruction including consideration of the effects of various fuels on fire pattern production, including: 18.3.2 *Excavation and Reconstruction*, 18.3.2.3 *Excavation*, 18.3.2.8 and 18.3.2.8.2 *Contents*, 18.3.3.2 *Description of Fuels*, 18.3.3.9 *Fuel Gas Systems*, and 18.4.1.1 *Consideration of All Patterns*.

It was detailed in the author's engineering report that the history of the 100-lb propane cylinder and local environmental conditions post-fire were unknown. The 100-lb cylinder was not documented at the scene in any fashion after the explosion/fire event. There was no in-situ photographic documentation of the cylinder as it was found after the incident. There was no reconstruction documentation or photographs of the cylinder relative to the structure, fuels, and other elements that were present at the fire scene. Some significant questions to consider included, but are not limited to: Where was the cylinder located, and what was its geometric positioning

relative to fuel loads, the structure immediately next to it, and other fire patterns present after the fire? What were the other fuel loads around the cylinder? What was the orientation of the cylinder and any alleged burn patterns on the cylinder in its as-found position? How long was the cylinder on the ground outside after the fire? What were the outdoor ambient and ground conditions over the time period it was there? Where is the documentation of the cylinder in each of the conditions it was originally located, moved, and stored in?

Metals exposed to elevated temperatures, such as very often happens in a fire, are subject to accelerated oxidation. When left exposed to the elements, various oxidation patterns can and do form post-incident on metals. For example, if the steel cylinder was lying on its side in the moist soil, fire debris or in a puddle of water for a period of time and later picked up, there can be an irregularly shaped oxidation pattern on the side of the cylinder reflecting where it was lying in the soil, debris, or water. The pattern depicted on the side of the cylinder could be just oxidation (rust) on a previously burned steel cylinder left out and exposed to the elements.

Furthermore, as implied above, another important question to consider is: What were the other fuels that were burning around the cylinder and their orientation relative to the alleged pattern on the cylinder? We know, for example, that the propane cylinder itself relieved gas through the relief valve multiple times as a normal consequence of the fire during the event. The regulator diaphragm (once quickly compromised by heat from the fire) would also have rapidly released gas into the fire. These events in themselves will create localized intense burning in close proximity to the propane cylinder. Flame impingement on the cylinder would be directionally dependent upon the sequence of events that occurred during the incident. In other words, localized intense burning can create patterns on one portion of the cylinder surface relative to the rest of the cylinder surface.

Compressor oil contained in the pressurized refrigerant lines of the air-conditioning units are another fuel source that can be released into the fire in close proximity to the cylinder and create areas of highly localized intense burning and the production of irregular patterns. Proper scene documentation, processing, and reconstruction as well as proper evidence identification, collection, documentation, and preservation would have allowed for a detailed and proper analysis of all the fire patterns and fuel loads in context with one another. Some additional relevant portions of NFPA 921 considered included [emphasis added]:

6.3.1.2.2. *The patterns seen by an investigator can represent much of the history of the fire. Each time another fuel package is ignited or the ventilation to the fire changes, the rate of energy production and heat distribution will change. Any burning item can produce a plume and thus a fire pattern… .*

6.3.1.2.1. *The production of lines and areas of demarcation depends on a combination of variables: the material itself, the rate of heat release of the fire, fire suppression activities, temperature of the heat source, ventilation, and the amount of time that the material is exposed to the heat. ... The investigator should keep this concept in mind while analyzing the nature of fire patterns… .*

10.1.2.1. *During fire or explosion events, disrupted fuel gas systems can provide additional fuel and can greatly change or increase fire spread rates, or can spread fire to areas of the structure that would not normally be burned. The flames issuing from broken fuel gas lines (often called flares) can spread fire and burn through structural components.*

There was no reliable scientific basis for opining that the isolated alleged fire pattern on the 100-lb cylinder was conclusively caused by differential heat processes primarily involving the liquids and vapors inside the cylinder and heat exposure. Aside from the absence of the history of the cylinder post-incident as previously described — and the unknown nature of other fuel packages, locations, quantities, positions, and the fire patterns associated with them — the observations in the following paragraphs are also relevant.

The allegation includes that the “fire pattern” formed while the cylinder was exposed to heat from the fire, after it fell over, rolled away, and was lying on the ground on its side — all the while still in a near liquid filled state with the bottom of the cylinder elevated above the top of the cylinder. Such conditions are not justifiable. The cylinder was reportedly connected to a soft copper pipe and installed in a vertical position adjacent to the office south wall. The cylinder service valve was open to the connected aluminum regulator and copper piping. The windows were blown out by the interior explosion, and the vertically oriented cylinder would be subjected to convective and radiant heat from the fire venting from inside the structure out through the breached window. The venting fire would

rapidly heat the cylinder, causing it to normally vent propane, as designed, through the pressure relief valve (PRV) to prevent overpressure and catastrophic failure of the cylinder.

At the same time, the heat and flames would rapidly compromise the rubber diaphragm and rubber orifice seat inside the regulator (attached to the top of the 100-lb propane cylinder at the open service valve), as well as the regulator aluminum housing, allowing high-pressure propane gas to rapidly free flow from the cylinder into the atmosphere through the regulator vent and housing. It is well known in the fire investigative industry that gas systems exposed to heat from fires are normally compromised and release their fuel contents into the fire, creating localized intense fire as a normal consequence. First responding witnesses also indicate there was no line or regulator attached to the cylinder service valve when they arrived at the scene. Evidence indicates that the regulator did, in fact, melt, and the connection to the cylinder failed. The rubber diaphragm would have failed sooner than the aluminum housing.

It is highly unlikely that the regulator diaphragm and housing were not compromised by the heat of the fire prior to the 100-lb propane cylinder falling over (resulting in the free flow of high pressure gas from the cylinder to the atmosphere). The cylinder was witnessed upright and venting through the PRV during the event, indicating that it was subjected to substantial heat before falling over. If the cylinder was subjected to high heat, so was the attached regulator at the top of the cylinder.

Furthermore, it is highly unlikely that the cylinder fell over with the cylinder top down and bottom sticking up without further compromising the heat damaged regulator and piping system, increasing the free flow of high-pressure propane to the atmosphere. Under such conditions, it is highly unlikely that the cylinder would still be in a state near liquid filled and exposed to fire while lying on the ground with a compromised attached piping and regulator system. Therefore, it would be unlikely to create an alleged "vapor bubble" fire pattern.

Finally and very significantly, the alleged "vapor bubble" fire pattern, purportedly formed by differential heating between the liquid filled regions and the vapor regions of the cylinder, extends into and across the foot ring. The foot ring is hollow and completely open to the atmosphere (i.e., is 100% air/vapor space and has no liquid in it), yet the pattern (with demarcation lines) continues completely across and to the bottom edge of the foot ring. By the plaintiff's expert hypothesis presented, there ought to be liquid propane present and contained in portions of the open to atmosphere foot ring, which is nonsensical.

Near the beginning of his deposition, the plaintiff's expert claimed he knew that the cylinder was overfilled because of the "vapor bubble" fire pattern and that the mere presence of the pattern precluded a pre-fire failure of the propane regulator rubber diaphragm. Had the diaphragm failed pre-fire, the contents of the cylinder would have been rapidly evacuated. Therefore, there would be no differential liquid/vapor space to create the observed pattern upon heat exposure. However, several hours later in his deposition, he contradicted himself when he opined that the regulator diaphragm failed pre-fire due to the introduction of liquid propane into the regulator chamber from the overfilled cylinder. In his opinion, when liquid propane entered the regulator chamber, it vaporized and produced a pressure of approximately 4,000 psi, which would have destroyed the rubber diaphragm and regulator.

Overfilled Cylinder Engineering Analysis Methodology

The plaintiff's expert examined the weather data for the day before the incident when the cylinder was allegedly filled as well as the weather data for the date of the incident. He concluded that the cylinder was filled at the refill station when the ambient temperature was 55°F; therefore, the propane in the 100-lb cylinder started at 55°F. He then concluded that at the time of the incident, the ambient temperature was 71°F; however, to account for solar radiation heating of the cylinder, an additional 18°F needed to be added. As a result, he opined that the temperature of the liquid propane in the cylinder (ending temperature) was at least 89°F at the time of the incident. Assuming a 100% liquid full cylinder, using a temperature differential of 34°F (i.e., 89°F to 55°F), multiplying that by a coefficient of thermal expansion interpolated from a rough graph, and then subtracting the gas volume consumed by the operating pilot on the heater, he concluded that the cylinder expelled a total of 0.91 gallons of liquid propane through the pressure relief valve of the regulator.

From this, he calculated that 0.91 gallons would convert to 28.2 ft^3 of pure propane gas and — when mixed with ambient air — form an explosive volume of between 294 ft^3 to 1,311 ft^3 outside and adjacent to the wall. He reasoned that this was more than sufficient volume to diffuse through the wall and be ignited inside. Although he estimated a discharge amount and calculated

corresponding explosive concentration volumes, his analysis did not compute any rates of discharge, which as will be discussed later are a significant factor in determining the potential for an explosion and fire to occur.

The Google Earth image depicted in previously referenced **Figure 7** indicates that the south wall, including the 100-lb propane cylinder, is well shaded in the afternoon due to the nearby stand of trees. The propane tank at the refilling store where the cylinder was allegedly filled was not significantly shaded, but substantially exposed to direct sunlight most of the day. **Figure 10** depicts the refilling station. The cylinder was allegedly filled near the end of the day.

When the plaintiff's expert was asked in his deposition why he did not factor in any solar heating of the tank at the refill station to his calculations, as he had done with the 100-lb cylinder, he deflected the question and ultimately ended up stating that the starting temperature was really irrelevant to the problem. Obviously, that is not true in the calculation that he performed. See **Equation 1**.

Equation 1: $\Delta V = Vi\beta(T_f - T_i)$

Where ΔV = change in volume
V_i = initial volume
β = volumetric temperature expansion coefficient
T_f = final temperature
T_i = initial temperature

Clearly, the closer the initial and final temperatures are to each other, the less change in volume there will be — and correspondingly the less potential exists for expelling any propane due to an alleged overfill condition.

In addition to ignoring any solar heating on the filling supply tank at the refill station, the plaintiff's expert assumed that the temperature of the liquid propane in the 100-lb cylinder was essentially the instantaneous outdoor temperature plus 18°F for solar radiation heating at any given time. For example, as the outdoor thermometer ticked to 71°F, the propane inside the cylinder at that instant was 71°F + 18°F = 89°F. He reasoned that this was true because of the high thermal conductivity of the steel cylinder, which would, in his view, more or less instantly heat the liquid propane inside to the same temperature.

Figure 10
Refilling station and supply tank. The refilling tank and pump station is circled in red. The pump station had a rain canopy. The vast majority of the tank is exposed.

It is well established that many engineering heat transfer problems are transient in nature and involve non-steady-state heating and cooling processes. For example, Holman[3] (page 139) notes the following:

...If a solid body is suddenly subjected to a change in environment, some time must elapse before an equilibrium temperature condition will prevail in the body…

In other words, objects do not generally heat up and cool down instantaneously, matching the immediate ambient environmental temperature into which they are placed. There is an initial temperature lag between the object and the environment it is placed in. The temperature difference will gradually approach zero over time as the object remains in the ambient environment and warms up or cools down to match the ambient temperature.

Transient heat transfer engineering problems associated specifically with propane cylinders have been studied and determined mathematically/experimentally to reliably follow and be predicted by the classical "Lumped Heat Capacity System"[4,5]. For example, Petersen[5] performed experimental testing and mathematical "Lumped Heat Capacity System" modeling calculations on propane cylinders placed in an outdoor environment with results indicating less than a 5 percent difference between the calculated and actual temperatures of the cylinder and the propane it contained.

Lumped Heat Capacity System engineering analysis addresses the transient heat transfer process and predicts resultant temperatures when placing a propane cylinder (including the liquid mass within) of a given temperature into an environment with variable ambient conditions (such as the outdoors). The analysis can include evaluating the diurnal cycle effects (i.e., evaluating the hourly ambient temperature, solar, and nocturnal radiation effects occurring during daylight and nighttime hours). These effects can include, if justified, the addition of degrees of temperature to the hourly ambient air temperature to model the overall complex heat transfer processes that occur at the air/surface and liquid/surface interface of the cylinder and mixing that goes on with the cylinder. The heat transfer and fluid mechanics occurring is more complex than simply looking at the thermal conductivity of the shell of the vessel. The general equation for Lumped Heat Capacity System analysis is expressed below. However, De Nevers[4] and Petersen[5] thoroughly cover the application to propane cylinders; therefore, the development and methodology will not be repeated.

Equation 2: $(T_o-T)/(T_o-T_1) = e^{(-hA/mc)t}$ where:

T_o = ambient temperature [°F]
T = temperature at the end of the time period [°F]
T_1 = initial temperature for the time period [°F]
h = heat transfer coefficient [Btu/(HR-°F-ft^2)]
A = container area, (exposed to liquid) [ft^2]
m = mass of propane and container [Lbm]
c = combined specific heat for propane and the container
t = time period, [Hr]

Mathematical Modeling Considerations for the Incident Case

Factors that may have impacted predicted temperatures of the cylinder and the mass of propane within the cylinder in question include the orientation and geometry of the 100-lb propane cylinder relative to the two window air-conditioners, roof overhang, and wall of the building, as well as the numerous surrounding trees. The dimensional measurements of the cylinder relative to the air-conditioning units, wall, and roof overhang of the building were not documented or preserved.

However, based on reported information, the 100-lb cylinder was located somewhere near the window units, which would likely provide some degree of shading effect for a period of time on the cylinder surface and reduce any potential overall solar heating effects. In addition to the air-conditioning units, the wall and roof overhang of the building also provide a shading effect from the sun for periods of time. Furthermore, there are considerable trees surrounding the area, which would also impact and substantially reduce any potential solar heating effects for periods of time (see **Figure 7**, depicting the trees and the corresponding shading of the building's south exterior wall where the cylinder was located).

The initial temperature of the propane in the 100-lb cylinder that would correspond to the temperature of the propane in the supply tank is also an important factor to consider as previously discussed. The temperature of propane in the supply tank is dependent upon several elements, including the quantity of propane in the tank, corresponding wetted surface area of the tank, the heat transfer coefficient, and diurnal cycling accounting for solar and nocturnal radiation before the 100-lb cylinder was filled. The amount of propane and temperature of the liquid propane that was in the supply tank at the time of the 100-lb cylinder filling is unknown. Commonly, such data is easily and reliably collected shortly after an incident by documenting the fill level gauge on the tank and

obtaining the tank pressure. There was no opportunity to document the condition of the supply tank within the immediate time frame of the incident. Again, it was over a year after the incident before the propane store was placed on notice via a lawsuit.

Thermal Expansion Modeling and Rates of Discharge for the Incident Case

Since there was an absence of some important data, an attempt to model the precise conditions of the incident was not performed. However, demonstrative modeling using the "Lumped Capacity Heat System" can still provide some useful information for analysis and opinions.

The heat transfer process associated with a liquid propane mass warming and cooling inside a cylinder located in outdoor ambient conditions is slow and gradual; therefore, the thermal expansion and contraction rates of the liquid propane in the cylinder are also slow and gradual. The "Lumped Heat Capacity System" model previously described can be used to reliably demonstrate the slow nature of the temperature changes and the corresponding expansion and contraction rates of the liquid propane over a normal diurnal cycle. Two demonstrative models were utilized to aid in the subject incident.

For both demonstration calculations, properties of liquid propane were obtained from the National Institute of Science and Technology (NIST), Material Measurement Laboratory database. The database is available free online at the NIST website. In addition, the hourly outdoor ambient weather conditions, as reported by the U.S. Department of Commerce, National Oceanic & Atmospheric Administration (NOAA) at the nearest observation station, were used. Some of the hourly weather data for the incident case, on the date of the incident is shown in **Figure 11**. The day prior is not included here to preserve space.

For purposes of the first demonstration, variables were selected in such a manner as to attempt to produce a forced expansion of liquid propane in an assumed liquid-full cylinder; such that, roughly, the quantity of propane alleged by the plaintiff's expert to have been released (0.91 gallons) would be discharged into the atmosphere. However, instead of simply determining a total quantity of gas released over an undefined time, the model places the release in the context of time and therefore provides an estimated average release rate. As previously mentioned, release rates are one critical factor in determining whether flammable gases will create conditions that may produce an explosion or fire hazard. Release rates are discussed

Date	Time (LST)	Station Type	Sky Conditions	Visibility (SM)	Weather Type	Dry Bulb Temp		Wet Bulb Temp		Dew Point Temp		Rel Humd %	Wind Speed (MPH)	Wind Dir	Wind Gusts (MPH)
						(F)	(C)	(F)	(C)	(F)	(C)				
1	2	3	4	5	6	7	8	9	10	11	12	13	14	15	16
15	0056	12	CLR	10.00		40	4.4	32	0.2	19	-7.2	43	3	290	
15	0156	12	CLR	10.00		35	1.7	30	-1.0	21	-6.1	57	0	000	
15	0256	12	CLR	10.00		33	0.6	29	-1.5	22	-5.6	64	0	000	
15	0356	12	CLR	10.00		31	-0.6	29	-1.9	24	-4.4	75	0	000	
15	0556	12	CLR	10.00		29	-1.7	27	-2.6	24	-4.4	82	0	000	
15	0656	12	CLR	10.00		30	-1.1	28	-2.2	24	-4.4	78	0	000	
15	0756	12	CLR	10.00		41	5.0	35	1.7	26	-3.3	55	3	180	
15	0856	12	CLR	10.00		48	8.9	39	3.7	25	-3.9	41	5	190	
15	0956	12	CLR	10.00		51	10.5	43	5.9	32	0.0	46	7	220	
15	1056	12	CLR	10.00		57	13.9	45	7.3	31	-0.6	37	10	230	16
15	1156	12	CLR	10.00		62	16.7	48	8.7	31	-0.6	31	8	250	20
15	1256	12	CLR	10.00		66	18.9	50	9.9	32	0.0	28	14	230	22
15	1356	12	CLR	10.00		68	20.0	51	10.7	34	1.1	29	15	250	22
15	1456	12	CLR	10.00		70	21.1	53	11.4	35	1.7	28	18	240	24
15	1556	12	CLR	10.00		71	21.7	53	11.8	36	2.2	28	16	230	29
15	1656	12	CLR	10.00		71	21.7	53	11.8	36	2.2	28	17	240	24
15	1756	12	CLR	10.00		69	20.6	53	11.6	37	2.8	31	13	220	22
15	1856	12	CLR	10.00		65	18.3	52	10.8	38	3.3	37	9	220	
15	1956	12	CLR	10.00		62	16.7	51	10.3	39	3.9	43	9	210	
15	2056	12	CLR	10.00		61	16.1	50	10.0	39	3.9	44	8	210	
15	2156	12	CLR	10.00		62	16.7	51	10.3	39	3.9	43	10	210	
15	2256	12	CLR	10.00		61	16.1	51	10.2	40	4.4	46	14	220	
15	2356	12	CLR	10.00		60	15.6	50	10.0	40	4.4	48	16	230	

Figure 11
Some of the hourly weather data for the incident case.

Time of Day (Clock)	Out Door Ambient |F| [With Applied Solar but No Nocturnal Radiation] |To|	Ending Temperature of the Propane and Cylinder |F| at the end of the time period	Total Volume of Liquid Propane in Cylinder |+ or -| Incremental Change in Volume	Liquid Propane (expansion or deficit) Beyond the Fixed Cylinder Volume = [Vcyl-Vf] in^3
4:00 to 5:00 PM	55	57.37	6594.6000	0.00
5:00 to 6:00 PM	53	56.44	6584.1274	-10.47
6:00 to 7:00 PM	53	55.72	6570.6106	-23.99
7:00 to 8:00 PM	49	54.30	6557.3080	-37.29
8:00 to 9:00 PM	45	52.34	6533.7613	-60.84
9:00 to 10:00 PM	41	49.94	6505.4156	-89.18
10:00 to 11:00 PM	45	48.90	6492.3363	-102.26
11:00 to 12:00 AM	45	48.08	6479.4705	-115.13
12:00 to 1:00 AM	44	47.22	6466.6094	-127.99
1:00 to 2:00 AM	40	45.69	6448.9535	-145.65
2:00 to 3:00 AM	35	43.44	6426.5073	-168.09
3:00 to 4:00 AM	33	41.23	6399.6925	-194.91
4:00 to 5:00 AM	31	39.07	6377.8899	-216.71
5:00 to 6:00 AM	30	37.16	6356.3045	-238.30
6:00 to 7:00 AM	29	35.44	6339.5160	-255.08
7:00 to 8:00 AM	48	38.09	6359.3551	-235.24
8:00 to 9:00 AM	59	42.50	6398.5248	-196.08
9:00 to 10:00 AM	66	47.46	6443.7028	-150.90
10:00 to 11:00 AM	69	52.01	6485.3257	-109.27
11:00 to 12:00 PM	75	56.86	6533.5734	-61.03
12:00 to 1:00 PM	80	61.75	6583.2502	-11.35
1:00 to 2:00 PM	84	66.44	6629.1678	34.57
2:00 to 3:00 PM (1/2 hr)	87	68.74	6619.4026	24.80
			Total in^3	59.37
			Gallons	0.26

Figure 12
Part of the spreadsheet calculations for the first demonstration.

along with other important factors later.

The manufacturer's fixed tare weight and water capacity data permanently engraved on the collar of the 100-lb cylinder were used to obtain the propane liquid volume of the cylinder, assuming 100% liquid filled, and the weight of the filled cylinder. The calculated combined **mc** term of **Equation 2** for the case in question was consistent with the calculated value for 100-lb propane cylinders referenced by De Nevers[4]. The calculated **hA** values of **Equation 2** were also likewise consistently comparable with De Nevers[4] and Petersen[5].

In the first demonstration calculations (**Figure 12**), for all daylight hours (beginning 30 minutes before sunup), an extremely unrealistic scenario, an assumed 18ºF solar effective temperature addition was added to the ambient hourly temperature. As a point of reference to the unrealistic nature of the assumption in the incident case, in one experimental test performed by Petersen[5] in Texarkana, Texas during the summertime, he added only 3 to 10 degrees for the incremental hours between 10 a.m. and 6 p.m. to adjust the model for solar loading gain to match the field experimental data. The case in question occurred during the winter time in South Carolina. Nevertheless, nocturnal radiative cooling was ignored, although likely significant, given the very cold (as low as 29°F) and clear night that had transpired. Shading was also ignored, although it was most likely a significant factor. A starting temperature of 58ºF was used for propane from the supply tank (3ºF above ambient), although it was substantially open and exposed to sunlight throughout the day.

Even with the extreme unrealistic conditions forced, the model calculates that only 0.26 gallons (as opposed to 0.91 gallons) would be released over a period of 1½ hours. **Figure 12** depicts a small part of the spreadsheet layout for the calculations performed. **Figure 13** depicts the model's predicted average vapor release rates and the total quantity of released gas vapor associated with the extreme unrealistic first demonstration. As can be seen, the discharge rates are extremely small, as is the total amount of gas discharged. **Figure 14** further illustrates and characterizes the extremely small quantities represented. Slow discharge rates provide substantial time for gas to disperse harmlessly, particularly in the outside open air. The propane cylinder regulator was several feet

above grade. There was wind movement around the time of hypothetical gas venting. Furthermore, there was plenty of air cross flow in the absence of underpinning. These factors are discussed in further detail below.

For purposes of the second demonstration, a baseline model was produced. In the baseline model, both solar and nocturnal radiation (for the cold clear night) assumed gains and losses are ignored, and simply the ambient air conditions are utilized. The initial starting temperature of the propane is assumed to be 55ºF. Results of the baseline model indicated the predicted average vapor release rates associated with the demonstration calculations are zero. Beginning with an assumed liquid filled cylinder at 55ºF — and allowing it to pass through the diurnal ambient temperature cycle that occurred during the incident case — the cylinder will retain a vapor head space (0.33 gallons) and not release any gas to the outside. This demonstration (like the first) also includes the gas consumption of the pilot. An analysis of any assumed solar gain (and/or losses via nocturnal radiation) beyond the baseline model would necessitate field testing an actual propane cylinder and its propane mass contents at the site for precise validation purposes. However, it is noteworthy that the cold ambient temperatures alone that night would have substantially cooled the cylinder and its propane mass contents down.

Dispersion Rate Factors and Migration of Gases

As discussed above, discharge rates are only one of the important considerations in analyzing a hypothesis related to an alleged gas leak or release potentially causing a fire or explosion hazard. For example, in discussing gas leaks that occur **inside** of buildings, Kennedy[6] notes additional factors that must be considered [emphasis added]:

> ***Spread and Diffusion of Fuel Gases***
> *When any fugitive fuel gas leaks into a structure, it will mix with the air by one or more of the following actions: turbulent jet mixing, the natural buoyancy of the gas, the turbulent action of building ventilation, or molecular*

Unrealistic Demonstration #1: Average*** Exterior Vapor Gas Release Rates (assuming a continuous discharge) Associated with (unrealistic) Demonstration Calculations; and Total Quantity Released to the Outside Air		
Time Period	**Vapor Gas Discharge Rate CFH**	**Vapor Gas Discharge Rate CFM**
1200-1300	0	0
1300-1400	5.44	0.0907
1400-1430	7.81	0.1302
Total Quantity in Cubic Feet over 1.5 hrs (90 min.)	**9.345 CF**	**9.345 CF**
*** Any alleged releases through the internal relief of the regulator would most likely be intermittent as opposed to a continuous release, as thermal warming under ambient conditions is slow and subsequently the incremental expansions of the propane is also slow and gradual, not instantaneous nor massive.		

Figure 13
Vapor gas release rates.

Unrealistic Demonstration #1: Average*** Liquid Propane Inlet Rates into the Regulator and total quantity discharged.		
Time Period	**Liquid Propane Inlet Rate Milliliters per Minute (ml/min)**	**Liquid Propane Inlet Rate Milliliters per Second (ml/s)**
1200-1300	0	0
1300-1400	9.4	0.157
1400-1430	13.5	0.226
Total quantity flowed over the elapsed time period	**0.26 gallons over 1.5 hours**	**0.26 gallons over 1.5 hours**
*** Any alleged releases through the internal relief of the regulator would most likely be intermittent as opposed to a continuous release, as thermal warming under ambient conditions is slow and subsequently the incremental expansions of the propane is also slow and gradual, not instantaneous nor massive.		

Figure 14
Liquid propane inlet rates.

> *diffusion. Mixing by molecular diffusion is extremely slow when compared to the others.* ***All of the mixing actions dilute the gas with air*** *more and more the farther from the gas leak source.* ***Gases once mixed with air tend to remain mixed with air and not separate due to density differences. If the gas is escaping under pressure from a small source such as an*** *open pipe or* ***hole*** *in a pipe,* ***air will be entrained into the sides of the gas plume*** *created by the turbulent jet. …If the gas is heavier than air, the plume will be less buoyant than the surrounding air and tend to settle downward in a three-dimensional flattened fan shape… .*

In the incident case, the allegedly small gas leakage (from the regulator vent) is on the exterior of the structure occurring in the outside open air, and, as a result, dispersion and dilution of the gas with air can be expected to be rapid. The alleged small leak rates of propane gas into the open outside air will be subject to mixing with the outside air. Mixing occurs as the gas is discharged out of the vent opening of the regulator and immediately entrains air into the discharging plume, diluting the gas. The diluted gas/air-mixed plume is then subject to additional dilution in the outside open air via molecular diffusion, thermal diffusion, and natural convection air currents around the localized discharge area. Molecular diffusion involves the natural mixing of gas molecules due to different concentration gradients between the gases[3]. The gases will diffuse together until the concentration gradient comes to equilibrium. Thermal diffusion (e.g., due to temperature differences between the gases or thermal gradients) accelerates the mixing process. Natural convection currents are present even in assumed still air conditions. For example, thermal gradients on different objects can induce small localized air currents. These air currents will further act to dilute gases in the ambient.

The above processes exclude any mixing due to air movement related to air breezes (forced convection currents). The open crawl space with no underpinning provides a clear avenue for substantial cross flowing airways. The weather data indicates wind speeds of 8 mph with gusts of 20 mph around 12 p.m. out of the west/southwest; wind speeds of 14 mph with gusts of 22 mph around 1 p.m.; wind speeds of 15 mph with gusts of 22 mph around 2 p.m.; and wind speeds of 18 mph with gusts of 24 mph around 3 p.m.

Sophisticated Computational Fluid Dynamics (CFD) models (e.g. NIST Fire Dynamics Simulator [FDS][7] or FLACS[8]) have been developed, tested and validated for use in evaluating the complex nature of gas discharge, dispersion and migration problems. The alleged leak rates and quantities for the case in question, however, were very small. More importantly, they occurred in the outside open air; therefore, there is no justifiable mechanism by which to produce a flammable concentration of gas inside the building.

Pressure relief valves (PRVs) incorporated with cylinder service valves and relief valves built into gas regulators are designed by manufacturers to release propane in a controlled manner under overpressure conditions. With the exception of the window, which was closed and sealed, there were no openings in the wall. Window air-conditioning units are intentionally designed not to communicate unconditioned air from the outside of a building to the inside.

Window air-conditioning units are installed in a window or through a wall and sealed around the perimeter to prevent outdoor unconditioned air from infiltrating inside, or indoor conditioned air from exfiltration to the outdoors. The owner stated that his installed air-conditioning units were sealed, which is the appropriate, ordinary, and common method of installing and using these units. The units simply draw air from inside the room, circulate it through the evaporator heat exchanger coil, and then discharge it back into the room. No outside air is drawn into the evaporator heat exchanger coil. In fact, it is separated from the outside by an internally sealed air (gas) barrier to specifically prevent such an occurrence.

The exterior wall of the office was reportedly constructed of overlapping T1-11 siding with the inner cavities being insulated and the interior side covered with OSB. No windows were open, and no other wall openings were reported; nor were the wall or window air-conditioning units made available for examination or reconstruction. Exterior walls are intended design barriers to minimize the migration of air or other gases through the wall in either direction. The purpose behind ordinary construction is to keep unconditioned air (gas) outside and conditioned air inside. Air and propane vapors gas are gases, and both would likewise be substantially kept outside by ordinary construction barriers.

There was no scientific basis (including any mathematical modeling, CFD, or experimental testing) that was presented in the incident case by the engineering plain-

tiff's expert to support his opinions.

The regulator, or remnants of the regulator, were not available for examination, identification, or potential testing (i.e., of exemplars), and the make and model of the regulator was unknown. However, design standards[9] require that regulator relief vents operate in a manner such as to maintain the outlet pressures at or below approximately 2 psi, with start-to-discharge settings occurring when the pressure climbs to 19 to 33 inches water column (0.685 to 1.19 psi). For example, the Fisher Emerson Process Management *Bulletin LP-15*[10] regarding LP gas regulators provides:

...the regulator vent will exhaust LP-Gas when the internal relief valve opens. Every second stage domestic and light commercial LP-Gas regulator reducing pressure down to appliance pressure must have an internal relief valve. An open internal relief valve can exhaust small bubbles of gas or large volumes of gas depending upon the condition that caused the overpressure situation…

...UL 144, Standard for LP-Gas Regulators requires that the second stage regulator internal relief valve must open (begin-to-bubble) between 170% and 300% of the regulator outlet setting.

The regulator that was connected to the cylinder service valve outlet was designed to receive high inlet pressure propane — most have a maximum input pressure rating of 250 psi. Any alleged liquid propane dripping or "sputtering" into the piping connected to the regulator and into the regulator inlet would immediately convert to vapor in the regulator chamber and as soon as sufficient gas pressure had built up in the chamber, the internal relief vent would operate and discharge (or bubble out) the gas vapor to the open outside air. Once the internal regulator pressure dropped below the start to discharge setting, it would close until the pressure built-up again.

The average discharge rates previously presented in **Figure 13** were used to estimate and illustrate the average liquid propane inlet rate into the regulator, which are presented in **Figure 14**. As shown, the rates are very small. The volumetric flow rates are comparable to a children's medicine dropper or a small graduated medicine dosage cup.

Fire Origin and Cause Conclusions

A complete independent origin and cause investigation could not be completed by the author due to the destruction of the scene and gross absence of any scene examination, documentation, and processing. The assistant fire chief was the only municipal authority to make an examination of the fire scene prior to its destruction as well as directly witness portions of the event itself. In addition, the chief spoke directly with the owner regarding the circumstances of the incident at the time it was occurring. Furthermore, the chief and the first-in firefighter both observed the 20-lb propane cylinder with the top mounted heater in the office. This information was ignored and then claimed to be false by the plaintiff.

The 20-lb propane cylinder and top-mounted heater located within the enclosed room was a valid and substantial potential source of explosive fuel to consider in the investigation of this explosion and fire. Connections between a heater and cylinder can potentially leak (e.g., due to a loose connection, damaged threads or seals, broken or cracked fittings, etc.) Likewise, damaged or defective gas-carrying portions of the heater connected to the cylinder may have been leaking gas and resulted in an explosion. Neither the propane cylinder nor a heater was available for laboratory examination. The 20-lb propane cylinder and top-mounted heater that was located in the office could not be ruled out as a potential source of fuel and an ignition source for the explosion and fire, or as the point of origin of the fire. The heavily damaged unvented wall heater could also not be ruled out as an ignition source for the explosion.

The explosion originated in the one-room office. The correct cause of the explosion and fire for this case is undetermined; however, a detailed engineering analysis eliminated an overfilled cylinder as a potential cause of the incident.

References

1. NFPA 921-2014. Guide for fire and explosion investigations. Quincy, MA; National Fire Protection Association.

2. NFPA 58-2008. Liquefied Petroleum Gas Code. Quincy, MA; National Fire Protection Association.

3. Holman JP. Heat transfer, 7th edition. New York, NY: McGraw-Hill, Inc.; 1990.

4. De Nevers N. Ambient and solar heating of propane containers. Fire Technology.1997;22(3).

5. Petersen J. Forensic engineering techniques for testing and predicting LP-gas container relief venting. Journal of the National Academy of Forensic Engineers. 2004;21(2).

6. Kennedy P, Kennedy J. Explosion investigation and analysis: Kennedy on explosions. Chicago, IL: Investigations Institute; 1990.

7. Pape R, Mniszewski KR. The use of FDS for estimation of flammable gas/vapor concentrations. Presented at: Society of Fire Protection Engineers, 3rd Technical Symposium on Computer Applications in Fire Protection Engineering; Sep 12-13, 2001; Baltimore, MD.

8. Gavelli F, Davis SG, Hansen OR. A modern tool for the investigation of indoor flammable gas migration. Proceedings, International Symposium on Fire Investigation Science and Technology, Hyattsville, MD, 2010.

9. ANSI/UL 144-2014. Standard for LP-gas regulators. Northbrook, IL; Underwriters Laboratories, Inc.

10. Bulletin LP-15-2011. Give a regulator the attention it deserves. McKinney, TX; Fisher Emerson Process Management.